BATCH AND CONTINUOUS BLENDING OF PARTICULATE MATERIAL STUDIED BY NEAR-INFRARED SPECTROSCOPY

Inauguraldissertation

zur

Erlangung der Würde eines Doktors der Philosophie

vorgelegt der

Philosophisch-Naturwissenschaftlichen Fakultät

der Universität Basel

von

Lizbeth Araceli Martínez Heredia

aus Mexiko

Basel, 2013

Genehmigt von der Philosophisch-Naturwissenschaftlichen Fakultät

auf Antrag von

Prof. Dr. Jörg Huwyler

Dr. Lorenz Liesum

Prof. Dr. Dr. h.c. mult. Hans Leuenberger

Basel, den 26 Marz 2013.

Prof. Dr. Jörg Schibler

Dekan

creative commons

Namensnennung-Keine kommerzielle Nutzung-Keine Bearbeitung 2.5 Schweiz

---

Sie dürfen:

das Werk vervielfältigen, verbreiten und öffentlich zugänglich machen

Zu den folgenden Bedingungen:

Namensnennung. Sie müssen den Namen des Autors/Rechteinhabers in der von ihm festgelegten Weise nennen (wodurch aber nicht der Eindruck entstehen darf, Sie oder die Nutzung des Werkes durch Sie würden entlohnt).

Keine kommerzielle Nutzung. Dieses Werk darf nicht für kommerzielle Zwecke verwendet werden.

Keine Bearbeitung. Dieses Werk darf nicht bearbeitet oder in anderer Weise verändert werden.

- Im Falle einer Verbreitung müssen Sie anderen die Lizenzbedingungen, unter welche dieses Werk fällt, mitteilen. Am Einfachsten ist es, einen Link auf diese Seite einzubinden.
- Jede der vorgenannten Bedingungen kann aufgehoben werden, sofern Sie die Einwilligung des Rechteinhabers dazu erhalten.
- Diese Lizenz lässt die Urheberpersönlichkeitsrechte unberührt.

Die gesetzlichen Schranken des Urheberrechts bleiben hiervon unberührt.

Die Commons Deed ist eine Zusammenfassung des Lizenzvertrags in allgemeinverständlicher Sprache: http://creativecommons.org/licenses/by-nc-nd/2.5/ch/legalcode.de

Haftungsausschluss:
Die Commons Deed ist kein Lizenzvertrag. Sie ist lediglich ein Referenztext, der den zugrundeliegenden Lizenzvertrag übersichtlich und in allgemeinverständlicher Sprache wiedergibt. Die Deed selbst entfaltet keine juristische Wirkung und erscheint im eigentlichen Lizenzvertrag nicht. Creative Commons ist keine Rechtsanwaltsgesellschaft und leistet keine Rechtsberatung. Die Weitergabe und Verlinkung des Commons Deeds führt zu keinem Mandatsverhältnis.

Quelle: http://creativecommons.org/licenses/by-nc-nd/2.5/ch/ Datum: 3.4.2009

To my parents

Acknowledgments

My gratitude goes to Dr. Lorenz Liesum for sharing with me his valuable experience, for the exposure that he gave me to the pharmaceutical industry, for helping me to focus my ideas in a structured way and mostly for his constant support throughout my entire PhD.

I am very grateful to Prof. Jörg Huwyler for accepting to be the Faculty responsible and for his valuable help for the successful conclusion of my PhD.

I would like to extend my gratitude to Prof. Hans Leuenberger who kindly accepted to review this thesis.

My general thanks to Novartis Pharma and University of Basel for their financial and nonfinancial support.

I would like to thank PD Dr. Gabriele Betz who gave me the opportunity to perform my PhD at the Industrial Pharmacy Lab.

I am very thankful to Dr. Antonio Peinado for his critical and valuable feedback and for the enthusiasm that he put into his explanations during my PhD.

I thank all my teachers who taught me during my PhD studies, especially PD. Dr. Joseph Dannacher for his useful lecture on diffuse reflectance.

I thank Dr. Ulrich Meier, Dr. Jay Lakshman, Dr. Vishal Koradia, Dr. Norbert Rasenack and Dr. Raju Vegesna for their comments on the manuscripts and thesis.

I want to thank the Process Analytical Technology Team and Global Pharma Engineering Department at Novartis Pharma. It was very motivational for my professional development to be in contact with experienced scientists who shared their valuable knowledge and expertise, especially to Dr. Lukas Doulakas and Dr. May Ling Yeow for the fruitful scientific conversations.

I would like to thank Evi Bieler from Zentrum Mikroskopie for the SEM micrographs.

Special thanks to Laura McLean for her valuable revision of this thesis.

My gratitude goes to the former members of the Industrial Pharmacy Lab at University of Basel, thank you for all the nice moments that we shared, Dr. Felicia Flicker, Dr. Krisanin Chansanroj, Dr. Imjak Jeon, Dr. Sameh Abdel-Hamid, Dr. Muhanned Saeed, Dr. Elaine Darronqui, and Branko Vranic.

I want to end with some personal acknowledgments. First I want to deeply thank my brother, Mario, for his unconditional support throughout all these years. I want to thank my dear friends in Basel and Mexico for always having the right motivational words.

I am deeply grateful to Heiko Brosy for his continuous support, encouragement, affection and love.

There are no words for thanking my parents whose wholehearted support was the main input for the successful completion of my studies; to them I dedicate this thesis.

Summary

Background: Pharmaceutical manufacturing is moving towards real-time release of the products. This objective can only be achieved by clearly understanding the process and by implementing suitable technologies for manufacturing and for process control. Near-infrared (NIR) spectroscopy is one technology that has attracted lot of attention from the pharmaceutical industry since it can analyze bulk solids without any pretreatment, therefore reducing or eliminating wet chemistry analysis. Consequently NIR spectroscopy is a powerful tool for the monitoring unit operations were bulk material is involved i.e. blending of powders.

Blending of powders is a complex and poorly understood unit operation. In the pharmaceutical industry blending has been performed batchwise and controlled by thief sampling. Thief sampling is an invasive process which is tedious and tends to introduce bias; therefore an alternative sampling method was highly needed. Here is where NIR found a perfect match with blend uniformity monitoring, thus NIR implementation offers several advantages: thief sampling is avoided, the process is continuously monitored, detection of blend-end point, and fast identification of process deviations.

NIR spectral data need to be correlated with the parameter of interest (physical or chemical). These computations are done by multivariate data analysis (MVDA). MVDA and NIR are a powerful combination for in-process control and their use has been promoted by the health authorities through the Process Analytical technology (PAT) initiative by the FDA.

Purpose: This thesis is focused on the study of powder blending, which is an essential unit operation for the manufacture of solid dosage forms. The purpose of this study was to develop two quantitative methods for the monitoring of the active ingredient concentration. One method was developed for the blend uniformity monitoring of a batch mixing process, and a second method for a continuous mixing process.

This study also tackles the relevance of the physical presentation of the powder on the final blend quality, by studying the influence of the particle size and the effect of the previous manufacturing steps on the NIR spectral data.

Methods: Particle size was studied by NIR in diffuse reflectance mode, using Kubelka-Munk function and the transformation of reflectance of absorbance values, in order to focus the analysis on the physical properties. Furthermore, an off-line NIR model was developed for the quantification of the mean particle size. The influence on segregation, that different particle size distribution of the formulation components, was studied.

Blend uniformity monitoring of a batch pharmaceutical mixing was achieved through a NIR off-line calibration method, which was used for the in-line drug quantification of a production scale mixing process.

NIR in diffuse reflectance mode was used in the study of a continuous blending system. The effect of the process parameters, i.e. flow rate and stirring rate, was analyzed. Moreover, a NIR method for the in-line drug quantification was developed.

In addition, NIR was implemented in a powder stream, in which the mass of powder measured by NIR was estimated.

Results and discussion: Regarding particle size, incompatibilities due to different particle size ranges between the formulation ingredients lead to severe segregation. Particle size and cohesion determined the quality of the powder blend; slight cohesion and broader particle size distribution improved the robustness of the final blend. NIR showed high sensitivity to particle size variations, thus it was possible to develop a quantitative model for the mean particle size determination with a prediction error of 16 micrometers.

Concerning batch mixing, an off-line calibration was generated for the quantification of two active ingredients contained in the formulation. The prediction errors varied from 0.4 to 2.3% m/m for each of the drugs respectively. Special emphasis was given on the proper wavelength selection for the quantitative analysis in order to focus the analysis on the active ingredients quantification.

In relation to continuous blending of particulate material, a quantitative NIR model was developed for the in-line prediction of the active ingredient concentration. The NIR model was tested under different process conditions of feeding rate and stirring rate. High stirring rates produce higher scattering of the NIR predictions. This was directly associated with the acceleration of the particles at the outlet of the blender affecting the dwell time of the particles with the NIR probe. The NIR model showed to be robust to moderate feed rate increments; however the NIR model under-predicted the drug concentration under moderate feed rate reductions of 30 kg/h. Furthermore, the continuous blending phases were clearly identified by principal component analysis, moving block of standard deviation, and relative standard deviation, all of them giving consistent results.

The NIR measurements in a powder stream involved the scanning of powder flowing in a chute. The flow of bulk solids is a complex phenomenon in which powder moves at a certain velocity. The motion of particles produces changes in the density and distribution of the voids. In this study, the velocity of the powder sliding down an inclined chute was measured and used for the estimation of the NIR measured mass. The mass observed during one NIR measurement was estimated to be 658 mg, which corresponded to less than one tablet.

Conclusions: This study proved the feasibility of applying NIR spectroscopy for the blend uniformity monitoring of batch and continuous powder mixing. Understanding the critical parameters of powder mixing lead to a robust process and reliable analytical methods. NIR proved to be a valuable and versatile analytical tool in the measurement of bulk solids.

Contents

List of figures

List of tables

Abbreviations

API	Active Pharmaceutical Ingredient
BU	Blend Uniformity
CB	Continuous Blending
CU	Content Uniformity
CV	Cross-Validation
FDA	Food and Drug Administration
GUI	Graphical User Interface
HPLC	High Pressure Liquid Chromatography
IBC	Intermediate Bulk Container
MBSD	Moving Block of Standard Deviation
MC	Mean Centering
MD	Mahalanobis Distance
MG	Melt Granulation
MVDA	Multivariate Data Analysis
NIR	Near-Infrared
OSC	Orthogonal Signal Correction
PAT	Process Analytical Technology
PB	Physical Blend
PCA	Principal Component Analysis
PLS	Partial Least Squares
QbD	Quality by Design
RMSECV	Root Mean Square Error of Cross Validation
RMSEE	Root Mean Square Error of Estimation
RMSEP	Root Mean Square Error of Prediction
RSD	Relative Standard Deviation
SEM	Scanning Electron Microscopy
SG	Savitzky Golay
SNV	Standard Normal Variate
USP	United States Pharmacopeia

1 Introduction

Pharmaceutical manufacturing is moving toward real-time release of pharmaceutical products. This goal can only be achieved by clearly understanding the manufacturing process and by implementing the suitable technology for manufacturing and for process control. Each unit operation brings challenges that need to be assessed in order to prevent compromising the quality of the final product. One of the technologies that has attracted a lot of attention from the pharmaceutical industries as well as the health authorities is near infrared (NIR) spectroscopy. NIR can measure bulk samples without any preceding treatment, thus making it a very appealing technology for the real-time monitoring of pharmaceutical processes. NIR spectral data needs to be correlated with the parameter of interest (physical or chemical); these computations are done by multivariate data analysis (MVDA). MVDA and NIR are a powerful combination for in-process control and their use has been promoted by the health authorities through the Process Analytical Technology (PAT) initiative of the FDA.

This thesis is focused on the study of powder blending, which is an essential unit operation for the manufacture of solid dosage forms. This study tackles the relevance of the physical presentation of the powder on the final blend quality by studying the influence of the particle size and the effect of the previous manufacturing steps on the NIR spectral data.

Blending of powders in the pharmaceutical industry has usually been performed batchwise. Batch blending has been traditionally controlled by thief-sampling which is tedious, quick to generate bias, and can potentially disrupt the blend, leaving plenty of room for improvement. By implementing NIR as a process analytical tool, the use of thief-sampling can be completely avoided. In this research a control strategy based on NIR and MVDA was developed for the blend uniformity monitoring of a batch process at an industrial scale.

Even though blend uniformity monitoring of a batch process by NIR is a huge achievement, it is still possible to go one step further: by employing continuous blending (CB) as a substitute of batch mixing. CB can handle higher production volumes and, when connected to the previous and following manufacturing steps, it is possible to avoid the manipulation of the formulation. The result is less operator interference and faster availability of the product. This scenario is only possible by having reliable control of the continuous blending process; as a result, in this study, NIR was used for monitoring the quality of the blend of the flowing powder at the outlet of a continuous blender. This study proved the feasibility of real-time monitoring of a continuous blending process of a pharmaceutical formulation.

Powder mixing has erroneously been considered a straightforward operation. The lack of scientific understanding, together with strong regulations, has kept the pharmaceutical industry behind other industries. The art of powder mixing needs a better scientific understanding towards the excellence in quality, efficiency and reliability of the product in order to bring to a safe treatment to the patient.

2 Theoretical Background

2.1 Blending

It is well known that powder mixing is a central and extremely important unit operation that is practiced to a great extent whenever particulate material is processed. In the pharmaceutical industry, blending is involved in the manufacture of solid dosage forms, which include tablets, capsules, and granules. Therefore, powder blending cannot be overlooked and a correct control strategy is fundamental. A clear example of the importance of the assessment of the blend homogeneity, known as the Barr Decision (US v. Barr Laboratories, Inc., 812 F. Supp. 458 - Dist. Court, D. New Jersey 1993), occurred in 1993. Barr laboratories faced a legal case against the FDA. The FDA found a series of failures during compliance inspections and, as a result of these investigations, blending of powders attracted a lot of interest. During the case special attention was placed on remixing, resampling, averaging, the importance of sample size and sampling locations, sampling procedures, mixing time, and particle size distribution. The case ended with numerous issued orders and product recalls, and a clear precedent was established concerning the importance of correct blending sampling and control. Bearing in mind that providing the best quality of the product is the main objective, the blend homogeneity has to be guaranteed by appropriate process control.

Solids mixing is a key unit operation by which two or more components (active ingredients and excipients) are randomized (Fan et al., 1970). The mixing of powders gains more and more economical importance since the mixing process adds value to the product and incorrect blend uniformity analysis can lead to out of specification products. Rees (1977) emphasized the importance of building quality into the product during development and manufacturing processes instead of relying and waiting for the control test of the final product. This statement clearly refers to the Quality by Design (QbD) context defined by the ICH (2009), where the quality of the final product cannot be tested in the product, but rather should be built-in by design through the development process.

Lacey (1954) suggested three possible mixing mechanisms for particulate material: convective mixing, which involved the transfer of neighbor particles from one location to another, involving the movement of large masses of particles (Williams, 1972); diffusive mixing, which is the distribution of particles over a freshly developed surface and random motion at small scale; and shear mixing, with setting up of slipping planes with the mass (Alexander and Muzzio, 2002; Bridgwater, 1994; Manjunath et al., 2004; Staniforth, 1982).

Mixing in tumbling blenders involves a fast convective stage followed by a slower dispersive or diffusive stage (Shinbrot and Muzzio, 2007). In Figure 2-1 the first stage of the mixing kinetic curve represents the reduction in heterogeneity. This period is associated with the rearrangement of large groups of particles, mainly due to convective and shear mixing mechanisms. The second stage corresponds to diffusive mixing characterized by the motion of individual particles (Massol-Chaudeur et al., 2002).

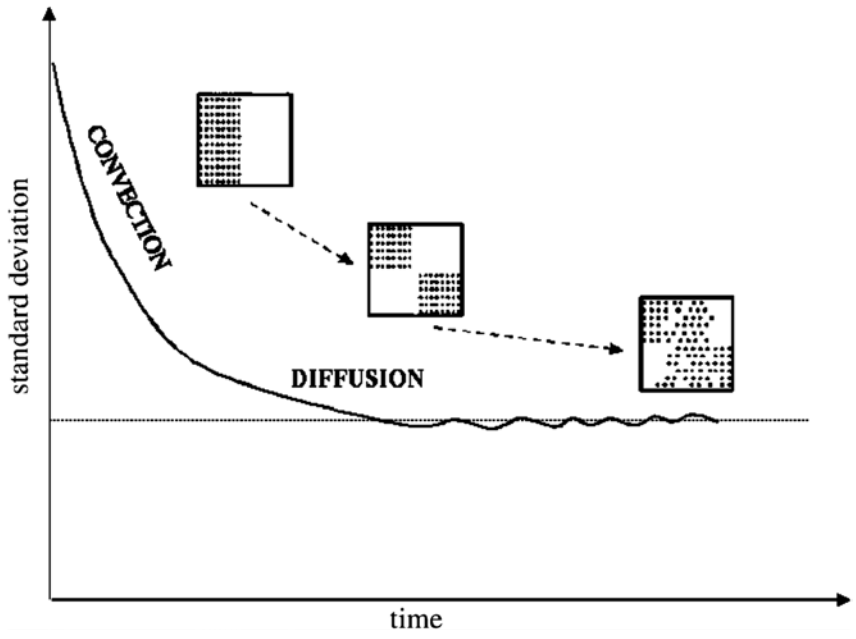

Figure 2-1 Mixing kinetic curve (Massol-Chaudeur et al., 2002).

At the end of the mixing process, two different types of blends can be obtained:

Ordered mixture (Figure 2-2a): requires particle interaction as adsorption, chemisorption, surface tension, frictional, electrostatic or any other form of adhesion (Hersey, 1975). An example is the adhesion of the fine component to the surface of coarse carrier particles as

the dominant mechanism of mixture (Fan et al., 1990). Depending on the attraction forces it is possible to find agglomerates in these kind of mixtures (Muzzio et al., 2004).

Random mixture (Figure 2-2b): this is the case for real mixtures, where the particles tend to show some heterogeneity, where the probability of a particle position is independent of the neighboring particles (Muzzio et al., 2004).

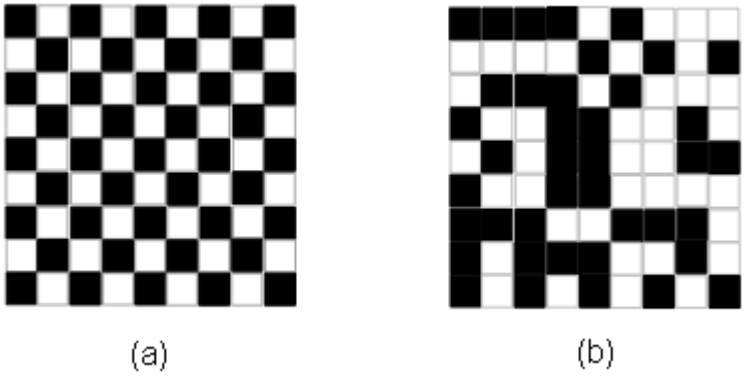

Figure 2-2 Types of blends (a) ordered mixture and (b) random mixture (Hersey, 1974).

In order to ensure safety and efficacy of the final product, the API needs to be uniformly distributed in the blend. The scale to which it needs to be homogeneously mixed is called scale of scrutiny. The scale of scrutiny of a product corresponds to the final unit dose in which the product will be commercialized, i.e. one tablet or one capsule (Train, 1959).

Some of the reasons for determining the degree of mixing are: for monitoring a blending process, for indicating the blend-end point, for evaluating the mixer efficiency, for determining the blending time required, and for establishing if the process critical attributes (e.g. API level) are under control (Twitchell, 2007).

It is important to bear in mind that there will always be some variation in composition from samples taken from a random mix. Thus, the objective is to keep these variations within acceptable limits (Twitchell, 2007). The EMEA (1996) mentioned that the acceptance limits should be within 95-105% of the nominal value for the active ingredients. The FDA (2003) established the acceptance criteria limits for a blend uniformity process (see Figure 2-3) to be between 90-110% of the label claim for the active ingredient as the acceptance criteria.

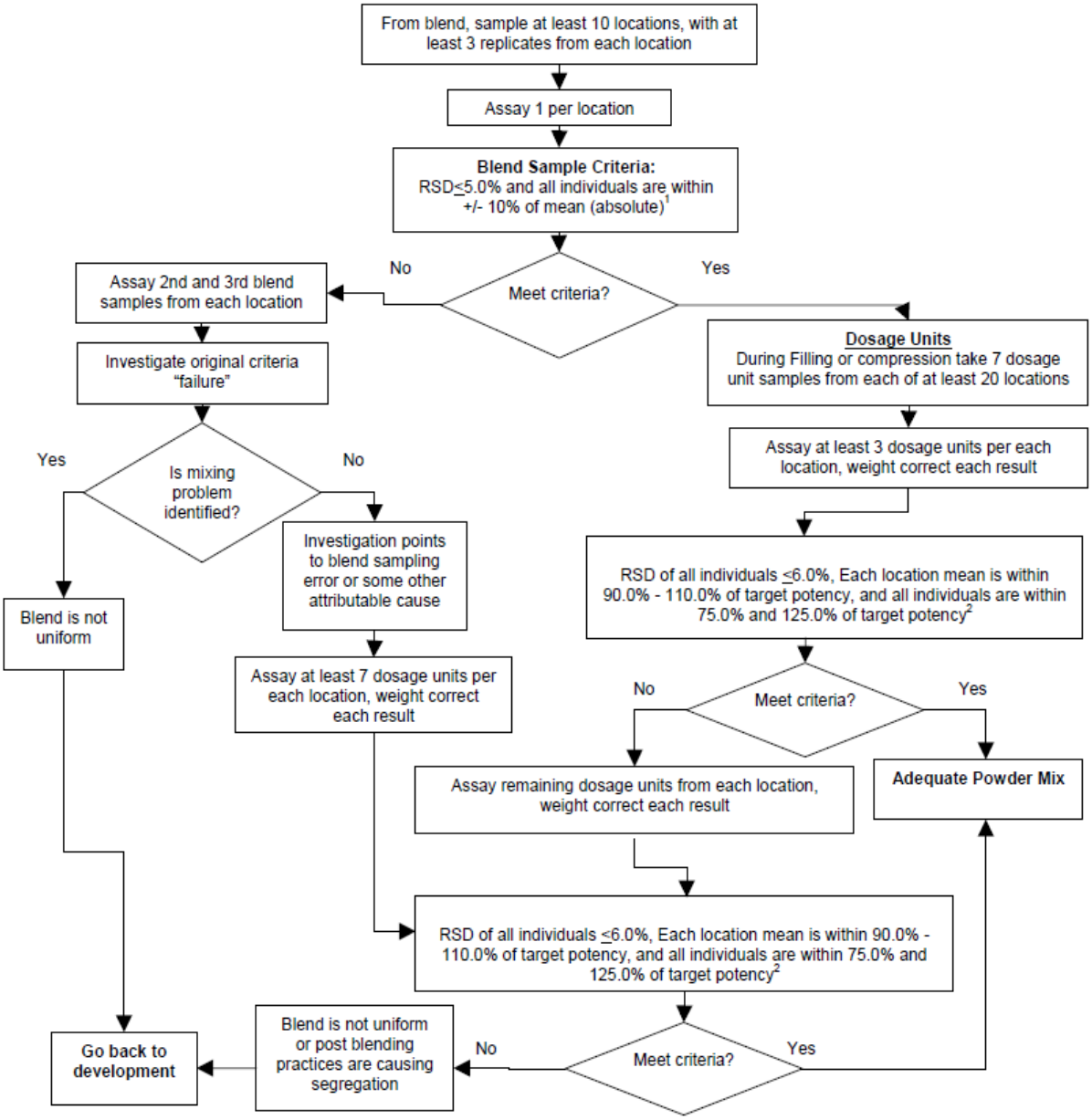

[1] Examples of "mean +/- 10% (absolute)" are: If the mean strength = 95%, then the interval is 95% +/- 10%; thus, all individuals must fall within 85.0% to 105.0%. If the mean strength = 103.0%, then the interval is 103.0% +/- 10.0%; thus all individuals must fall within 93.0% to 113.0%.

[2] When comparing individual dosage units to 75.0% - 125.0% of target strength, use the *as is* results (not corrected for weight).

Figure 2-3 Guidance for Industry for Powder Blends and Finished Dosage Units (FDA, 2003).

The homogeneity or the degree of mixing is often determined by a mixing index. Most of the mixing indexes are founded on variance-based statistics of the component of interest; the reader is referred to the following reviews which cover numerous mathematical models for the computation of the degree of mixing (Bridgwater, 2012; Fan et al., 1970). One common and widely used mixing index is the Relative Standard Deviation (RSD), given in Equation 2-1:

Equation 2-1

$$\%\boldsymbol{RSD} = \mathbf{100} * \frac{\sqrt{\sum_{i=1}^{n} \frac{(X_i - \bar{X})^2}{n-1}}}{\bar{X}} = \mathbf{100} * \frac{\sigma}{\bar{X}}$$

where $\boldsymbol{X_i}$ is the API concentration in the sample at time point t_i, n is the total number of samples, $\bar{\boldsymbol{X}}$ is the average of the concentration and σ is the standard deviation of the concentration. The lower RSD indicates less variability of the samples thus higher homogeneity. As a blend uniformity criteria, the FDA (2003) established the RSD limit to be 5% (see Figure 2-3).

2.2 Impact variables on solids mixing

Pharmaceutical powders can be very diverse in their physical and chemical nature. The powders may come from a milling process after crystallization of the main active ingredient. Under these conditions the API may be cohesive and with bad flow behavior; an alternative is that the API was further processed through an agglomeration technique (such as granulation) resulting in bigger particles with improved flow behavior and lower cohesion. Therefore, the API can vary in mean particle size, particle shape, particle size distribution, porosity, density, flow character, etc. Moreover, the API will be blended with other components, either excipients or other APIs, which also possess their own physical characteristics. Thus, it is well known that the blending performance is largely dependent on the physical characteristics of the materials (Bellamy et al., 2008; Chaudhuri et al., 2006; Venables and Wells, 2001; Virtanen et al., 2007) and the process conditions (Sudah, et al., 2002). This is exemplified by a fishbone diagram in Figure 2-4. It is clear that the assessment of a good blend quality requires a good understanding of the variables that can have a strong impact on the powder blend. This thesis is focused on the study of different mixing modalities, such as batch and continuous mixing, which differ on feeding techniques, mixing times, mixer geometry, blending speed, sampling rate, etc. Additionally the influence that different particle size distributions and agglomeration (by hot-melt granulation) exerted on the final blend was of primary interest.

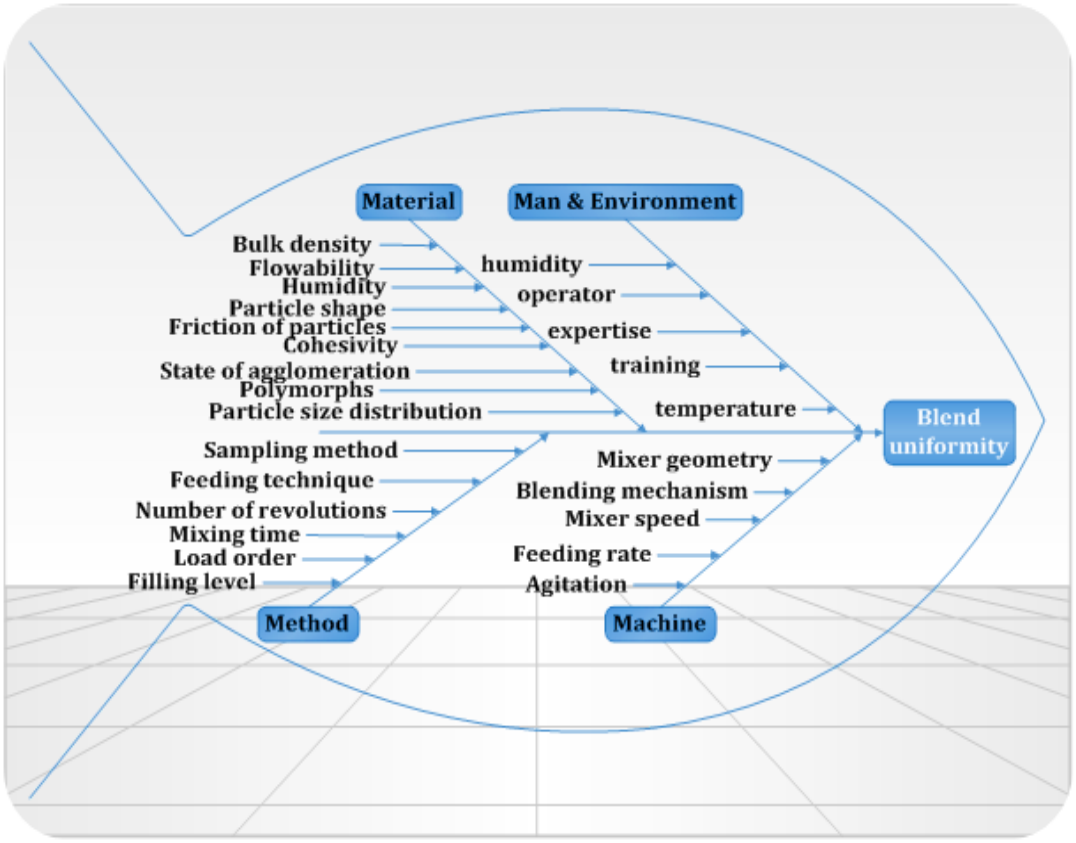

Figure 2-4 Fish-bone diagram for blend uniformity.

Segregation

In practice, segregation or demixing is a potential issue that will have a direct influence on the content uniformity of the final product. The mechanisms of segregation include (Figure 2-5):

- Percolation: This mechanism refers to the movement of the small particles through the voids in the powder bed. This is considered the main mechanism of segregation for non-aerated blends. Percolation can appear due to differences in size and density between the formulation components.
- Trajectory segregation during a free fall: Particles under motion possess kinetic energy. This may result in preferential separation
- Densification: density differences of the formulation components can cause large particles to move to the surface of the powder bed while smaller particles move to the

bottom. Vibration during handling, transportation, or tableting can induce densification (Aiache and Beyssac, 2007).

- Elutriation: This mechanism occurs in upwards flow, e.g. fluidized beds. Elutriation can also occur in pipelines in combination with trajectory segregation.

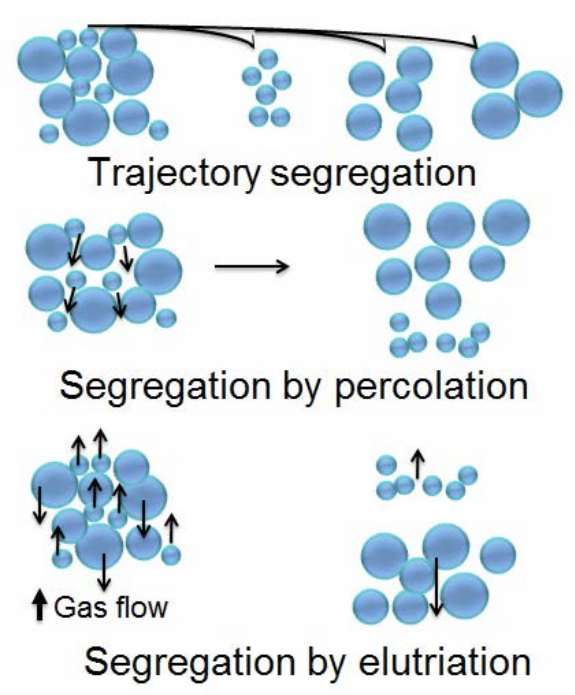

Figure 2-5 Mechanisms of segregation.

It is recommended to choose particles with similar characteristics, such as particle size and density, to avoid segregation (Williams, 1972). Angle of repose, coefficient of friction, and flow behavior are closely related. Particulate material holding small repose angles, good flow behavior, and small coefficient of friction may cause mixing problems, since segregation can occur due to their rapid movement (Fan et al., 1970). Segregation can also occur when the mixer is emptied, during transportation and storage, and, in general, wrong handling procedures can induce powder segregation.

2.3 Batch mixing equipment

The pharmaceutical industry has been batchwise driven. The two most common types of blenders are tumbling and convective blenders. Tumbling mixers are a container or vessel

that is rotated. Examples of these blenders (see Figure 2-6) are the cylindrical drum, double cone, off-center cone, V-mixer, tote mixer, and bin mixer. One tumbling mixer that is used in production areas is the bin blender, also known as an intermediate bulk container (IBC). These blenders are designed as storage vessels which are loaded with the formulation components, mounted into the axis and then rotated. The functionality is similar to the double cone mixer (Sudah et al., 2002). The bin blender has the advantage that the bin containing the final blend can be transported to the next production area (e.g. compaction room) and the powder can be discharged directly into the hopper of the tableting machine. Additionally, the contact of the operator to the blend is reduced.

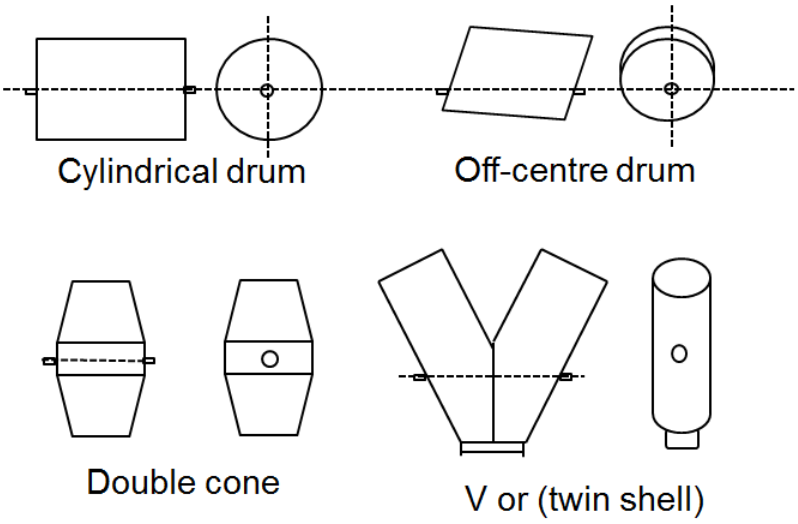

Figure 2-6 Tumbling mixers (Bridgwater, 2012).

The second class of blenders is the convective mixers. These mixers have a stirring device such as paddles or impellers. Some examples are the centrifugal mixer, ribbon mixer, planetary mixer, and orbiting screw mixer (Nauta mixer). Many convective mixers can be adjusted for continuous processing of material (Bridgwater, 2012; Muzzio et al., 2004).

2.4 Continuous mixing

The aim of continuous mixing is to continuously feed and blend the ingredients in a single pass so that the resulting blend is ready for the next unit operation (Manjunath et al, 2004; Weinekötter and Gericke, 2006). The advantages of a continuous blender are listed below

(Manjunath et al, 2004; Pernenkil and Cooney, 2006; Pernenkil, 2008; Weinekötter and Gericke, 2006; Williams and Rahman, 1970):

- Reduction of intermediate handling and segregation: connecting the continuous mixer to the previous and next unit operation is of great industrial value, since segregation of the powder blend may occur during the handling of the final blend. The vibrations during the transportation of the container from one production area to another as well as the storage of the blend can produce different degrees of segregation.
- Continuity of production: the product availability is faster compared to a batchwise process.
- High production capacity: continuous blenders can produce larger quantities of a powder mixture compared to batch mixers.
- Better dispersion of minor components: the ingredients can be mixed more efficiently due to the intense mixing.
- Better blend quality: the presence of axial and radial mixing together with better dispersion of the minor components lead to a better mixed product.
- Residence time: is a critical parameter which refers to the time that the powder stays inside the blender.

Low hold-up: this is achieved due to lower residence times inside the blender compared to batch mixing. Reduction of storage space: this is only feasible when the blender is connected to the previous or next processing step.

- Automatic control: allows for the correct monitoring of the process parameters, such as stirring rate, mass flow rate, feeding rate of each ingredient.
- Easier scale-up: can be achieved by extension of the blender total runtime.
- Faster product availability by using a PAT tool: real-time monitoring of the process would provide a valuable way of measuring the API level as a quality attribute. Additionally, the product would already be tested once it arrives at the next unit operation.

- Reduce the analytical time and sampling: this can be achieved with a non-invasive spectroscopic technique such as NIR, so the requirements of reagents and off-line analytical tests are skipped.
- Lower production and analytical costs: the continuous production combined with a suitable PAT tool can dramatically reduce the amount of off-line tests and production costs, although the continuous blender, feeding system, PAT equipment, and automation costs can be higher than in a batch system.
- Less labor work: minimum operator work is needed since filling and emptying is done automatically and sampling can be avoided.

Continuous blending also holds some disadvantages. Usually the continuous blender is product-specific and switching to another product is not a simple process. Also, the breakdown of the equipment or the malfunctioning of the feeding system can stop the production chain. In the pharmaceutical industry, the definition of a batch in a continuous process needs to be clearly specified. The feeding system needs to be accurate and reliable. Calibration of the equipment, mostly of the feeding system, requires careful and narrow ranges. Cohesive powders can be challenging for the feeding system. If the removal of samples is required, it must be done with a good sampling procedure in order to avoid biased and misleading results. If the control technique includes a MVDA method, this needs to be reliable and accurate as well. The automation system has to react quickly to any process deviations.

Continuous blending characterization

The continuous blender has to homogenize the material in the radial and axial directions. Radial means lateral to the direction of the material conveyance into the mixer and axial is in the direction of the material's conveyance (Figure 2-7). Radial mixing can be achieved by paddles and axial mixing and back mixing can dampen the effect of feed fluctuations (Manjunath et al, 2004; Weinekötter and Gericke, 2006; Williams and Rahman, 1970). Axial

mixing will dampen the variability introduced by the feeders, while shear forces and radial mixing will homogenize the original components.

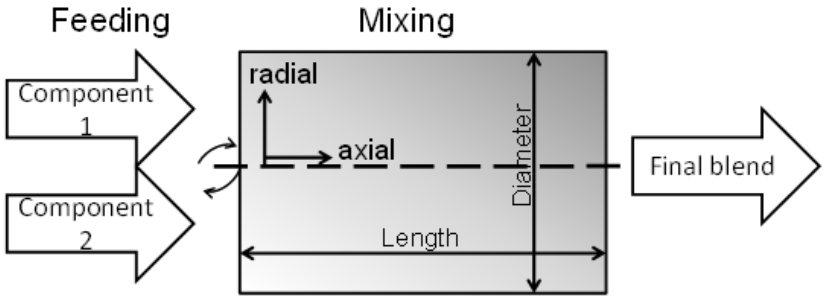

Figure 2-7 Continuous mixing of two components (Weinekötter and Gericke, 2006).

Williams and Rahman (1970) gave a list of physical parameters that can be used to characterize a continuous blender. These measurements include average rate of flow and hold-up. Average flow rate is the amount of outflow during the run, divided by the total time. Hold-up is the mass contained inside the blender once it has reached the steady state. These are important since they can be used to determine the average residence time and the strain underwent by the powder (Vanarase and Muzzio, 2011).

Residence time distribution (RTD) indicates the time that the powders stay inside the blender. This value can be measured by injecting a tracer into the blender and measuring the time that it takes to leave the blender. A broad RTD indicates extensive axial mixing. On the other hand, RTD does not indicate the rate of shear or radial mixing applied to the powder bed (Portillo et al. 2009; Weinekötter and Gericke, 2006). The RTD,$E(t)$, is defined mathematically by Equation 2-2. Gao et al. (2011) and Vanarase and Muzzio (2011) used a pulse-test and monitored the tracer concentration, $c(t)$ for the determination of RTD. The tracer concentration was measured by retrieving samples from the outlet of the blender and performing off-line measurements.

Equation 2-2 $$\boldsymbol{E(t) = \frac{c(t)}{\int_0^\infty c(t)dt}}$$

Danckwerts (1953) proposed the variance reduction ratio (VRR) as an option for the evaluation of blender efficiency. The VRR is the ratio between the variances at the inlet (σ^2_{inlet}) and outlet (σ^2_{outlet}) of the mixer, see Equation 2-3. The VRR can be quantified experimentally by measuring a determined signal (spectroscopic methods) at the inlet and comparing it with the signal of the outlet. A good mixer will have a high VRR. A low σ^2_{outlet} VRR as well as the RTD give an insight into the performance of the blender and the blend quality. Conversely, in the pharmaceutical industry the acceptance criteria for determining the quality of the blend are given only by the RSD of the active ingredient (see Figure 2-3).

Equation 2-3 $$\boldsymbol{VRR = \frac{\sigma^2_{inlet}}{\sigma^2_{outlet}}}$$

Operating variables that influence the quality of the final blend are: the inclination of the blender, the rotation speed, the length-diameter ratio of the blender, the number of paddles, paddle inclination, filling level, and size of the inlets and outlets. The feeders are also critical for achieving optimum blend quality.

In order to improve the quality of the final blend, a better understanding of the operating conditions is needed. Portillo et al. (2008, 2009) showed how the powder residence time and API concentration are highly influenced by the rotation rate, mixing angle and cohesion. Rotation rate influences the rate of shear, axial mixing, mean residence time, the intensity of the material dispersion, and the number of blade passes. All these factors will determine the API homogeneity in the blend. Cohesion can also influence the blending performance by affecting the flow rate in the feeding system.

Feeding and weighing equipment

A continuous blender consists of a feeding system with a feeder unit, a measurement section, and a control system. The ingredients can be fed gravimetrically or volumetrically. Volumetric feeding is used for liquids or uniform solids in which bulk density does not fluctuate. Gravimetric feeders are more accurate and are recommended for cohesive powders as well as for materials with bulk density fluctuations. In this study we used loss-in-

weight feeders, which are a type of gravimetric feeder. The general mechanism consists of a feeder unit with a hopper placed over the weighing system. A load cell in the feeding system measures the weight at regular time intervals and the weight loss per unit time corresponding to the actual feed rate. The actual feed rate is compared with the set point and the feeder adjusts the flow in order to equal the set point (Weinekötter and Gericke, 2006).

Accurate performance of the feeding system is essential in a continuous blending process. Figure 2-8 shows the curve of the mass flow ($\dot{m}$) over time (t). At the beginning of the production the mass flow ($\dot{m}_1$) is in the proximity of the set point and by the end of the process, the mass flow ($\dot{m}_2$) deviation from the set point is greater. This situation can appear when the bulk density changes over time thereby influencing the volumetric feeding.

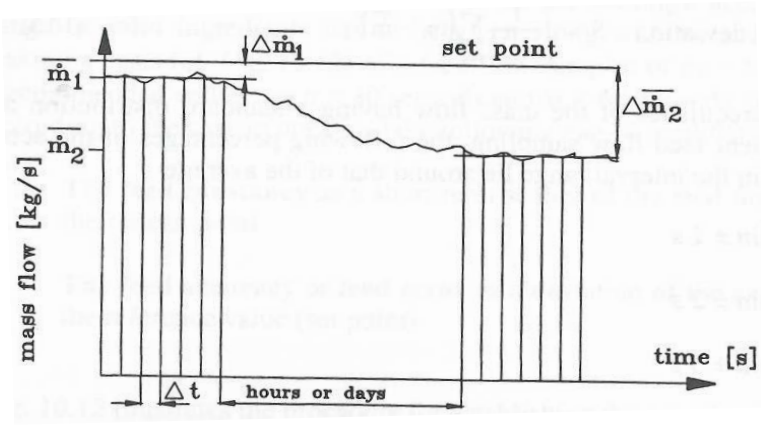

Figure 2-8 Drift in a continuous feeding system (Weinekötter and Gericke, 2006).

2.5 Sampling

Sampling of static powder

The main goal of sampling is to collect an amount of powder that is representative of the batch. The most frequently used method for determining the performance of a mixer is by withdrawing samples and then using the variance of the concentration of these samples as a measure of mixture quality (Cooke et al., 1976).

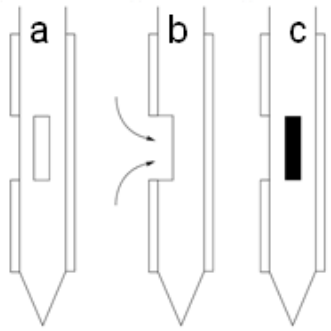

Figure 2-9 Side-sampling thief (a) close position, (b) open position, and (c) close position with a sample inside (Brittain, 2002).

One common technique for sampling a batch blending process is by inserting a probe, known as a thief sampler (Figure 2-9). A thief sampler consists of two concentric tubes, where the outer tube is pointed and contains holes in selected positions. The holes are opened or closed in order to capture material. Important parameters that need to be considered are sample size, number of samples and location of sampling points. The selection of sampling locations and sampling number can be done by following the existing guidelines. The thief sampling technique suffers from two main disadvantages: the samples withdrawn can be heavily contaminated from neighbor particles, and the thief can also have preferential retention of particles (Harnby, 1997). Thief sampling can disrupt the powder bed causing systematic errors (Muzzio et al., 1997; Schofield, 1976) as shown in Figure 2-10. Figure 2-10a shows the side-sampling thief which relies on free particle flow; thus the particles with easier mobility and better flow behavior can be overrepresented on the final sample. Figure 2-10b corresponds to an end-sampling thief. In this probe particles are forced into the cavity but can substantially disrupt the blend (Muzzio et al., 2004).

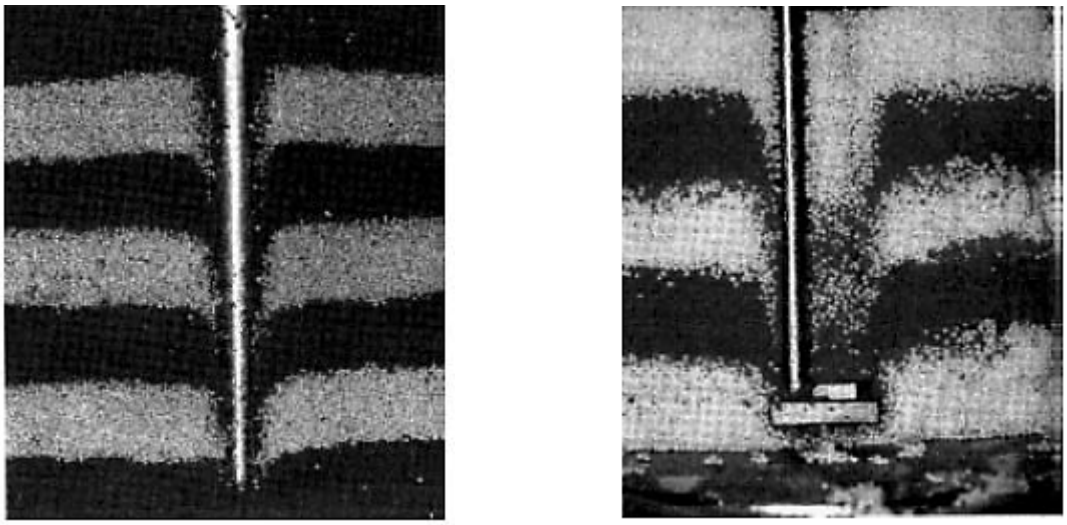

(a) (b)

Figure 2-10 (a) error introduced by a side-sampling thief and by an (b) end-sampling thief. Layer configuration of small (dark) and large (light) particles (Muzzio, 2004).

As Hersey (1975) mentioned, all sampling operations can lead to some degree of segregation. The number of samples is important and the more samples taken, the smaller the error.

Here are three sampling recommendations (Allen, 2003; Harnby, 1997):

- The powder should be sampled while in motion
- Sample frequently and avoid a sample frequency that coincides with a process cycle
- Sample the entire section of the powder stream

It is clear that thief sampling does not follow all these recommendations since the blender needs to be stopped in order to collect the samples from the static powders and from selected regions. Testing the homogeneity of a blend is a challenging task that can suffer from inconsistencies due to bad sampling techniques, thus causing confusion on whether the batch is inhomogeneous or if the results are biased due to incorrect sampling. Here is where NIR found a generous field for improving the process analytics.

Sampling in powder streams

One of the golden rules of sampling is to take the sample while the powder is in motion. This can be achieved easily in continuous processes. When sampling falling powders, special care must be used when introducing and removing the sampler. In addition, the entire stream needs to be considered rather than only the central or peripheral parts. Figure 2-11b shows correct stream sampling, in which the removal of the sample needs to be in the same direction upon insertion and removal in order to avoid segregation and selective particle sampling. Figure 2-11a shows an incorrect way of sampling which lead to an excess of bigger particles since the surface of the powder bed is sampled for a longer period of time than the rest of the stream. The surface of the powder bed could contain higher amounts of coarse particles compared to the lower region, thus leading to unwanted selective particle size sampling. The best sampling method is shown in Figure 2-11c where the sample is collected through the entire sample stream (Allen, 2003). Meyer (2008) developed a device for sampling a powder stream, in which consisted of a sampling train connected to a motor. The speed of the motor was adjusted according to the flowability of the powder blend together with the desired sampled mass. This example proved the feasibility of sampling while in motion together with a frequent sampling corresponding to the mixing process cycle.

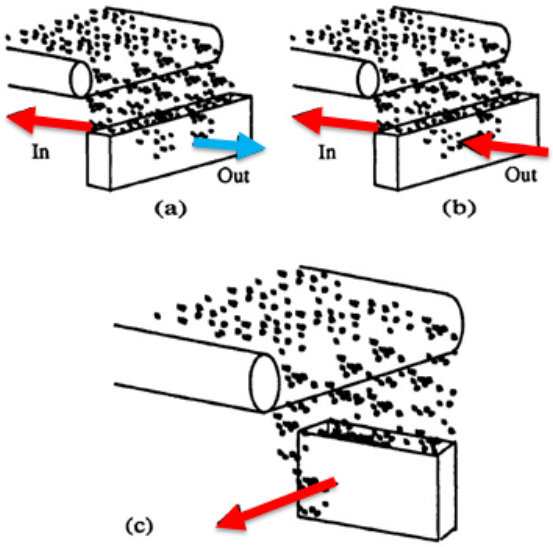

Figure 2-11 Sampling from falling streams. (a) bad sampling technique, (b) good sampling technique, (c) sampling procedure adopted for high mass flow rate (Allen, 2003).

Several sampling techniques are available for sampling under powder motion (see Figure 2-12a-d), such as sample strippers, pendulum samplers, chute sampler splitters, and spin riffling, among others. The selection of the best sampling method needs to be evaluated according to the process needs, space availability, and further analytical tests.

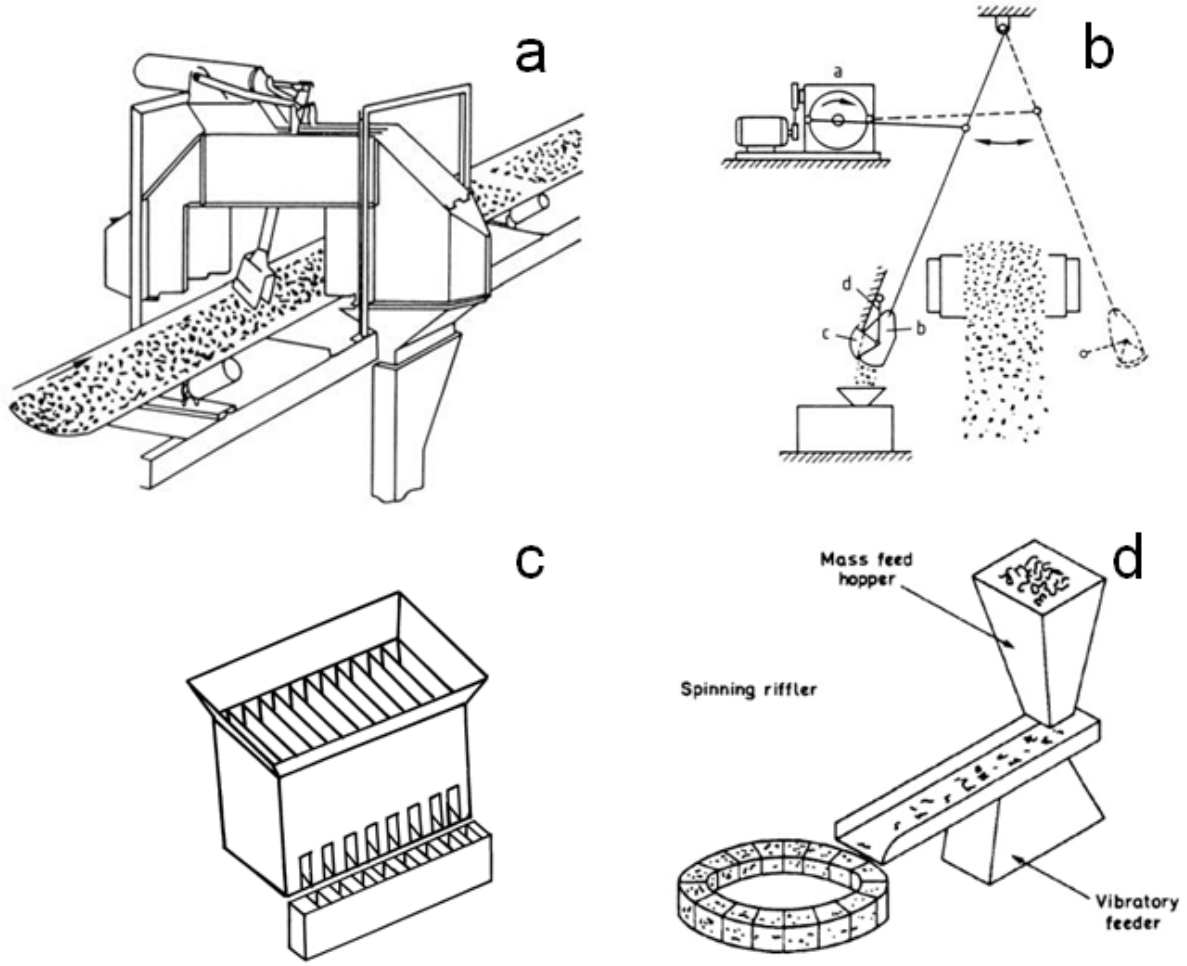

Figure 2-12 sampling under dynamic conditions, (a) sample stripper, (b) pendulum sampler, (c) chute sample splitter, and (d) spinning riffler (Allen, 2003; Brittain, 2002; Sommer, 2012).

Sampling error

The total variance measured on a sample is given by Equation 2-4. The measured variance is the combination of the variance from the sampling, the variance related to the homogeneity of the blend and the contributed variance from the analytical method (Manjunath et al., 2004).

Equation 2-4 $$\sigma^2_{measured} = \sigma^2_{mixture} + \sigma^2_{sampling} + \sigma^2_{analytical}$$

The sampling uncertainties as well as the analytical variance are required values in order to assess the homogeneity of the blend. In an ideal situation the errors due to sampling and analytical method should be negligible; hence the measured variance will be equivalent to the variance of the process. On the other hand, sampling error should never be underestimated, since the physical removal of powder (in a batch or in a continuous process) can lead to serious misleading results if the sampling is performed incorrectly or if the wrong sampling technique is chosen. Muzzio et al. (1997) quantified the maximum sampling error for three different thief samplers: side-sampling thief (Globe Pharma Thief) can reach 100%, slug sampler (end-sampling thief) as much as 30%, and Rutgers (end-sampling thief) up to 20%.

In order to avoid physical sampling methods and also to increase the sampling rate, non-invasive techniques are on the scope of the industries that deal with particulate materials. One analytical tool that is non-invasive and has shown great potential for blend uniformity is near infrared spectroscopy (See section 2.9 Near Infrared Spectroscopy). Using NIR will eliminate the term $\sigma^2_{sampling}$ from Equation 2-4, thus the sample variance will be ruled by the variance of the mixing process as well as the uncertainty belonging to the NIR-MVDA method.

2.6 Melt Granulation

Granulation is a common pharmaceutical unit operation. During the granulation process the primary powder particles adhere to form larger entities called granules. Some of the reasons for performing a granulation step are (Kristensen and Schaefer, 1987; Summers and Aulton, 2007):

- To improve the flow properties by reducing cohesion, increasing particle size, and generating isodiametric granules.

- To improve compaction by better distributing the binder, thus helping the bond formation.
- To improve the blending by reducing segregation due to particle differences, although problems due to segregation and percolation may appear if there is a pronounced difference between the size of the granules and the other formulation.
- To improve the die filling.
- To reduce dust
- To modify the appearance
- To improve stability during storage, reducing the cake formation.
- To modify or control the dissolution of the API.

Granulation can be divided in wet or dry granulation. Wet granulation includes the addition of a liquid containing a binder. Dry granulation involves high pressures in order to compact the original powders. The resulting product undergoes milling and sieving processes for controlling the final particle size. Table 2-1 lists dry and wet granulation methods with their further preprocessing.

Table 2-1 Granulation techniques (Parikh, 2005).

	Process	**Further processing**
Dry granulation	Direct compression	Blending
	Slugging	Milling-Blending
	Roller compaction	Milling-Blending
Wet granulation	Low-shear mixer	Drying-Milling-Blending
	High-shear mixer	Drying-Milling-Blending
	Fluidized bed	Drying-Milling-Blending
	Extrusion/ spheronization	Drying-Milling-Blending
	Spray-dryer	Sieving-Blending
	Continuous mixer granulator	Milling-Blending
	Continuous fluid-bed granulator	Milling-Blending

This study is focused on a special granulation technique named melt-granulation, which in some aspects follows similar principles as wet granulation; the main difference is that it uses a molten binder as a granulation fluid. Some of the advantages of melt granulation over wet granulation are (Vervaet and Remon, 2009):

- No need of solvents, thus the drying step is eliminated, reducing the process time and energy requirements.
- Moisture-sensitive materials can be agglomerated, although it is not suitable for thermo-sensitive APIs that can suffer thermal degradation.

Melt granulation involves the melting of the binder which will produce the particle agglomeration and consolidation, followed by a cooling step. Successively the resulting product undergoes a milling step. All the steps for melt granulation can be performed in sequence.

The binder for a melt-granulation process can be hydrophilic or lipophilic. Hydrophilic binders will lead to immediate release while lipophilic binders can produce sustained-release forms (Zhang and Schwartz, 2003).

Melt granulation can be performed in high shear mixers (Schaefer et al., 1992) and in fluidized bed granulators (Abberger et al., 2002), hence the granules production was batch wise. One manufacture alternative is to use an extruder as a granulator; in this manner melt granulation can be performed as a continuous unit operation. Van Melkebeke et al. (2006) successfully used a twin-screw extruder for preparing melt granules of an immediate release formulation.

The selection of a suitable technology for each unit operation (e.g. granulation) can improve the quality and performance of the final product; it can also reduce the manufacturing time and material and manpower. Melt granulation used in a continuous modality can be linked to the previous and following steps, thus reducing the material handling and product storage. In

addition, a correct in-line process control can reduce the analytical time and characterization of the granules.

2.7 Continuous manufacturing in pharmaceutics

Continuous manufacturing is attracting interest and investment from the pharmaceutical industry due to two main reasons: cost reduction and quality improvement.

Pharmaceutical manufacture of solid dosage forms often contains continuous processing steps; some examples for drying, granulation, and blending are given on Table 2-2.

Table 2-2 Continuous processes in pharmaceutical manufacture.

Unit operation	Use	Reference
Granulation	Continuous granulation (Review)	Vervaet and Remon, 2005.
	Roller compaction	Kleinebudde, 2004.
	Melt granulation in twin-screw extruders	Djuric et al., 2009, Djuric and Kleinebudde, 2010.
	Melt Extrusion	Gamlen and Eardley, 1986.
	Cold extrusion	Keleb et al., 2001.
	High-shear mixer (quasicontinuous)	Betz et al., 2003.
	Twin-screw high-shear granulator	Fonteyne et al., 2012; Vercruysse et al., 2012.
Drying	Fluidized bed drying	Betz et al., 2003; Burgschweiger and Tsotsas, 2002.
	Spray drying	Gonissen et al., 2008.
Blending	Continuous blending, convective mixers	Pernenkil and Cooney, 2006; Portillo et al., 2008.

Schaber et al. (2011) studied the implementation of an integrated continuous production of tablets and a process that can work for 335 working days per year, with 30 days for cleaning, maintenance, start-up and shut down. This effective working time in a continuous modality is higher than in batch modality, since batch manufacture needs more time for filling, emptying, cleaning, and transport from one process area to the next one. Schaber et al. (2011) estimated an overall cost savings of 9 to 40%, depending on the technology and reagents

selected for the manufacture. On the other hand, this estimation did not include the expenses associated with the analytical methods used. These savings could increase further by having an efficient, reliable and non-invasive in-process control.

The continuous manufacture of a product requires a robust process that can soften raw material variability since the quality in the product must be constant (Remon and Vervaet, 2007). Continuous manufacturing already takes place in the Merck facility in Elkton, Virginia (see Figure 2-13). In this process the operators load the material in the bulk unit load container and this is the only interaction that they have with the process. The correct implementation of a continuous process requires automation and a well-understood process. The transfer of the powder and the feeding into the next unit operation need to be mass controlled and discharged in the correct weight proportions.

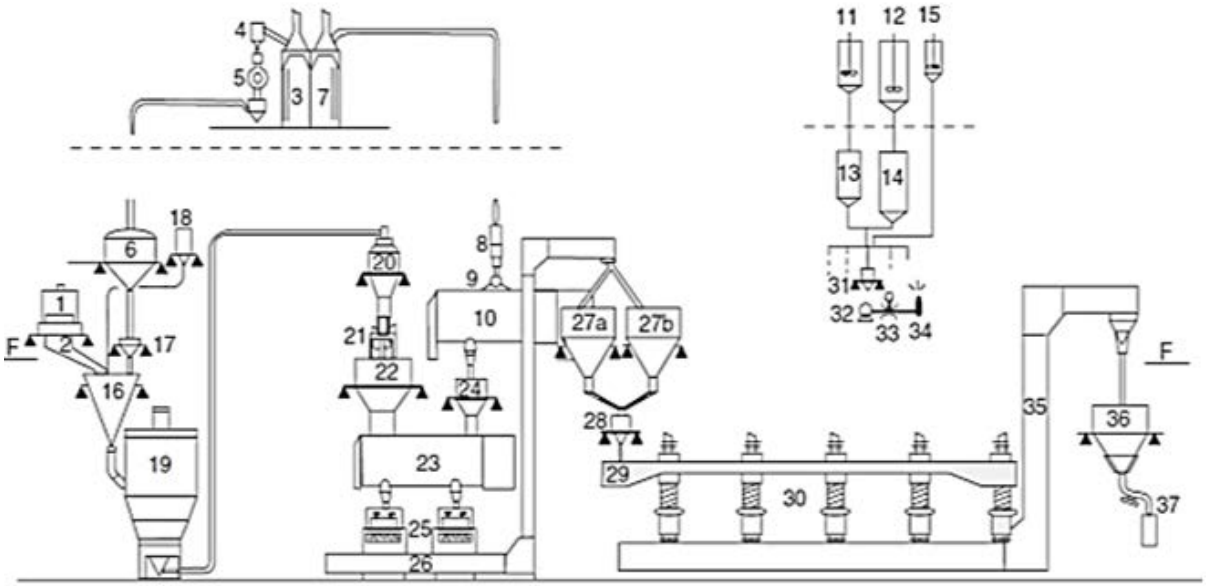

Figure 2-13 Flow diagram of the continuous production line of Merck. (1) Bulk unit load container; (2) weigh‑discharge unit; (3) ethylcellulose hood; (4) Vac-U-Max (ethylcellulose); (5) rotary sifter; (6) bulk ethylcellulose hopper; (7) adds materials hood; (8) Vac-U-Max; (9) rotary sifter; (10) adds ribbon blender; (11) clear-coat make-up tank; (12) color-coat make-up tank; (13) clear-coat use tank; (14) color-coat use tank; (15) purge solvent tank; (16) Nauta mixer; (17) ethylcellulose dosing hopper; (18) alcohol dosing tank; (19) fluid bed dryer; (20) mill feed hopper; (21) Fitzmill; (22) bulk granule hopper; (23) lubrication ribbon blender; (24) adds dosing hopper; (25) Manesty Mark III; (26) bucket conveyor; (27) bulk tablet hoppers; (28) tablet dosing hopper; (29) ploughed conveyor; (30) 18-in. coating columns; (31) coating dosing hoppers; (32) Nordson pump; (33) thermal mass flow meter; (34) spray system nozzle; (35) bucket conveyor; (36) coated tablet hopper‑dryer; (37) conveyor (Remon and Vervaet, 2007).

2.8 PAT

The process analytical technology (PAT) initiative launched by the FDA (2004) is defined as "*a system for designing, analyzing and controlling manufacture processes with the goal of ensuring final product quality*". A key point of PAT is: "*quality cannot be tested into products; it should be built-in or should be by design*". The PAT initiative has encouraged the pharmaceutical industry to increase its research into new analytical technologies, which enable the measurement or monitoring of critical process parameters. These technologies can be used to control and understand the manufacturing process and ensure improved product quality. Near-infrared (NIR) spectroscopy is one of the techniques found to be appropriate for a variety of PAT applications, and is the subject of many studies in the pharmaceutical field. Major advantages of NIR spectroscopy are its non-destructive nature and its immediate delivery of results.

There are primarily three types of process measurements:

- At-line: Measurement where the sample is removed, isolated from, and analyzed in close proximity to the process stream.
- On-line: Measurement where the sample is diverted from the manufacturing process, and may be returned to the process stream.
- In-line: Measurement where the sample is not removed from the process stream and can be invasive or non-invasive.

2.9 Near Infrared Spectroscopy

Historical development

The study of light has been of high interest for scientists. The interaction of light with matter, the physical definition and composition of light, and its analytical applications have been widely studied. In 1800 Herschel published the first reference to near infrared radiation. Herschel was an astronomer who fabricated telescopes, and he was interested in knowing

which chromatic component of light was responsible for heat. He dispersed the sun rays into colors and measured the temperature of each color. He found that there was an invisible light near the red color that was releasing most of the heat.

Coblentz (1908) studied the infrared reflection and transmission including the “extreme infrared”. The spectrometer that Coblentz used consisted of a wire grating made of copper wires, a mirror galvanometer, a thermophile, and a prism. He measured the infrared spectra for several substances and all gave unique spectra.

NIR region was not considered attractive for analytical purposes, due to the overlapping peaks and weak intensity. Contrarily, weak NIR intensities were considered a drawback in the past whereas nowadays it is a valuable advantage for process monitoring.

The fast development of the computer and important scientific developments such as the Kubelka-Munk theory with the possibility to measure solids, as well as Hotellings and Mahalanobis mathematical approaches were key events for the further implementation of NIR (Hindle, 2001). Multivariate data analysis, powerful software, and fast instrumentation development facilitated the fast evolution of NIR technology. As a result, NIR is continuously gaining more acceptance as an analytical technique in many sectors, including the pharmaceutical industry.

Basic concepts

Electromagnetic radiation can be considered as a stream of photons traveling at the speed of light. The energy of a photon (E) is related to the wavelength (λ), frequency (ν), and speed of light (c) by Equation 2-5, where h is Planck’s constant (Hof, 2003).

Equation 2-5 $$\boldsymbol{E = h\nu = hc/\lambda}$$

In spectroscopy, the interaction of light with matter (molecules) involves energy transfer. The energy absorbed by the molecule is specific to the frequency of the radiation and can cause reorientation of nuclear or electron spin states, changes in the energy of valence electrons,

changes in vibrational –rotational energy, and ejection of inner electrons, among others. Vibrational spectroscopy, such as IR, is based on the interaction of light with molecules which molecular bonds will vibrate at characteristic frequencies. Molecules that exhibit a dipole moment will absorb in the infrared radiation. The intensity of the vibrational absorption is proportional to the square of the dipole moment change (Duerst, 2007). Another name for the dipole model is ideal harmonic oscillator; the frequency at which the ideal harmonic oscillator vibrates (stretches or bends) depends on the bond strength and the masses of the atoms. The total energy in the bond is proportional to the frequency of the vibration. According to the harmonic model the transitions between vibrational states can only occur from one level to the next (Workman and Burns, 2001). In the harmonic model, the potential energy curve is symmetric and the bonds displacement has a maximum dipole displacement (Figure 2-14B). According to the harmonic oscillator model, overtones and combinations are not allowed; nonetheless they appear due to anharmonicity.

The harmonic oscillator has limits and the anharmonic oscillator allows a more realistic description of the overtone transitions. The anharmonic oscillator considers that two atoms in close proximity repel one another, and also considers that the distance between the atoms is important and has limits in which the bond dissociates (Figure 2-14A). Thus the anharmonic model is more useful to predict the behavior of real molecules (Workman and Burns, 2001).

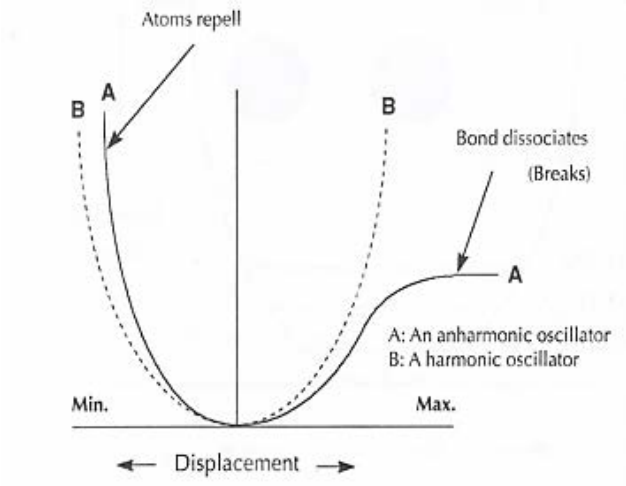

Figure 2-14 Potential energy curves for an anharmonic (A) and a (B) harmonic oscillators.

Vibrations in the near-infrared region consist of bending and stretching combinations and overtone bands. Stretching vibrations involve changes in the bond length and bending refers to a change in the bond angle between two atoms. Combination bands arise from the summation of fundamental bands. In Table 2-3 the wavelength regions for the IR are divided by the vibrational changes that can be observed, thus mid-infrared detects fundamental transitions and near-infrared overtones and combinations.

Table 2-3 Spectroscopic regions for IR.

Region	Wavelength (nm)	Wavenumber (cm^{-1})	Characteristics
Near-Infrared	700-2500	14,000-4000	First (2ν), second (3ν), third (4ν) overtones and combination bands
Mid-Infrared	2500-25000	4000-400	Fundamental (ν) vibrations: stretching, bending, wagging, and scissoring
Far-Infrared	25000-500000	400-20	Molecular rotation

Table 2-4 contains some functional groups associated with their characteristic wavelength region and the type of vibration observed. Most of the peaks in the NIR region derive from the X-H stretching modes because of energy considerations; the overtones are 10 to 1000 times weaker than the fundamental bands. This weak intensity was initially a drawback; nowadays it allows the measurement of concentrated samples and is therefore a valuable advantage for process analysis (Ciurczak, 2001).

Table 2-4 NIR absorption regions.

Group	Vibration ($\nu = stretching, \delta = bending$)	Wavenumber (cm^{-1})	Wavelength (nm)
Free OH	3 ν*	10400-10200	960-980
	2 ν	7140-7040	1400-1420
	Combination ν+2δ and 3δ	5210-5050	1920-1980
Bound OH	3 ν	10000-8850	1000-1130
C-H (CH_3, CH_2)	3 ν	8700-8200	1150-1220
	Combination 2 ν+2δ	7350-7200	1360-1390
	Combination 2 ν+δ	7090-6900	1410-1450
	Combination ν+δ	4440-4200	2250-2380

Group	Vibration ($\nu = stretching, \delta = bending$)	Wavenumber (cm^{-1})	Wavelength (nm)
CH_3 and CH_2	2 ν	6020-5550	1660-1800
Free NH	2 ν	6710-6500	1490-1540
Hydrogen bonded NH	2 ν	6620-6250	1510-1600
S-H	2 ν	5780-5710	1730-1750
C=O	3 ν	5230-5130	1910-1950

*ν= fundamental, 2ν= first overtone, 3ν= second overtone, and 4ν=third overtone.

Diffuse reflectance spectroscopy

The incident light coming from the spectrometer has an intensity of I_0. This light can be partially reflected (I_R), scattered (I_S), and absorbed (I_A) and the remaining light will be transmitted (I_T) as shown in Figure 2-15. The light intensities can be detected by selecting the position of the detector (Steiner, 2003).

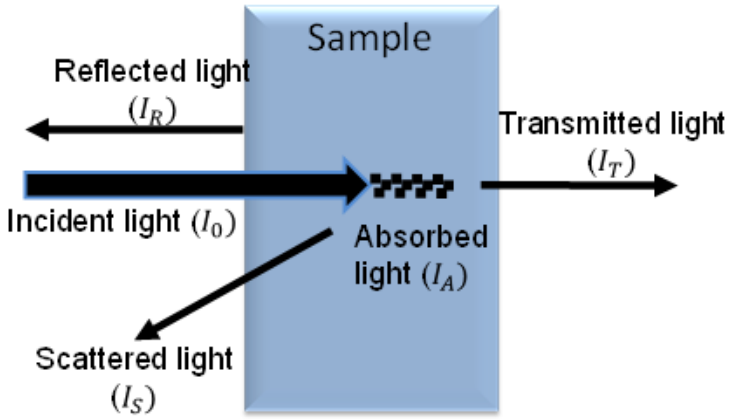

Figure 2-15 Energy balance of incident light.

Samples can be non-scattering or scattering. In a non-scattering sample, the absorbing power can be determined directly and it is not highly influenced by the sampling, and the contribution of a constituent to the total absorption is proportional to its concentration. In a particulate (scattering) material, such as powders, the determination of the absorption coefficients is complicated and the value is influenced by the properties of the sample e.g. size, porosity, shape, surface, etc. (Dahm and Dahm, 2007).

According to the sample surface, the light can be specularly reflected as in polished surfaces or diffused as in rough surface like in the powders. Many cases are the combination of

diffuse and specular reflection (Figure 2-16). Diffuse reflection considers the interaction of light with a sample, in which the incident light is partly absorbed and scattered.

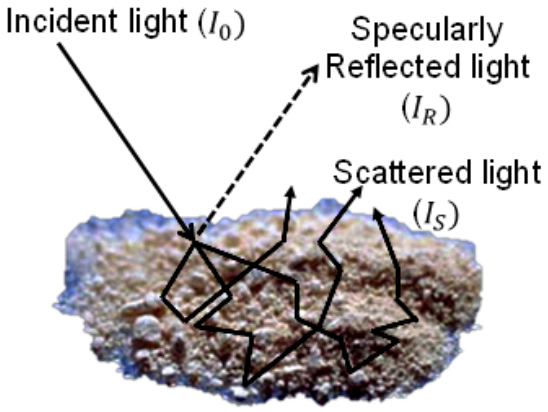

Figure 2-16 Incident light in a scattering sample (powder).

Near infrared spectra contain chemical information related to differences in bond strengths, chemical species, electronegativity, and hydrogen bonding. When NIR is used for solids measurements, information about scattering, diffuse reflectance, specular reflectance, surface gloss, refractive index and polarization are all superimposed on the NIR spectra (Workman and Burns, 2001).

The intensity of reflected energy depends on angle of incidence, particle packaging, density, particle size distribution, crystalline structure, refractive index, and absorptive and scattering properties (Workman and Burns, 2001).

Diffuse reflection theories

The case of specular reflection occurring in a smooth surface is well-described by the Fresnel law. On the other hand, there is not a general theory that completely covers diffuse reflection, but most of the proposed formulas include a version of the Lambert Cosine Law (Dahm and Dahm, 2007).

According to Lambert Cosine Law, the remitted radiation has constant intensity at all angles of observation. In Equation 2-6 the radiation strength (B) is given by the incident light (I_0) multiplied by the cosine of the angle of incidence (α) and the angle of observation (θ).

Equation 2-6 $$\boldsymbol{B = (I_0/\pi) cos\alpha cos\theta}$$

Lambert Cosine Law considers an ideal diffuse reflector that is not used in practice, and it applies only when both angles (α and θ) are very small (Ollinger et al., 2001).

Another scattering theory was proposed by Rayleigh. This theory deals with the scattering of particles that are smaller than the wavelength of incident radiation. Mie (1908) also investigated the scattering phenomena in particles of any size. Some generalizations of this model are that for very small particles the scatter is isotropic (gives similar results as Rayleigh). In the case of large particles the scatter is not isotropic while for particles in the same order of magnitude as the wavelength, significant diffraction ripples can be observed (Andrews, 1999; Dahm and Dahm, 2007; Ollinger et al., 2001).

A linear relationship for absorption and concentration is described by the Kubelka-Munk function, Equation 2-7.

Equation 2-7 $$\boldsymbol{f(R_\infty) = \frac{1-R_\infty}{2R_\infty} = \frac{k}{s}}$$

Where R_∞ is the reflectance of an infinitely thick sample (approx. 5mm or more), k and s describe the absorbing and scattering properties respectively. This empirical model assumes that s does not depend on the wavelength, scattering is isotropic, particles are smaller than the thickness of the sampled layer but larger than the wavelength of incident radiation, and scattering particles are distributed homogeneously over the entire sample. Because of the simplified solution of Equation 2-7 and it can be experimentally calculated, the Kubelka-Munk approximation is widely accepted (Heise, 2007; Ollinger et al., 2001; Steiner, 2003).

Dahm and Dahm (2007) proposed the representative layer theory which uses plane parallel mathematics and a two-flux approximation for describing the absorption-remission function expressed as fractions of incident light absorbed, remitted or transmitted.

NIR is applied for samples with high scattering where the ratio of particle size to wavelength is greater than one, and the particle packaging brings interferences between scattered rays. No general quantitative solution exists for multiple scattering (Ollinger et al., 2001), therefore the use of advance statistics such as chemometrics is needed. As Dahm and Dahm mentioned "*good statistics compensate for bad theory*" or, in other words, chemometrics find complex and particular relationships of the highly scattering samples that up to now cannot be fully quantified by a single theory.

Instrumentation

The fast growth of NIR in the analytical area has provided a wide range of spectrometers. According to their spectral characteristics, the spectrometers can be classified according to wavelength range, accuracy, precision, photometric accuracy, noise, bandwidth (resolution), baseline, scan speed, signal-to-noise, and scan modes (Shaw and Mantsch, 1999; Workman and Burns, 2001).

The basic configuration of a NIR reflectance spectrometer consists of a light source, a monochromator, a sample holder, and a detector, as shown in Figure 2-17. The most common light source used for NIR is the tungsten-halogen lamp due to its resistance, long life, and high energy delivery all over the NIR region.

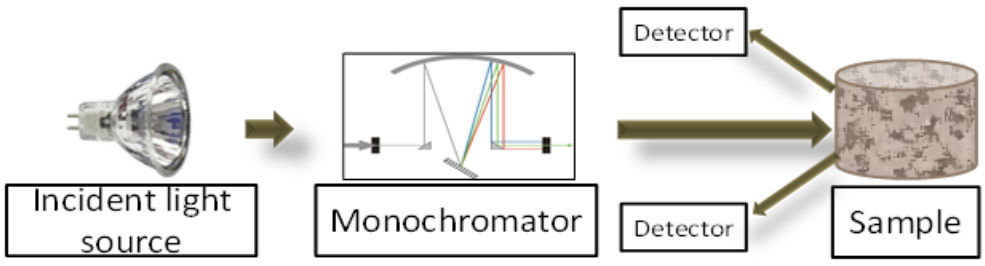

Figure 2-17 Basic configuration for a reflectance spectrometer.

There are different kinds of detectors which are applied at different frequencies (Sablinskas, 2003):

- Ge detector 600-1800 nm
- Si detector 400-1100 nm
- InGaAs detector 900-1700 nm
- Extended InGaAs1100-2800 nm
- PbS detector 1100-3500 nm
- InAs detector 1100-2800 nm
- InSb detector 2000-4000 nm
- PbSe detector 1100-4000 nm

The commonly used detectors are silicon photodiodes, lead sulfide (PbS) or lead selenide (PbSe) photoconductors, which provide good signal-to-noise ratio at room temperature. The InGaAs detector has fast detection; it can have an extended wavelength range at the expense of some sensitivity (Reich, 2005; Shaw and Mantsch, 1999).

According to their measurement principles the NIR spectrometers can be (Sablinskas, 2003; Shaw and Mantsch, 1999):

1. Scanning-grating spectrometers: These spectrometers can scan the UV/VIS region to the NIR region. They may have two detectors; one for each region. The advantages of these spectrometers are that they provide a broad spectral range, speed and accuracy.

2. Diode array spectrometers: These spectrometers have no moving parts. They consist of a fixed grating that spreads the spectrum across the array of detector elements; thus each element senses a different wavelength. The resolution will depend on the number of elements in the array and the wavelength range. Diode arrays can have silicon photodiode detector or charge coupled device (CCD) arrays, with thermoelectrically cooled InGaAs arrays. A great advantage is the possibility of miniaturization.

3. Filter spectrometers: A typical instrument consist of filters mounted on a rotating wheel. The wheel can have selected filters for the desired wavelength region. These are robust and low cost spectrometers.

4. AOTF (Acousto-Optical Tunable Filter): AOTF spectrometers consist of a crystal which is used for the wavelength selection. This is done by generating an acoustic wave; the frequency changes in the acoustic wave change the wavelength of the diffracted light in the crystal. A common set-up is a TeO_2 crystal with one or more transducers act as a monochromator. The resolution is given by the physical size of the crystal, by the length of the light crystal interaction. Advantages are the high resolution, high speed, no moving parts, compact size, and imaging capabilities.

5. LED (Light Emitting Diode) spectrometers: LED spectrometers emit radiation of discrete wavelengths, these spectrometers do not need a wavelength selector they only require a small interference filter to select the center wavelength and the bandwidth. Advantages of LED spectrometers are the possibility of miniaturization and LED sources stability.

6. Fourier Transform (FT) spectrometers: FT spectrometers consist of a radiation source, an interferometer, a beamsplitter, a laser, a detector and other optical components (Figure 2-18). The interferometer is what distinguishes FT spectroscopy from the others. The interferometer modulates the radiation, giving a frequency of kHz which can be transformed to an electromagnetic frequency. A simple interferometer (Michelson interferometer) consists of two mutually perpendicular mirrors and a beamsplitter. One of the mirrors moves along its axis at a given velocity. The beamsplitter divides the radiation into the fixed and the moving mirror, afterwards the radiation is recombined and sent to the detector. A laser (Helium-Neon) is used to control the mirror movement to ensure the alignment with the interferometer and the

wavelength precision. The FT spectrometers can achieve high resolution without compromising signal-to-noise ratio (McCarthy and Kemeny, 2001).

In this study three different spectrometers in reflectance mode were used. The first one was a NIRFlex-N500 Fourier transform spectrometer with a reflectance cell (Büchi Labortechnik, Switzerland). The second was a SentroPAT Blend Uniformity TL, NIR spectrometer (Sentronic GmbH, Dresden, Germany) based on a micro-electromechanical system, equipped with an onboard computer, two tunable laser sources, and Indium Galium Arsenide detector. The third spectrometer was a SentroPAT FO (Sentronic GmbH, Dresden, Germany) that includes a diode array detector and acquires data by a fiber optical connector from the diffuse reflectance probe SentroProbe DR LS (Sentronic GmbH, Dresden, Germany). The probe has tungsten halogen bulbs as its light source.

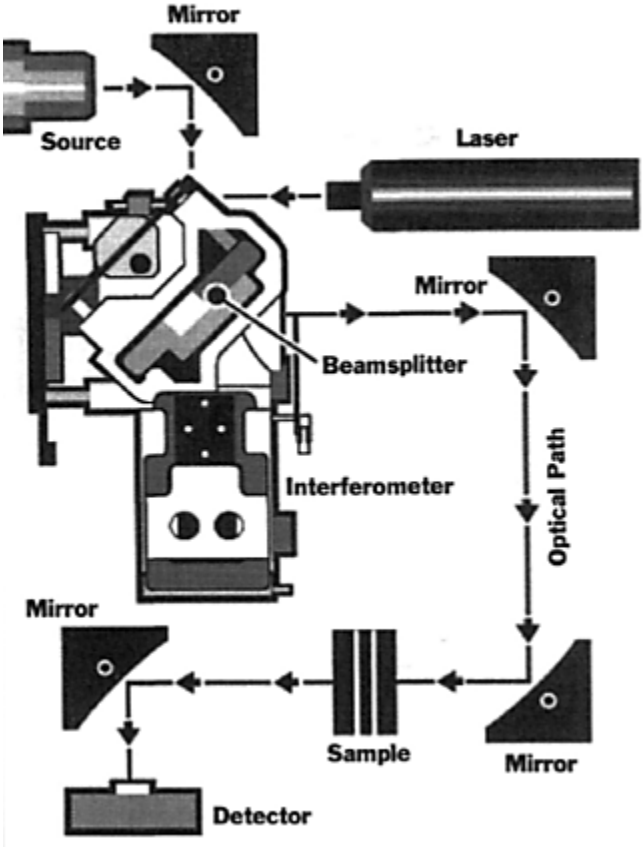

Figure 2-18 Design of a FT-NIR spectrometer.

Process control

A common approach in most production areas is to retrieve samples from the process stream followed by off-line quality control. One step further is to continuously monitor the quality and correct performance of the process and to monitor the intermediate steps without waiting to test the final product. Continuous process monitoring of a large volume production or in continuous manufacturing can be achieved by the correct selection of the analyzer, since it needs to measure over long periods of time and needs to give reliable measurements throughout the total duration of the unit operation. Faulty conditions can appear, such as bubbles in the measurement cell, clogging, and lack of sample. Therefore the implementation of supervisory diagnostics is fundamental (Kemeny, 2001).

In process control the rate of analysis is highly important, because it is used to control the process. The data acquisition must be done fast enough to monitor and/or identify changes in the critical quality attribute (API concentration). NIR can perform fast measurements, which should be twice as fast as the frequency of expected fluctuations (Kemeny, 2001).

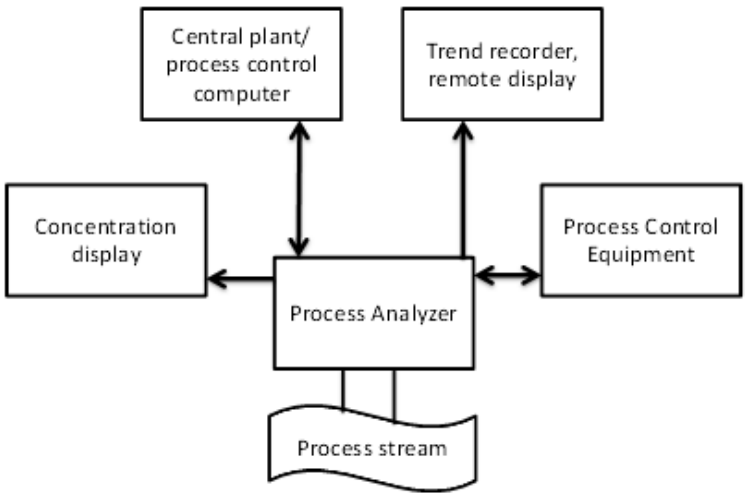

Figure 2-19 Process control

The integration of the analytical and process related measurements can lead to a powerful process control strategy. The process information, including API concentration, can be displayed locally and remotely in order to allow the operators to follow the process trend and to let them make decisions when needed (Figure 2-19). The whole production process can

be supervised by the remote control computer, by displaying and storing trends, computed statistics, outliers, deviations, etc. (Kemeny, 2001).

One of the main aims of monitoring a process is to be able to correct a deviation in the process as soon as it is detected. NIR has been used for process monitoring of a wide range of pharmaceutical unit operations from raw material identification to the final product, greatly improving process understanding. NIR imaging and spectroscopy have been successfully applied as analytical tools in order to get a deeper understanding of the pharmaceutical manufacture.

Roggo et al. (2005) used NIR as the analytical tool for getting information of the process, identifying qualitatively the influence of melt-granulation, compression and coating parameters on the tablet dissolution. Moes et al. (2008) successfully applied NIR from the blend uniformity monitoring through the content uniformity determination on tablets, and finally the thickness of the coating, thus showing the high versatility of NIR applications. The readers are referred to the reviews of Reich (2005), Roggo et al., (2007), and Gendrin et al. (2008) for an overview of NIR pharmaceutical applications.

2.10 Blending and NIR

As mentioned before, blending of powders is an essential unit operation that has been traditionally controlled by removing samples from the bulk and then analyzing these samples by means of an off-line method (mainly HPLC). This approach is slow and the sampling procedure may disrupt the blend and may also bias the measurements. Under these circumstances NIR is an attractive alternative for continuously monitoring the blending process by scanning the blend without the need of stopping the equipment, removing material by thief sampling, and disrupting the blend equilibrium. NIR blend uniformity monitoring also complies with the sampling recommendations of the health authorities (see Figure 2-3), since the “sampling” is performed continuously thus several measurements are acquired during batch or continuous blending.

The identification of the blending end-point has been one of the main research topics for NIR and powder blending. Different approaches have been developed; a summary is given in Table 2-5.

Table 2-5 Summary of NIR applications on batch blend uniformity monitoring.

Objective	Description	Reference
Blend end-point determination	Identification of the homogenous state, by dissimilarity with the mixture spectrum, PCA. SIMPLISMA was used for the identification of the wavelengths with higher purity; this approach is based on Beer's law.	Cuesta-Sánchez et al., 1995
Blend homogeneity determination	Combination of NIR and Polar Qualification System (PQS). PQS converts the absolute pretreated values into a polar coordinate system. The aim is to randomly distribute the noise, thus reducing noise influence.	Plugge and Vlies, 1996
Blend uniformity determination	Determination of the blend homogeneity by the boot strap algorithm and chi-square analysis.	Wargo and Drennen, 1996
Blend end-point determination	Homogeneity determined by the calculation of the moving block of standard deviation of the spectral standard deviation. Identification of the drop in variability as a function of time.	Sekulic et al., 1996; 1998.
On-line monitoring of powder blending	By means of different approaches such as: average standard deviation between spectra, measurements dissimilarity, Shewhart charts and Hotelling's T2, and PCA.	De Maesschalck et al., 1998
Blend homogeneity	Determine the mean square of differences between spectra for blend uniformity monitoring. This method does not require a reference spectrum.	Blanco et al., 2002
Blend end-point determination	Comparison of different methods for the blend end-point determination: Root mean square from nominal value, student's t test, API concentration profile, and moving block of standard deviation. Use of two sensors, for identifying blending variability.	Shi et al., 2008
Blend homogeneity in small scale	Small batches of approximately 50 g were monitored by moving block of standard deviation, autocorrelation functions, and partial least square discriminant analysis.	Storme-Paris et al., 2009
Blend homogeneity	Use of Hotelling's T2 and scores distance for monitoring the blend homogeneity.	Puchert et al., 2011
Blend end-point determination	Development of a PAT method for the real-time end point identification, by using a Caterpillar algorithm, this method evaluates spectral changes by moving windows followed by an F test for the comparison of the signal variations.	Flåten et al., 2012

Moving Block of Standard Deviation

One method for the identification of the blend end-point is the moving block of standard deviation (MBSD). This technique consists of calculating the standard deviation of each wavelength absorbance value (or pretreated) over a certain number of measurements and is referred to as the window size. The computation follows several iterations so the total number of measurements is considered (Figure 2-20a). The results correspond to the standard deviation calculated at different time points and at each wavelength point (Figure 2-20b). The standard deviations are expected to get closer to zero as homogeneity is approached, thus higher standard values are obtained at the beginning of the blending process.

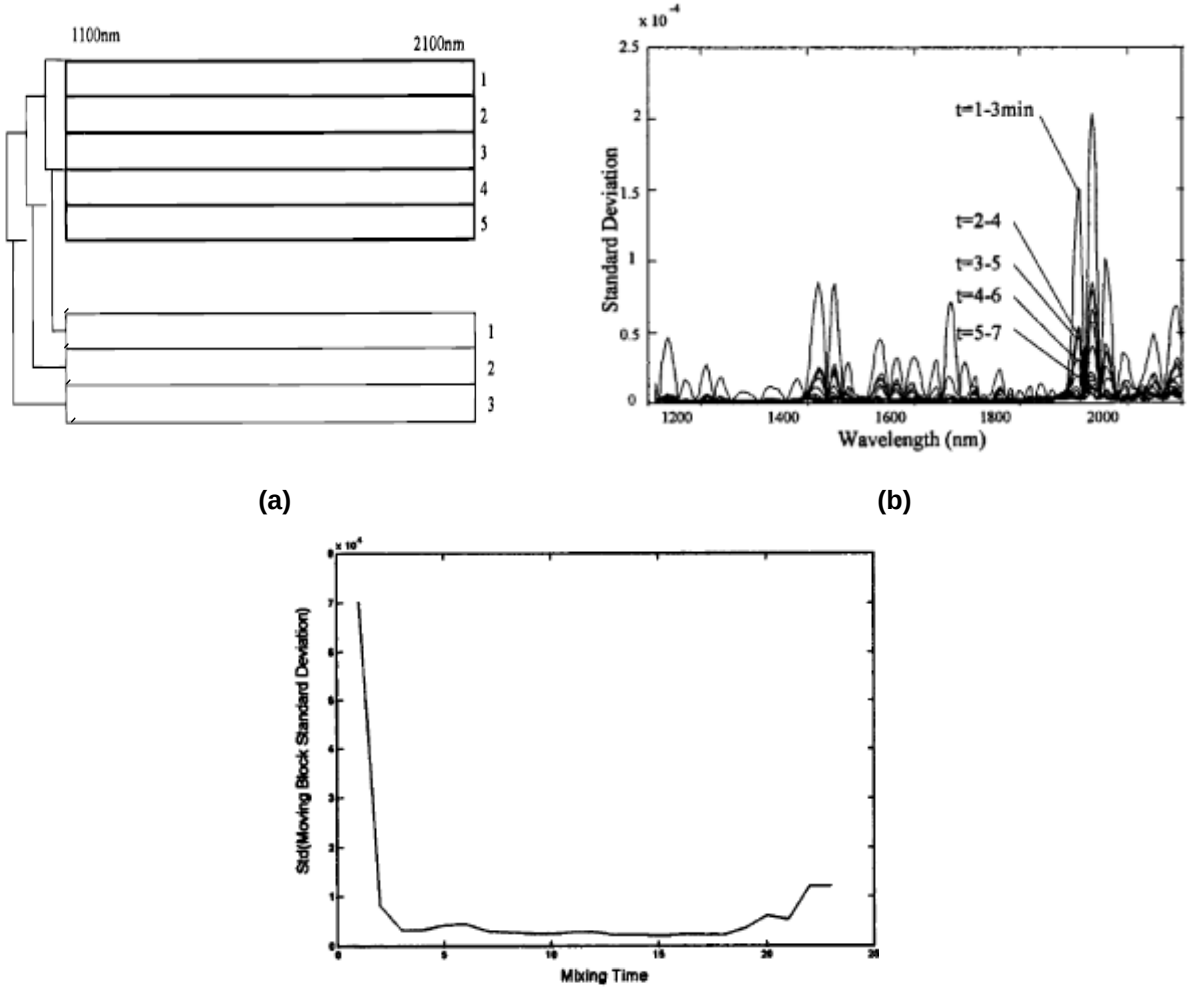

Figure 2-20 (a) MBSD calculation scheme, (b) MBSD for each wavelength (Sekulic et al., 1996).

The next step corresponds to the identification of the time at which the blend is homogeneous; this is carried out by the computation of the standard deviation of the already calculated moving block of standard deviation (Sekulic et al., 1996). The final result is a curve that monitors the standard deviation over the mixing time (Figure 2-20c). The MBSD shows a decay and then the values stabilize, this steady stage corresponds to the homogeneity of the blend.

Calibration approaches

A second challenge of the NIR blend uniformity monitoring is the acquisition of calibration samples for the construction of the quantification model. Some studies have chosen an off-line calibration approach (Sulub et al., 2009) since a bigger amount of blends can be measured and the API concentration is well-known. Another approach consists of stopping the blender at different time points to scan the powder bed by NIR and to take samples for off-line analysis (Wu et al., 2009). There are several methods for the spectral acquisitions which differ on the scale of mixing, the dynamic or static measurement, on-line or off-line, gravimetric or chromatographic reference methods, etc. Karande et al. (2010) compared three different methods for the calibration samples acquisition: (1) laboratory mixing and static spectral acquisition, (2) IBC mixing and static spectra acquisition and (3) IBC mixing and dynamic spectral acquisition. The calibration approach that included the variability of the process was by using IBC and dynamic spectral collection. Several studies have been performed in order to establish the best calibration procedure, the best scanning region (Shi et al., 2008), the optimal number of sensors (El-Hagrasy et al., 2001), etc. All these studies have the same objective, to develop a robust and accurate model for the blend uniformity monitoring.

After choosing a calibration method, developing and validating a quantification model, and selecting the strategy for the blend-end point determination, the final goal is to develop an automated system that continuously monitors the blending process (e.g. API level and homogeneity state) as well as the mixer parameters (Hailey et al., 1996).

Continuous blending

The study and characterization of blend uniformity monitoring of a continuous blender by NIR in the pharmaceutical industry has been scarcely performed. Vanarase et al. (2010) developed a quantification model for the real-time monitoring of a continuous blending process of acetaminophen, showing promising results for the industrial implementation of NIR as a PAT tool.

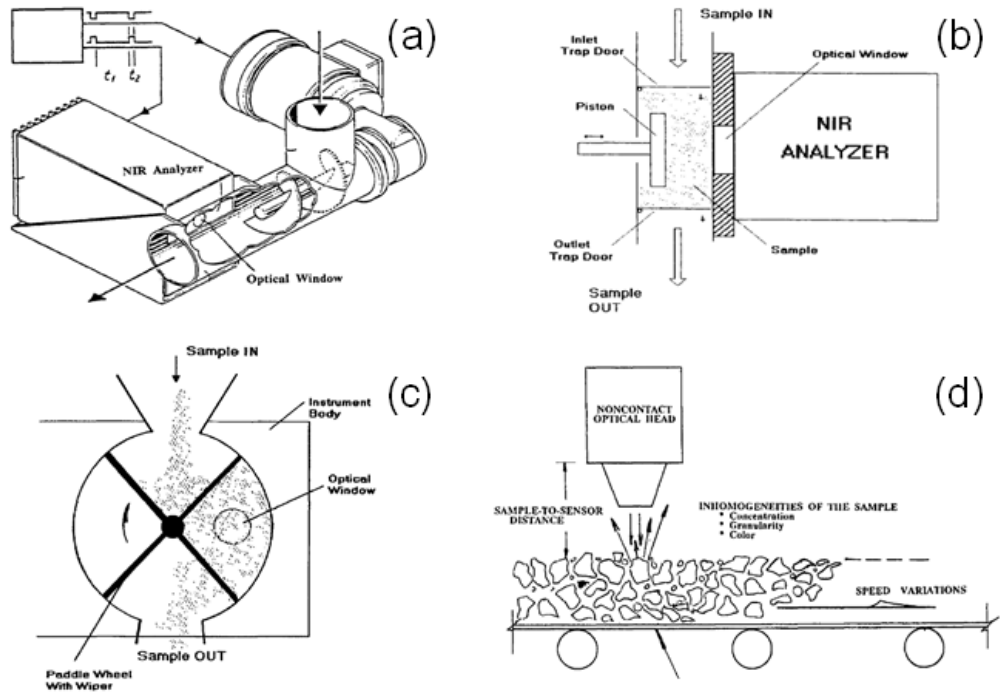

Figure 2-21 Spectroscopic monitoring and sampling systems.

Even though not many studies are available for continuous blending monitoring, there are some studies on the NIR implementation on powder streams or voiding of powders. Since the monitoring of a continuous blending is performed at the outlet of the blender when the blend is forming a powder stream, it is possible to gather information from relevant studies on powder streams. Figure 2-21 shows different set-ups for the spectroscopic measurement of particulate materials. Figure 2-21a shows a screw conveyer consisting of a sample trap where the material is slightly compacted in order to provide a constant sample (constant density) presentation to the NIR spectrometer. Another example, in which the sample is diverted from the process stream, is given in Figure 2-21b. Here the particulate material is

compressed by a piston and presented to the NIR probe. Figure 2-21c refers to a paddle wheel, in which the flowing powder is filled and analyzed through an optical window. Figure 2-21d shows an example of non-contact spectroscopy, where a conveyor belt is continuously been monitored by a spectroscopic method (Kemeny, 2001).

Ropero et al. (2009) evaluated the voiding from a funnel by NIR-scanning of the powder flow, gathering physical information of the flow and showing that even under flowing conditions the chemical attributes of the samples are detectable and could be used for further quantification. Barajas et al. (2007) studied the appearance of segregation and the particle size changes during voiding, showing that it is feasible to distinguish particle size variations.

The study of granular materials flow is complex task where particle size, angle of repose, particle interactions, and process conditions such as chute design are relevant for the final flow of the particles. Several studies have been performed on the powder flow down inclined chutes (Kruyt and Verël, 1992; Santomaso and Canu, 2001; Tamara et al., 2006; Weingerl and Schaflinger, 2000) and the majority of industrial chute applications involve rapid or accelerated flow conditions in which a “thin” stream is present, where the thickness of the powder bed is less than the width of the chute (Roberts, 2003). Under these conditions the powder will have a velocity profile. Andersson et al., (2005) studied the influence of the particle velocity on a Fourier transform NIR spectrometer. They identified that the flow conditions such as particle velocity can present artifacts on the spectral data, influencing the quality of the results. It is important to point out that the mass flow rate as well as velocity variations will influence the interaction of the NIR radiation with the sample, which will impact the amount of powder seen by the NIR probe.

2.11 Chemometrics

Over the past years a transition on the analytical methods has been taking place. In the past, scientists had only a few measurements available which were expensive, labor-intensive, and time-consuming; now the analytical methods allow high-quality measurements and fast

and high amounts of data acquisition. This high amount of data is collected for further analysis. The multivariate responses of the analytical equipment and the easy access to computers and potent software generation allow the appearance and fast development of Chemometrics.

Massart and Buydens (1988) defined chemometrics as “the chemical discipline that uses mathematical, statistical and other methods of formal logic to design or select optimal procedures and experiments and to provide maximum chemical information by analyzing chemical data”. Chemometrics is also defined as “how to get chemically relevant information out of measured chemical data, how to represent and display this information, and how to get such information into data” (Wold, 1995). Therefore chemometrics aim is to structure the chemical information into a form that can be expressed as a mathematical relation in order to extract the relevant information.

Chemometrics include several approaches for the study of multivariate data such as pattern recognition, classification, linear and non-linear mapping, and predictive models. Multivariate empirical modeling (e.g. Principal Component Analysis and Partial Least Squares) shows unexpected patterns because of the consideration of all the variables, contrary to traditional analysis which often considers one or few variables at the same time (Wold, 1995). However, the empirical models generated through chemometric tools need to be consistent with theory, thus theory and chemometrics are complementary in the study of a chemical system.

A mathematical model is designed for describing reality; all the models have an error due to the noise, variability, uncertainties, and non-linearity contained in the measured data (Wold, 1995; Wold and Sjöström, 1998). This experimental error can come from known or unknown sources that can hide the relevant information contained in the dataset. Using calibrated equipment and appropriate sampling techniques for acquiring representative samples will reduce this error. Consequently, chemometrics tools are used for extracting the relevant information from the noisy data.

Spectral Pre-processing

Dissimilarities on near-infrared spectral data are the result of chemical and physical sample variations. Mathematical preprocessing of the data is applied In order to reduce the influence of particle size, shape, density, particle packaging and other physical differences between the samples. A good data pretreatment will enhance the chemical information while a wrong pretreatment will diminish or eliminate the information correlated to the parameter of interest. Therefore the correct selection of the preprocessing technique is fundamental and should be carefully chosen.

Standard Normal Variate (SNV)

SNV was designed for reducing the undesirable multiplicative effects of particle size. SNV calculates the standard normal variation at each wavelength and removes the slope variation on a sample basis (Barnes et al., 1989).

Equation 2-8

$$^{SNV}\boldsymbol{x_{ij}} = \frac{\boldsymbol{x_{ij}} - \bar{\boldsymbol{x}}_{\boldsymbol{j}}}{\sqrt{\sum_{\boldsymbol{k}}(\boldsymbol{x_{ij}} - \bar{\boldsymbol{x}}_{\boldsymbol{i}})^{\boldsymbol{2}}/\boldsymbol{I}}}$$

Where $^{SNV}x_{ij}$ is the matrix **x** after SNV preprocessing, $\boldsymbol{x}_{ij}$is the **x** data matrix of i rows (samples) and j columns (variables) and I is the number of points.

Mean centering

This operation intends to mean-center the columns by subtracting the mean of each column (variable) so that:

Equation 2-9

$$^{mc}\boldsymbol{x_{ij}} = \boldsymbol{x_{ij}} - \bar{\boldsymbol{x}}_{\boldsymbol{j}}$$

where $^{mc}x_{ij}$ is the mean centered matrix. After mean centering, the score plot appears centered around the origin. Mean centering has a significant effect on the size of the first eigenvalue, which is reduced dramatically and can influence the significant number of principal components (PC) (Brereton, 2003).

Derivatives

Derivatives are used to remove additive and multiplicative effects in the spectra. The first derivative removes baseline, while the second removes baseline and linear trend. In the second derivative the peaks appear at the same wavelengths, whereas in the first derivative they become zero. Simple derivation is not feasible in real measurements due to the noisy nature of the spectral data. Therefore derivation of spectral data normally includes a smoothing step. Savitzky and Golay (1964) described an algorithm that performs a local polynomial regression in a symmetric window in the raw data; subsequently the derivative of any order can be calculated.

Orthogonal Signal Correction (OSC)

NIR spectra often contain systematic variation that is unrelated to the response (**Y**). SNV and derivatives and other preprocessing techniques may remove information on the **X** matrix related to **Y**. Wold et al. (1998) proposed a method for signal correction that removes variation on **X** that is not related to **Y** by removing the orthogonal components to **Y**. This method is called orthogonal signal correction (OSC) and the basic format is given in Equation 2-10:

Equation 2-10

$$^{OSC}\boldsymbol{x_{ij}} = \boldsymbol{x_{ij}} - \boldsymbol{t_{OSC}}\boldsymbol{P_{OSC}^{t}}$$

where $^{OSC}x_{ij}$ is the matrix **X** after OSC, t_{OSC} is the OSC scores and the P_{OSC}^{t} is the transpose of the OSC loadings matrix.

Pattern recognition

PCA

One of the aims of pattern recognition is to enable the visualization of n-dimensional data by reducing the n-dimensional space to two dimensional coordinates (Massart and Buydens, 1988). Principal component analysis (PCA) is one of the multivariate tools that can be used for pattern recognition, to identify similarities on the data, and to detect trends and outliers;

this is done by the projection of the large data space into a smaller space that is easier to analyze (Geladi, 2003). The data matrix $\boldsymbol{X}$ is decomposed into principal components (PCs) that maximize the explained variance and each successive component is orthogonal to the previous one (Figure 2-22), the mathematical relation is explained as the product of scores and loadings.

Equation 2-11 $$\boldsymbol{X = TP^T + E = t_1 p_1^T + t_2 p_2^T + \cdots + t_A p_A^T + E}$$

Where $\boldsymbol{T}$ are the scores and have as many rows as the original data matrix, $\boldsymbol{P}$ are the loadings and have as many columns as the original data $\boldsymbol{X}$, and $\boldsymbol{E}$ is the residual matrix, the variance not explained, and A is the number of calculated PCs.

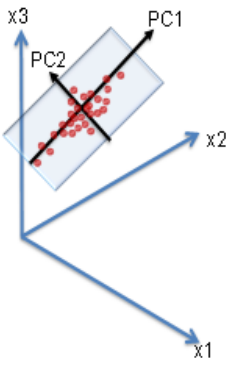

Figure 2-22 Graphic PCA representation in a three variables space.

The aim of PCA is to explain as much as variability related to X as possible by considering the minimal number of PCs. The scores and loadings can also be used in line and scatter plots to facilitate the interpretation of the data. The noise is left in the residuals.

The next step is to determine the number of significant PCs to be used. In an ideal case the number of PCs is equal to the number of substantial components, for example in a formulation with three ingredients, we expect three PCs. In reality noise can interfere with the ideal situation and then interfere with the rank determination (Brereton, 2003). The size of each PC can be measured and the size is referred as an eigenvalue (g). The earlier PCs have larger eigenvalues and therefore are more significant. A simple definition of an eigenvalue is the sum of squares of the scores:

Equation 2-12 $$g_A = \sum t_A^2$$

In practice the cumulative percentage of the eigenvalue is often used to determine what portion of the data was modeled by the PCA (Brereton, 2003; Rajalahti and Kvalheim, 2011).

Calibration

NIR spectra are multivariate in nature because the detectors allow the detection of the reflected or transmitted radiation at many wavelengths simultaneously. Each absorption value at each wavelength is a variable, each variable may be correlated to different extents to the concentration of the substance of interest. PLS (Partial Least squares Projection to Latent Variables) is a quantitative multivariate method, used for developing a model that would relate $\mathbf{X}$ and $\mathbf{Y}$ (Wold, 1991).

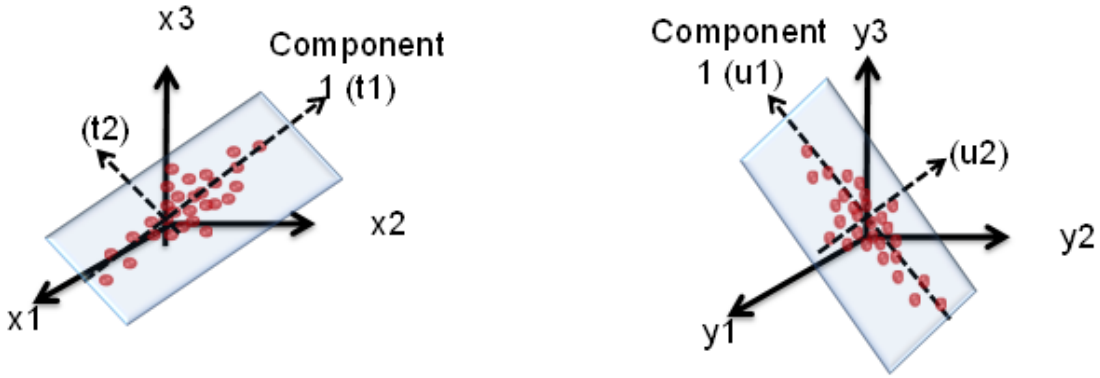

Figure 2-23 Graphical representation of observations in the X-space and Y-space.

Figure 2-23 shows an example of a matrix **X** and matrix **Y**, each one formed with three variables. By projecting the observations, it is possible to obtain the scores $\mathbf{t_1}$ and $\mathbf{u_1}$ for **X** and **Y** respectively. The correlation between both matrices **X** and **Y** can be assessed by plotting the scores $\mathbf{t_1}$ and $\mathbf{u_1}$ in a scatter plot (Eriksson et al., 2006). **X** and **Y** can be expressed according to:

Equation 2-13 $$\boldsymbol{X} = \mathbf{1}\bar{\boldsymbol{x}}' + \boldsymbol{TP}' + \boldsymbol{E}$$

Equation 2-14 $$\boldsymbol{Y} = \mathbf{1}\bar{\boldsymbol{y}}' + \boldsymbol{UC}' + \boldsymbol{F}$$

Where $1\bar{x}'$ and $1\bar{y}'$ are terms originated from the preprocessing and averaging techniques, T and U are the score matrices, P' is the X-loading matrix, C' is the Y-weight matrix, E and F are the residual matrices (Eriksson et al., 2006).

In practice it is possible to work with the one Y value e.g. concentration, thus Y will be a vector **u**, known as PLS1. If several Y variables are to be modeled at the same time, then **Y** scores will be **U**, known as PLS2.

Model validation

One of the most important aspects of calibration models is the validation. Cross-validation (CV) is one chemometric tool in which part of the calibration set is used for testing the model. CV is a useful technique for establishing the required number of PLS components. Figure 2-24 shows the parameter R^2 which indicates the explained variation in the model, where the higher the number of PLS components more variation will be explained. Q^2 is the predicted variation, in other words, the prediction ability. Increasing the number of components does not necessary imply that the prediction ability will improve; Q^2 will reach a plateau followed by Q^2 decrease (Eriksson et al., 2006). Therefore it is important to identify an area with good fit and good predictive ability. CV gives an overall performance of each of the PLS components.

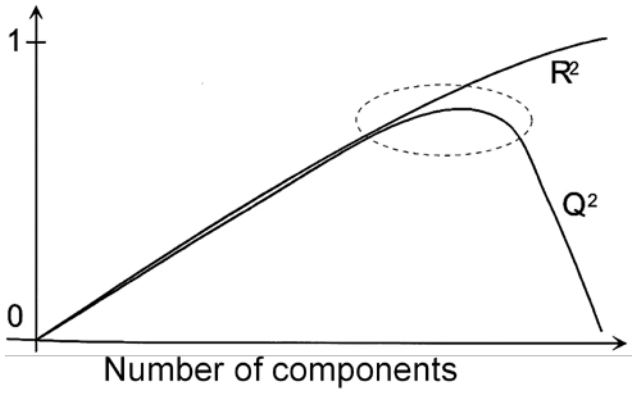

Figure 2-24 Selection of PLS components.

One disadvantage of CV is that it depends on the original dataset. In order to overcome this situation, the use of independent test sets is recommended. The Root Mean Square Error of the Prediction (RMSEP) can be used for the determination of the quality of the model.

Equation 2-15 $$RMSEP = \sqrt{\frac{\sum_{i=1}^{n}(y_{ref}-\hat{y}_{test})^2}{n}}$$

Where n is the number of samples, y_{ref} is the reference value, and $\hat{y}_{test}$ is the predicted value.

DmodX

The residuals are a diagnostic value for the quality of the model; an inspection of the residuals enables the detection of outliers. The standard deviation of the X- residuals is proportional to the distance between the data point and the model plane in the X-space. This value is called DModX. A DModX larger than 2.5 times the overall SD of the X-residuals indicates that the observation is an outlier (Wold et al., 2001). DModX is a useful tool for moderate outliers identification.

Mahalanobis distance and Hotelling's T2

Many multivariate methods are based on the measurement of distances between objects. The most known distances are the Euclidean distance and the Mahalanobis distance (MD). In the case of Euclidean distance, each measurement assumes equal significance; therefore variables that may be irrelevant can considerably influence the analysis. On the other hand, MD of the original dataset considers the correlation of the data and is computed through the inverse of the variance-covariance matrix of the dataset. Figure 2-25 illustrates an example of the Euclidean Distance and the Mahalanobis distance for the same dataset. Euclidean distances in Figure 2-25a indicate that the measurements located on the outer circles have lower probability to occur, which is not the case. Therefore the use of MD is more accurate when correlated variables are under study. The ellipse in Figure 2-25b considers the correlation between the variables, hence the measurements that are located in the outer

ellipse have greater MD and the probability of new measurements landing in that area is lower.

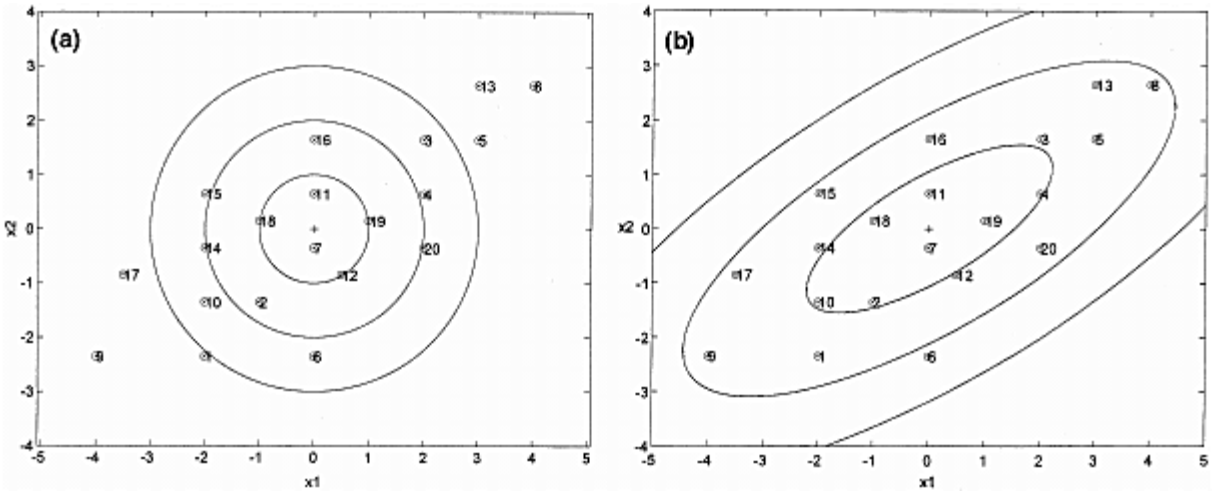

Figure 2-25 Plots of two variables X1 and x2. (a) The circles represent equal Euclidean distances to the center. (b) The ellipses represent equal Mahalanobis distances to the center (De Maesschalck et al., 2000).

MD can be calculated on the principal component space, once the variable reduction has taken place. MD can be used for the outliers detection, selection of calibration samples, and for the calculation of Hotelling's T^2 (De Maesschalck et al., 2000; Brereton, 2003). The squared MD values are called Hotelling's T^2, which is a widely used statistical tool for process control charts, where the calculated T^2 values are compared to the critical T^2 (De Maesschalck et al., 2000). In the case of pharmaceutical applications concretely mixing of powders, T^2 values have been used for the monitoring of the blend uniformity (De Maesschalck et al., 1998, Putchert et al., 2011).

PAT and Chemometrics

MVDA is a basic tool for the PAT initiative. According to the complexity of the data incorporated on a chemometric model, there are four levels (Figure 2-26) in which MVDA can be applied (Eriksson et al., 2008):

Level 1-MVDA off-line calibration: this refers to off-line analysis i.e. concentration of API or impurities in the final product, moisture content.

Level 2-MVDA for classification and / or calibration: The objective is to classify samples, i.e. for identifying similarities or dissimilarities.

Level 3- MVDA on a single process step: At this level, Multivariate Statistical Process Control and real-time process monitoring are the main objectives. All available data are used for end-point identification as well as unforeseen deviations.

Level 4- MVDA on the entire process: This is the final level, in which information obtained from all the different unit operations are integrated, thus giving an overview of the complete process. Therefore, it is possible to associate the information of process deviation and its impact on the quality of the final product. This level of process understanding is one of the major achievements of the PAT initiative.

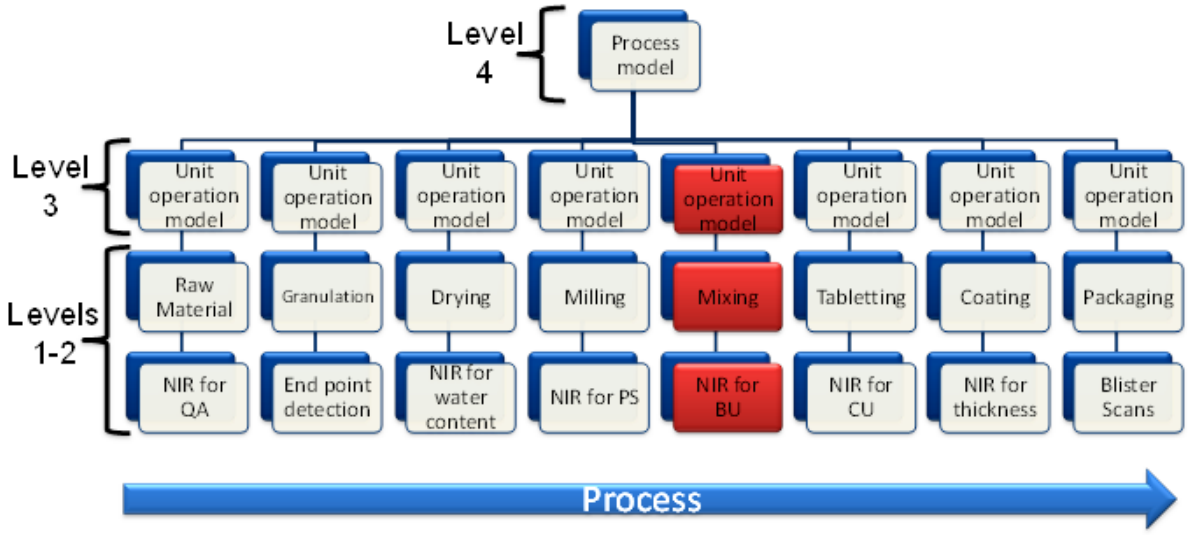

Figure 2-26 Combination of all unit operations for a complete process overview (Eriksson et al., 2008), with special emphasis on NIR and powder mixing.

References

Abberger, T., Seo, A., Schaefer, T., 2002. The effect of droplet size and powder particle size on the mechanisms of nucleation and growth in fluid bed melt agglomeration. Int. J. Pharm. 249, 185-197.

Aiache, J.-M., Beyssac, E., 2007. Powders as Dosage Forms, in: Swarbrick, J. (Ed.), Encyclopedia of Pharmaceutical Technology, 3rd Informa Healthcare USA, Inc, New York, pp. 2971-2982.

Alexander, A.W., Muzzio, F.J., 2002. Batch Size Increase in Dry Blending and Mixing, in: Levine, M. (Ed.), Pharmaceutical Process Scale-Up, Marcel Dekker, New York, pp. 115-132.

Allen, T. (2003) Powder Sampling and Particle Size Determination, Elsevier, Amsterdam, pp. 1-55.

Andersson, M., Svensson, O., Folestad, S., Josefson, M., Wahlund, K.-G., 2005. NIR spectroscopy on moving solids using a scanning grating spectrometer-impact on multivariate process analysis. Chemometr. Intell. Lab. Syst. 75, 1-11.

Andrews, D.L., 1999. Rayleigh Scattering and Raman Effect Theory, in: Tranter, G., Holmes, J., Lindon, J., (Eds.), Encyclopedia of Spectroscopy and Spectrometry, Academic Press, pp.1993-2000.

Barajas, M.J., Rodriguez-Cassiani, A., Vargas, W., Conde, C., Ropero, J., Figueroa, J., Romañach, R.J., 2007. Near-Infrared Spectroscopic Method for Real-Time Monitoring of Pharmaceutical Powders During Voiding. Appl. Spectrosc. 61, 490-496.

Barnes, R.J., Dhanoa, M.S., Lister, S.J., 1989. Standard Normal Variate Transformation and De-trending on Near-Infrared Diffuse Reflectance Spectra. Appl. Spectrosc. 43, 772-777.

Bellamy, L.J., Nordon, A., Littlejohn, D., 2008. Effects of particle size and cohesive properties on mixing studied by non-contact NIR. Int. J. Pharm. 361, 87-91.

Betz, G., Junker-Büzgin, P., Leuenberger, H., 2003. Batch and continuous processing in the production of pharmaceutical granules. Pharm. Dev. Technol. 8, 289-297.

Blanco, M., González-Bañó, R., Bertran, E., 2002. Monitoring powder blending in pharmaceutical processes by use of near infrared spectroscopy. Talanta 56, 203-212.

Brereton, R.G., 2003. Chemometrics: Data Analysis for the Laboratory and Chemical Plant. John Wiley & sons Ltd. England.

Bridgwater, J., 1994. Chapter 10 Mixing, in: Chulia, D., Deleuil, M., Pourcelot, Y. (Eds.), Powder Technology and Pharmaceutical Processes, Elsevier, Amsterdam, pp. 347-357.

Bridgwater, J., 2012. Mixing of powders and granular materials by mechanical means- A perspective. Particuology 10, 397-427.

Brittain, H.G., 2002. Particle-Sire Distribution II: The Problem of Sampling Powdered Solids. Pharm. Tech. Jul, 67-73.

Burgschweiger, J., Tsotsas, E., 2002. Experimental investigation and modeling of continuous fluidized bed during steady-state and dynamic conditions. Chem. Eng. Sci. 57, 5021-5038.

Chaudhuri, B., Mehrotra, A., Muzzio, F.J., Tomassone, M.S., 2006. Cohesive effects in powder mixing in a tumbling blender. Powder Tech. 165, 105-114.

Ciurczak, E.W., 2001. Principles of Near-Infrared Spectroscopy, in: Burns, D.A., Ciurczak, E.W., Handbook of Near-Infrared Analysis, 2nd. CRC Taylor & Francis, USA, pp. 7-18.

Coblentz, W.W., 1908. Supplementary investigations of infra-red spectra. Carnegie Institution of Washington, Washington D.C.

Cooke, M.H., Stephens, D.J., Bridgwater, J., 1976. Powder Mixing- A Literature Survey. Powder Tech. 15, 1-20.

Cuesta-Sánchez, F., Toft, J., van den Bogaert, B., Massart, D.L., Dive, S.S., Hailey, P., 1995. Monitoring powder blending by NIR spectroscopy. Fresenius J. Anal. Chem. 352, 771-778.

Dahm, D.J., Dahm, K.D., 2007. Interpreting Diffuse Reflectance and Transmittance, IM Publications, Norfolk, UK.

Danckwerts, P.V., 1953. Continuous flow systems. Distribution of residence times. Chem. Eng. Sci. 2, 1-13.

De Maesschalck, R., Cuesta-Sánchez, F., Massart, D.L., Doherty, P., 1998. On-Line Monitoring of Powder Blending with Near-Infrared Spectroscopy. Appl. Spectrosc. 52, 725-731.

De Maesschalck, R., Jouan-Rimbaud, D., Massart, D.L., 2000. The Mahalanobis distance. Chemometr. Intell. Lab. Sys. 50, 1-18.

Djuric, D., Van Melkebeke, B., Kleinebudde, P., Remon, J.P., Vervaet, C., 2009. Comparison of two twin-screw extruders for continuous granulation. Eur. J. Pharm. Biopharm. 71, 155-160.

Djuric, D., Kleinebudde, P., 2010. Continuous granulation with a twin-screw extruder: impact of material throughput. Pharm. Dev. Technol. 15, 518-525.

Duerst, M.D., 2007. Spectroscopic methods of analysis-infrared spectroscopy, in: Swarbrick, J. (Ed.), Encyclopedia of Pharmaceutical Technology, 3rd Informa Healthcare USA, Inc, New York, pp. 3405-3418.

El-Hagrasy, A., Morris, H.R., D'Amico, F., Lodder, R.A., Drennen III, J.K., 2001. Near-Infrared Spectroscopy and Imaging for the Monitoring of Powder Blend Homogeneity. J. Pharm. Sci. 9, 1298-1307.

Eriksson, L., Johansson, E., Kettaneh-Wold, N., Trygg, J., Wikström, C., Wold, S., 2006. Multi- and Megavariate Data Analasys. Part I Basic Principles and Applications. Umetrics Academy, Umeå.

Eriksson, L., Johansson, E., Kettaneh-Wold, N., Wikström, C., Wold, S., 2008. Design of Experiments, Umetrics Academy, Umeå, pp. 387-398.

European Medicines Agency, 1996. Note for Guidance on Manufacture of Finished Dosage Form. http://www.ema.europa.eu/docs/en_GB/document_library/Scientific_guideline/2009/09/WC500002916.pdf, accessed May 2012.

Fan, L.T., Chen, S.J., Watson, C.A., 1970. Solids Mixing. Ind. Eng. Chem. 62, 53-69.

Fan, L.T., Chen, Y.-M., Lai, F.S., 1990. Recent Developments in Solids Mixing. Powder Tech. 61, 255-287.

FDA, 2003, Guidance for Industry: Powder Blends and Finished Dosage Units- Stratified In-Process Dosage Unit Sampling and Assessment. http://www.fda.gov/downloads/Drugs/GuidanceComplianceRegulatoryInformation/Guidances/ucm070314.pdf, accessed June 2012.

FDA, 2004. Guidance for Industry: PAT – A Framework for Innovative Pharmaceutical Development, Manufacturing, and Quality Assurance. http://www.fda.gov/downloads/Drugs/GuidanceComplianceRegulatoryInformation/Guidances/ucm070305.pdf, accessed June 2012.

Flåten, G.R., Ferreira, A.P., Bellamy, L., Frake, P., 2012. PAT within the QbD Framework: Real-Time End Point Detection for Powder Blends in a Compliant Environment. J. Pharm. Innov. 7, 38-45.

Fonteyne, M., Soares, S., Vercruysse, J., Peeters, E., Burggraeve, A., Vervaet, C., Remon, J.P., Sandler, N., De Beer, T., 2012. Prediction of quality attributes of continuously produced granules using complementary pat tools. Eur. J. Pharm. Biopharm. http://dx.doi.org/10.1016/j.ejpb.2012.07.017

Gamlen, M.J., Eardley, C., 1986. Continuous extrusion using a Baker Perkins MP50 (multipurpose) extruder. Drug Dev. Ind. Pharm. 12, 1701-1713.

Gao, Y., Vanarase, A., Muzzio, F., Ierapetritou, M., 2011. Characterizing continuous powder mixing using residence time distribution. Chem. Eng. Sci. 66, 417-425.

Geladi, P., 2003. Chemometrics in spectroscopy. Part 1. Classical chemometrics.Spectrochim. Acta B 58, 762-782.

Gendrin, C., Roggo, Y., Collet, C., 2008. Pharmaceutical applications of vibrational chemical imaging and chemometrics: A review. J. Pharm. Biomed. Sci. 48, 533-553.

Gonnissen, Y., Gonçalves, S.I.V., De Geest, B.G., Remon, J.P., Vervaet, C., 2008. Process design applied to optimize a directly compressible powder produced via a continuous manufacturing process. Eur. J. Pharm. Biopharm. 68, 760-770.

Hailey, P.A., Doherty, P., Tapsell, P., Oliver, T., Aldridge, P.K., 1996. Automated system for the on-line monitoring of powder blending processes using near-infrared spectroscopy Part I. System development and control. J. Pharm. Biomed. Anal. 14, 551-559.

Harnby, N. ,1997. Characterization of powder mixtures in Harnby, N., Edwards, M.F., Nienow, A.W. (Eds), Mixing in the Process Industries, 2nd. Butterworth-Heinemann. London, pp. 25-41.

Heise, H.M., 2007. Spectroscopic Methods of Analysis: Diffuse Reflectance Spectroscopy, in: Swarbrick, J. (Ed.), Encyclopedia of Pharmaceutical Technology, 3rd Informa Healthcare USA, Inc, New York, pp. 3375-3386.

Herschel, W., 1800. Investigations of the Powers of the Prismatic Colours to Heat and Illuminate Objects; With Remarks That Prove the Different Refrangibility of Radiant Heat. To Which Is Added, and Inquiry into the Method of Viewing the Sun Advantageously, with Telescopes of Large Apertures and High Magnifying Powers. Phil. Trans. R. Soc. 900, 255-283.

Hersey, J.A., 1975. Ordered Mixing: A New Concept in Powder Mixing Practice. Powder Tech. 11, 41-44.

Hindle, P.H., 2001. Historical Development, in: Burns, D.A., Ciurczak, E.W., Handbook of Near-Infrared Analysis, 2nd. CRC Taylor & Francis, USA, pp. 1-6.

Hof, M., 2003. Basics of Optical Spectroscopy, in: Gauglitz, G., Vo-Dihn, T. (Eds.), Handbook of Spectroscopy. Wiley-VCH Verlag GmbH & Co. KGaA, Weinheim, Germany, pp. 39-47.

International Conference on Harmonization, ICH Q8 (R2), 2009. Pharmaceutical Development. http://www.ich.org/fileadmin/Public_Web_Site/ICH_Products/Guidelines/Quality/Q8_R1/Step4/Q8_R2_Guideline.pdf, accessed August 2012.

Karande, A.D., Liew, C.V., Heng, P.W.S., 2010. Calibration sampling paradox in near infrared spectroscopy: A case study of multi-component powder blend. Int. J. Pharm. 395, 91-97.

Keleb, E.I., Vermeire, A., Vervaet, C., Remon, J.P., 2001. Cold extrusion as a continuous single-step granulation and tabletting process. Eur. J. Pharm. Biopharm. 52, 359-368.

Kemeny, G.J., 2001. Process Analysis in: Burns, D.A., Ciurczak, E.W., Handbook of Near-Infrared Analysis, 2nd. CRC Taylor & Francis, USA, pp. 729-782.

Kleinebudde, P., 2004. Roll compaction/dry granulation: pharmaceutical applications. Eur. J. Pharm. Biopharm. 58, 317-326.

Kristensen, H.G., Schaefer, T., 1987. Granulation, A review on pharmaceutical wet-granulation. Drug Dev, Ind. Pharm. 13, 803-872.

Kruyt, N.P., Verël, W.J.T., 1992. Experimental and theoretical study of rapid flows of cohesionless granular materials down inclined chutes. Powder Tech. 73, 109-115.

Lacey, P.M.C., 1954. Developments in the theory of particle mixing. J. Appl. Chem. 4, 257-268.

Manjunath, K., Dhodapkar, S., Jacob, K., 2004. Solids Mixing, Part B: Mixing of Particulate Solids in the Process Industries, in: Paul, E.L., Atiemo-Obeng, V.A., Kresta, S.M., (Eds.), Handbook of Industrial Mixing: Science and Practice, John Wiley & Sons, Inc, New Jersey, pp. 924-985.

Massart, D.L., Buydens, L., 1988. Chemometrics in pharmaceutical analysis. J. Pharm. Biomed. Anal. 6, 535-545.

Massol-Chaudeur, S., Berthiaux, H., Dodds, J.A., 2002. Experimental study of the mixing kinetics of binary pharmaceutical powder mixtures in a laboratory hoop mixer. Chem. Eng. Sci. 57, 4053-4065.

McCarthy, W.J., Kemeny,G.J., 2001. Fourier Transform Spectrometers in the Near-Infrared, in: Burns, D.A., Ciurczak, E.W., Handbook of Near-Infrared Analysis, 2nd. CRC Taylor & Francis, USA, pp. 71-89.

Meyer, T.A., 2008. Novel Determination of Powder Mixing Qualitites and Study of Dry Coated Particles. PhD Thesis, University of Basel, Switzerland.

Mie, G., 1908. Beiträge zur Optik trüber Medien, speziell kolloidaler Metallösungen. Ann. Physik 25, 377-445.

Moes, J.J., Ruijken, m.M., Gout, E., Frijlink, H.W., Ugwoke, M.I., 2008. Application of process analytical technology in tablet process development using NIR spectroscopy: Blend uniformity, content uniformity and coating thickness measurements. Int. J. Pharm. 357, 108-118.

Muzzio, F.J., Robinson, P., Wightman, C., Brone, D., 1997. Sampling practices in powder blending. Int. J. Pharm. 155, 153-178.

Muzzio, F.J., Alexander, A., Goodridge, C., Shen, E., Shinbrot, T., 2004. Solids Mixing, Part A: Fundamentals of Solids Mixing, in: Paul, E.L., Atiemo-Obeng, V.A., Kresta, S.M., (Eds.), Handbook of Industrial Mixing: Science and Practice, John Wiley & Sons, Inc, New Jersey, pp. 887-923.

Ollinger, J.M., Griffiths, P.R., Burger, T., 2001. Theory of Diffuse Reflection in the NIR Region, in Burns, D.A., Ciurczak, E.W., Handbook of Near-Infrared Analysis, 2nd. CRC Taylor & Francis, USA, pp. 19-51.

Parikh, D.M., 2005. Introduction, in: Swarbrick, J. (Ed), Handbook of Pharmaceutical Granulation Technology, 2nd, Taylor & Francis Group, USA, pp. 1-5.

Pernenkil, L., Cooney, C.L., 2006. A review on the continuous blending of powders. Chem. Eng. Sci. 61, 720-742.

Pernenkil, L., 2008. Continuous Blending of Dry Pharmaceutical Powders. PhD thesis Massachusetts institute of Technology, USA.

Plugge, W., van der Vlies, C., 1996. Near-infrared spectroscopy as a tool to improve quality. J. Pharm. Biomed. Anal. 14, 891-898.

Portillo, P.M., Ierapetritou, M.G., Muzzio, F.J., 2008. Characterization of continuous convective powder mixing processes. Powder Tech. 182, 368-378.

Portillo, P.M., Ierapetritou, M.G., Muzzio, F., 2009. Effects of rotation rate, mixing angle, and cohesion in two continuous powder mixers- A statistical approach. Powder Tech. 194, 217-227.

Puchert, T., Holzhauer, C.-V., Menezes, J.C., Lochmann, D., Reich, G., 2011. A new PAT/QbD approach for the determination of blend homogeneity: Combination of on-line NIRS with PC Scores Distance Analysis (PC-SDA). Eur. J. Pharm. Biopharm. 78, 173-182.

Rajalahti, T., Kvalheim, O.M., 2011. Multivariate data analysis in pharmaceutics: A tutorial review. Int. J. Pharm. 417, 280-290.

Rees, J.E., 1977. Mixing of particulate solids to ensure homogeneity of dosage forms: The need for a critical approach to pharmaceutical process development. Boll. Chim. Farm. 116, 445-462.

Reich, G., 2005. Near-infrared spectroscopy and imaging: basic principles and pharmaceutical applications. Adv. Drug Deliv. Rev. 57, 1109-1143.

Remon, J.P., Vervaet, C., 2007. Continuous Processing of Pharmaceuticals, in: Swarbrick, J. (Ed.), Encyclopedia of Pharmaceutical Technology, 3rd Informa Healthcare USA, Inc, New York, pp. 743-749.

Roberts, A., 2003. Chute Performance and Design for Rapid Flow Conditions. Chem. Eng. Technol. 26, 163-170.

Roggo, Y., Jent, N., Edmond, E., Chalus, P., Ulmschneider, M., 2005. Characterizing process effects on pharmaceutical solid forms using near-infrared spectroscopy and infrared imaging. Eur. J. Pharm. Biopharm. 61, 100-110.

Roggo, Y., Chalus, P., Maurer, L., Lema-Martinez, C., Edmond, A., Jent, N., 2007. A review of near infrared spectroscopy and chemometrics in pharmaceutical technologies. J. Pharm. Biomed. Anal. 44, 683-700.

Ropero, J., Beach, L., Alcalà, M., Rentas, R., Davé, R.N., Romañach, R.J., 2009. Near-infrared Spectroscopy for the In-line Characterization of Powder Voiding Part I: Development of the Methodology. J. Pharm. Innov. 4. 187-197.

Sablinskas, V., 2003. Instrumentation, in: Gauglitz, G., Vo-Dihn, T. (Eds.), Handbook of Spectroscopy. Wiley-VCH Verlag GmbH & Co. KGaA, Weinheim, Germany, pp. 48-69.

Santomaso, A.C., Canu, P., 2001. Transition to movement in granular chute flows. Chem. Eng. Sci. 56, 3563-3573.

Savitzky, A., Golay, M.J.E., 1964. Smoothing and Differentiation of Data by Simplified Least Squares Procedures. Anal. Chem. 36, 1627-1639.

Schaber, S.D., Gerogiorgis, D.I., Ramachandran, R., Evans, J.M.B., Barton, P.L., Trout, B.L., 2011. Economic Analysis of Integrated Continuous and Batch Pharmaceutical Manufacturing: A Case Study. Ind. Eng. Chem. Res. 50, 10083-10092.

Schaefer, T., Holm, P., Kristensen, H.G., 1992. Melt pelletization in a high shear mixer. 1. Effects of process variables and binder. Acta Pharm. Nord. 4, 133-140.

Schofield, C., 1976. The Definition and Assessment of Mixture Quality in Mixtures of Particulate Solids. Powder tech. 15, 169-180.

Shaw, R.A., Mantsch, H.H., 1999. Near-IR Spectrometers, in: Tranter, G., Holmes, J., Lindon, J., (Eds.), Encyclopedia of Spectroscopy and Spectrometry, Academic Press, pp.1451-1461.

Sekulic, S.S., Ward II, H.W., Brannegan, D.R., Stanley, e.D., Evans, C., Sciavolino, S.T., Aldridge, P.K., 1996. On-Line Monitoring of Powder Blend Homogeneity by Near-Infrared Spectroscopy. Anal. Chem. 68, 509-513.

Sekulic, S.S., Wakeman, J., Doherty, P., Hailey, P.A., 1998. Automated system for the on-line monitoring of powder blending processes using near-infrared spectroscopy Part II. Qualitative approaches to blend evaluation. Pharm. Biomed. Anal. 17, 1285-1309.

Shi, Z., Cogdill, R.P., Short, S.M., Anderson, C.A., 2008. Process characterization of powder blending by near-infrared spectroscopy: Blend end-points and beyond. J. Pharm. Biomed. Anal. 47, 738-745.

Shinbrot, T., Muzzio, F.J., 2007. Mixing and Segregation in tumbling Blenders, in: Swarbrick, J. (Ed.), Encyclopedia of Pharmaceutical Technology, 3rd Informa Healthcare USA, Inc, New York, pp. 2352-2367.

Sommer, K., 2012. Mixing of Solids, in: Ullmann's Encyclopedia of Industrial Chemistry, 7th Wiley-VCH Verlag GmbH & Co. KGaA, Weinheim, pp. 403-419.

Staniforth, J.N., 1982. Advances in powder mixing and segregation in relation to pharmaceutical processing. Int. J. Pharm. Tech. & Prod. Mfr., 3 (Suppl), 1-12.

Steiner, G., 2003. Measurement techniques, in: Gauglitz, G., Vo-Dihn, T. (Eds.), Handbook of Spectroscopy. Wiley-VCH Verlag GmbH & Co. KGaA, Weinheim, Germany, pp. 70-88.

Storme-Paris, I., Clarot, I., Esposito, S., Chaumeil, J.C., Nicolas, A., Brion, F., 2009. Near Infrared Spectroscopy homogeneity evaluation of complex powder blends in a small-scale pharmaceutical preformulation process, a real-life application. Eur. J. Pharm. Biopharm. 72, 189-198.

Sudah, O.S., Coffin-Beach, D., Muzzio, F.J., 2002. Effects of blender rotational speed and discharge on the homogeneity of cohesive and free-flowing mixtures. Int. J. Pharm. 247, 57-68.

Sulub, Y., Wabuyele, B., Gargiulo, P., Pazdan, J., Cheney, J., Berry, J., Gupta, A., Shah, R., Wu, H., Khan, M., 2009. Real-time on-line blend uniformity monitoring using near-infrared reflectance spectrometry: A noninvasive off-line calibration approach. J. Pharm. Biomed. Anal. 49, 48-54.

Summers, M.P., Aulton, M.E., 2007. Granulation, in: Aulton, M.E. (Ed), Aulton's Pharmaceutics The Design and Manufacture of Medicines, 3rd Churchill Livingstone Elsevier, Hungary, pp.410-424.

Tamara, A.J., Yap, C., Mannan, M.A., 2006. Gravity flow of polymeric bulk solids in pneumatic conveying system. Chem. Eng. Sci. 61, 7836-7849.

Train, D., 1959. Mixing of Pharmaceutical Solids: The General Approach. J. Am. Pharmaceut. Assoc. 49, 265-271.

Twitchell, A.M., 2007. Mixing, in: Aulton, M.E. (Ed), Aulton's Pharmaceutics, The design and manufacture of medicines, 3rd Churchill Livinstone Elsevier, Hungary, pp. 152-167.

US v. Barr Laboratories, Inc., 812 F. Supp. 458 - Dist. Court, D. New Jersey 1993.

Van Melkebeke, B., Vermeulen, B.,Vervaet, C., Remon, J.P., 2006. Melt granulation using a twin-screw extruder: A case study. Int. J. Pharm. 326, 89-93.

Vanarase, A.U., Alcalà, M., Jerez-Rozo, J. I., Muzzio, F.J., Romañach, R.J., 2010. Real-time monitoring of drug concentration in a continuous powder mixing process using NIR spectroscopy. Chem. Eng. Sci. 65, 5728-5733.

Vanarase, A.U., Muzzio, F.J., 2011. Effect of operating conditions and design parameters in a continuous powder mixer. Powder Tech. 208, 26-36.

Venables, H.J., Wells, J.I., 2001. Powder Mixing. Drug Dev. Ind. Pharm. 27, 599-612.

Vercruysse, J., Córdoba Díaz, D., Peeters, E., Fonteyne, M., Delaet, U., Van Assche, I., De Beer, T., Remon, J.P., Vervaet, C., 2012. Continuous twin screw granulation: Influence of process variables on granule and tablet quality. Eur. J. Pharm. Biopharm. http://dx.doi.org/10.1016/j.ejpb.2012.05.010

Vervaet, C., Remon, J.P., 2005. Continuous granulation in the pharmaceutical industry. Chem. Eng. Sci. 60, 3949-3957.

Vervaet, C., Remon, J.P., 2009. Melt Granulation in: Parikh, D.M. (Ed), Handbook of Pharmaceutical Granulation Technology, 3rd, Informa Healthcare, pp. 435-448.

Virtanen, S., Antikainen, O., Yliruusi, J., 2007. Uniformity of poorly miscible powders determined by near infrared spectroscopy. Int. J. Pharm. 345, 108-115.

Wargo, D.J., Drennen, J.K., 1996. Near-infrared spectroscopic characterization of pharmaceutical powder blends. J. Pharm. Biomed. Anal. 14, 1415-1423.

Weinekötter, R., Gericke, H., 2006. Mixing of solids. Springer, Dordrecht, pp. 107-129.

Weingerl, U., Schaflinger, U., 2000. Feeding of granular material on conveyer bands or chutes. Powder Tech. 108, 1-5.

Williams, J.C., Rahman, M.A., 1970. The continuous mixing of particulate solids. J. Soc. Cosmetic Chemists 21, 3-36.

Williams, J.C., 1972. The Mixing of Solid Particles. Pharm. Ind. 34, 816-820.

Wold, S., 1991. Chemometrics, why, what and where to next? J. Pharm. Biomed. Anal. 9, 589-596.

Wold, S., 1995. Chemometrics; what do mean with it, and what do we want from it? Chemometr. Intell. Lab. Sys. 30, 109-115.

Wold, S., Sjöström, M., 1998. Chemometrics, present and future success. Chemometr. Intell. Lab. Sys. 44, 3-14.

Wold, S., Antti, H., Lindgren, F., Öhman, J., 1998. Orthogonal signal correction of near-infrared spectra. Chemom. Intell, Lab. Syst. 44, 175-185.

Wold, S., Sjöström,M., Eriksson, L., 2001. PLS-regression. A basic tool of chemometrics. Chemom. Intell. Lab. Syst. 58, 109-130.

Workman, J.J., Burns, D.A., 2001. Commercial NIR Instrumentation, in: Burns, D.A., Ciurczak, E.W., Handbook of Near-Infrared Analysis, 2nd. CRC Taylor & Francis, USA, pp. 53-70.

Wu, H., Tawakkul, M., White, M., Khan, M.A., 2009. Quality-by-Design (QbD): An integrated multivariate approach for the component quantification in powder blends. Int. J. Pharm. 372, 39-48.

Zhang, Y.E., Schwartz, J.B., 2003. Melt granulation and heat treatment for wax matrix-controlled drug release. Drug Dev. Ind. Pharm. 29, 131-138.

3 Research aims

The overall aim of this study was to evaluate different factors affecting the final quality of a pharmaceutical blend using NIR spectroscopy in diffuse reflectance modality as the analytical tool.

The first study aimed to identify segregation tendency due to physical incompatibilities among the formulation components by an optical tracer and by an off-line NIR-based method. The physical parameters under study were mean particle size, particle size distribution, density, and flow behavior.

The aim of the second study was the real-time blend uniformity monitoring of two active ingredients in a batch mixing process by NIR, as well as to investigate the influence of melt-granulation on the spectroscopic features of the formulation.

The objective of the third study was to develop an analytical method based on NIR spectroscopy for the in-line quantification of drug content in a continuous blending process. A second aim was to examine the influence that the process parameters such as stirring rate and mass flow rate exert on the NIR measurements.

The objectives of the fourth study include the development of a NIR calibration method for powder flowing down a chute, as well as to estimate the NIR sampled mass by considering the powder velocity.

Overall, the four sections give an insight into the batch and continuous mixing of powders, and the critical factors associated to the homogeneity of a pharmaceutical formulation.

4 Particle size and segregation studied by NIR

This work was presented at the FIP World Congress of Pharmacy and Pharmaceutical Sciences, Hyderabad, India, 2011. Awarded the Best Young Pharmacist Presentation of the Industrial Pharmacy Section.

This work was presented at the 16th International Conference of Near Infrared Spectroscopy, La Grande-Motte, 2013. Granted the Q-interline Sampling Award 2013.

Graphical abstract

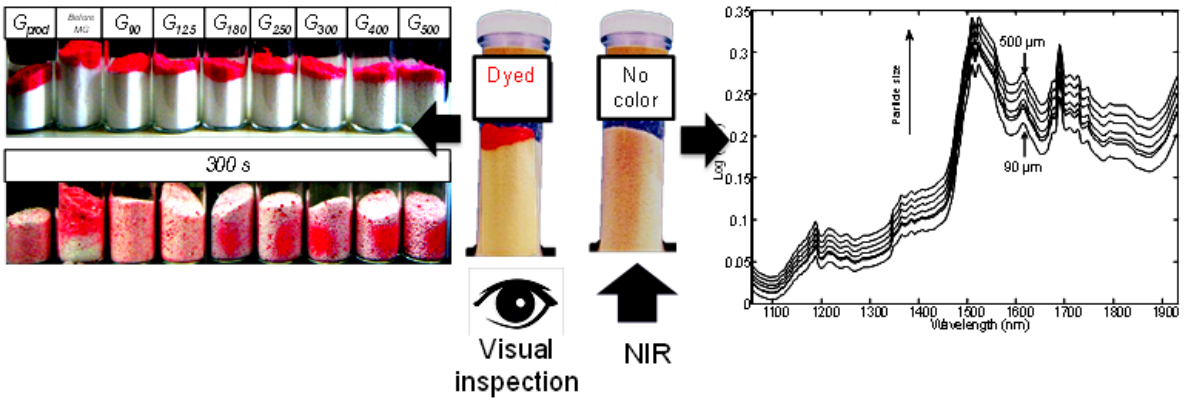

4.1 Abstract

The aim of this study was to evaluate the influence of the granules particle size on the segregation of a second API. Binary blends consisting of granulated material (96 %m/m) and an API (4% m/m) were prepared. The granules particle size was studied by near-infrared (NIR) spectroscopy using Kubelka-Munk function and the transformation of reflectance toabsorbance values in order to focus the analysis on the physical properties. Furthermore, an off-line NIR model was developed for the quantification of the granules mean particle size.

Additionally, a gravimetric procedure for the low dose drug quantification was established for the reference values acquisition. The method consisted of accurately weighing each formulation component into glass vials. Thus, the reference values were the mass weighed. Vials containing the powder samples were mixed and subsequently scanned in diffuse reflectance mode on a Fourier Transform NIR spectrometer. Partial least square regression was applied for correlating the spectral data with the reference values. The content of the low dose drug was accurately predicted. The gravimetric method was shown to be accurate, fast and convenient.

Keywords

PAT, blending, NIR, homogeneity, melt granulation, particle size, segregation, Kubelka-Munk.

4.2 Introduction

Segregation, or demixing, is a potential issue in the pharmaceutical environment. Segregation is associated with problems in the content uniformity of tablets. Segregation can occur due to vibrations during the handling and storage of the blend; it can also appear during the discharge of the blend. The presence of segregation is due to the separation of the components due to physical attributes e.g. size, shape, cohesion, density, etc. There are many segregation mechanisms reported in literature, examples include percolation, elutriation, trajectory segregation (Aiache and Beyssac, 2007), and one of the major segregation causes is particle size incompatibilities. The importance of particle size cannot be underestimated and has been widely demonstrated (Johnson, 1975; Rees, 1977; Train, 1959; Yalkowsky and Bolton, 1990; Zhang and Johnson, 1997).

Physical properties of the material can provide hints about possible segregation problems. Fan et al. (1970) reported that particulate material holding small repose angles, good flow behavior and small friction coefficient may have mixing problems since segregation can occur due to their rapid movement.

Particle-particle interactions play an important role in the powder flow behavior. For free-flowing mixtures it is often necessary to restrict the freedom of movement of the particulate material. On the other hand, for cohesive blends the problem is the opposite. A cohesive powder aggregate needs to be broken down in order to allow the individual particles to relocate (Harnby, 2000). The flow behavior of a material is associated with the surface of a particle; particles having large diameters (above 100 µm) behave as cohesionless blends, since gravitational force dominates over interparticle electrostatic forces. Under this particle range, cohesive powders dominate, thus interparticle interactions are significant (Fan et al., 1990). However, it is important to point out that there is no specific classification size limit for free-flowing and cohesive materials.

Granulation is a common process in the pharmaceutical industry; in most cases the aim of granulation is to increase the mean particle size and to improve the flow character of the

powder. The granules can be further blended with other excipients or APIs, thus a correct identification of the particle size range is fundamental in order to prevent segregation of the blend.

Near-Infrared (NIR) spectroscopy has been widely applied in the measurement of particulate materials and the influence of physical properties on the NIR spectrum is well-known. Several preprocessing techniques have been developed in order to reduce the effect of particle size, particle shape and packaging differences. These techniques include first and second derivatives, standard normal variate (Barnes et al., 1989) and multiple scattering correction (Geladi et al., 1985; Martens and Stark, 1991), which are meant to focus the analysis into the chemical information contained in the spectra. It is also possible to take advantage of the physic-chemical nature of NIR spectra in order to extract the physical information of the material. NIR has been successfully applied for particle size measurements (Gamble and Barnett, 1937; O'Neil et al., 1998; 2003, Pasikatan, et al., 2001), proving that NIR is a potential tool for particle size measurements.

One of the challenges of particle size measurements by NIR is to extract the information referred to the size variations from the rest of the physical and chemical information. As mentioned before, most of the preprocessing techniques are focused on reducing this source of variability. In this study two different approaches were applied. The first approach was the transformation of reflectance to absorbance and the second was the Kubelka-Munk function (Kubelka, 1948).

The aim of this study was to evaluate the influence of the particle size of granules on the homogeneity of a second API by NIR and visual inspection. PLS-models for the prediction of the granules mean particle size and quantification of the API in a lower concentration were developed.

4.3 Materials and methods

The binary blends consisted of a granulated material (96 % m/m) and an active pharmaceutical ingredient (4% m/m), referred to as A2. The granulated material contained a polymer and an API which will be referred to as A1.

Powder characterization

The morphological characterization was performed by scanning electron microscopy (SEM) (ESEM XL 30 FEG, Philips, The Netherlands) at an applied voltage of 10 kV and magnifications of 100-2000 times. The sample preparation included placing the powder on carbon adhesive followed by gold plating.

The average particle size was measured using a laser diffraction system (Mastersizer S long bed, Malvern, Worcestershire, UK). The lens range was within the particle size range of 4.2-3500 µm. The samples were dispersed through a dry powder feeder and the measurements were carried out five times. The obscuration value was kept between 10-30% and the residual value under 1%. The analysis was set in “polydisperse” mode. The volume mean diameter (D [4, 3]), the mass median diameter (D [v, 0.5]) and the span values were recorded.

For the flowability determination, approximately 100 g of powder were poured in a volumetric cylinder and the unsettled apparent volume (V_0) was measured, then the sample was tapped until no volume changes occurred (V_f), the final volume was recorded and bulk (ρ_{bulk}) and tapped (ρ_{tapped}) densities were computed. The compressibility index and the Hausner ratio of the API A before and after the MG process were determined following the procedure given in the USP 35:

Equation 4-1 Compressibility Index =100 x [($\boldsymbol{\rho_{tapped}}$ -$\boldsymbol{\rho_{bulk}}$) /$\boldsymbol{\rho_{tapped}}$]

Equation 4-2 Hausner Ratio= ($\boldsymbol{\rho_{tapped}}$ /$\boldsymbol{\rho_{bulk}}$)

Melt-granulation and milling

The API A was combined with a cellulose based polymer, the powders were fed into a twin screw extruder (Leistritz Extrusionstechnik GmbH, Nuremberg, Germany), the extrusion temperatures ranged from 20 to 135 °C (under the melting point of the API A), and the screw speed was set at 90 rpm.

The extruded product was split into two groups. The first group was milled in a Frewitt hammer mill (Friburg, Switzerland) with knives forward at 2100 rpm and the screen size was fixed at 1000 µm, the milled extruded product was used without further particle selection in order to keep a broad particle size distribution, these granules will be referred as G_{BROAD}. The second set of extruded API was milled in a FitzMill Type L1A (The Fitzpatrick Company Europe, Sint-Niklaas, Belgium) at 3000 rpm with a screen size of 1000 µm, the milled extruded was sieved using a sieve shaker (Vibro, Retsch, Haan, Germany) at level 40 for 15 min with sieve openings of 90, 125, 180, 250, 315, 400, 500, and 700 µm. The sieve fraction of 700 µm was discarded. The granules will be referred as G_{90}, G_{125}, G_{180}, G_{250}, G_{315}, G_{400}, and G_{500} where the subscript indicates the sieve opening.

Tracer preparation

As an optical tracer, A2 was selected in order to resemble to the original component characteristics. The dying solution consisted of Erythorsine which was sprayed over a thin layer of A2 disposed in a tray. The drying phase was performed at 50°C on a static oven. Finally the dyed A2 powder was screened with a mesh of 300 µm. The tracer was used only for visual inspection and its resulting blends were not measured by NIR.

Mixing and segregation test

Vials with a 4 mL capacity were filled with 900 mg of different sieve fractions: G_{90}, G_{125}, G_{180}, G_{250}, G_{315}, G_{400}, and G_{500}, extra samples corresponding G_{BROAD}, as well as a physical blend of polymer and A2 (before melt-granulation) were included in the study. Subsequently 100 mg

of the tracer were added to each vial. The vials were blended for 0.5, 1, 2, 5, and 10 minutes. After each time point the distribution of the tracer in the vial was observed.

Blending and NIR instrumentation

All NIR measurements were performed on a NIRFlex-N500 Fourier transform spectrometer with a reflectance cell (Büchi Labortechnik, Switzerland). Spectral data acquisition was done over the wavelength range of 4000-10000 cm^{-1}, with 4 cm^{-1} resolution with an illuminated spot of 8 mm diameter. The samples were scanned through a borosilicate vial. The vial dimensions were 4mm diameter and 15 mm height and the illuminated spot was 8 mm.

The wavenumbers (1/cm) were converted to namometers according to Equation 4-3:

Equation 4-3

$$\boldsymbol{Wavelength\ (nm)} = \frac{\mathbf{10^7}}{\boldsymbol{wavenumber}\left(\frac{\mathbf{1}}{\boldsymbol{cm}}\right)}$$

The software used for the chemometrical analysis were Matlab (The Mathworks Inc.) version 2012Ra with PLS_toolbox (Eigenvector Research Inc.) version 6.7.1

Calibration samples

Calibration model for the G_{BROAD} granules

The G_{BROAD} granules were used without further selection in order to keep a wide particle size distribution. Sample preparation included accurately weighing (Mettler Toledo XS204 Delta range) G_{BROAD} and A2, followed by a mixing step (Turbula type T2C, W. Bachofen, Switzerland) of 5 minutes. The binary calibration samples covered a range of 70-130% of A2 target value (4 % m/m). Each vial was measured through the bottom of the vial by NIR, using the gravimetric values as reference. The reference values were matched to their spectral data and a PLS model was developed for A2 quantification. The validation set corresponded to one third of the samples previously excluded from the calibration set.

Calibration model for the sieve fractions of 90 and 125 µm

The sieve fractions of the granules corresponding to G_{90} and G_{125} were collected separately. Binary blends from each of the sieve fractions were prepared by accurately weighing the granules and A2 powder into the vials. The binary calibration samples covered a range of 70-130% of A2 target value (4% m/m). Each sample was measured through the bottom of the vial by NIR, using the gravimetric values as reference. Spectral data from the binary blends of both sieve fractions (90 and 125 µm) were used for the computation of independent PLS models. The gravimetric reference values were matched to their spectral data and a PLS model was developed for A2 quantification. The validation set corresponded to one third of the samples previously excluded from the calibration set.

Mixing kinetics

Mixing profiles were obtained under different conditions of loading order and particle size for the target formulation.

In order to test the loading order influence, five vials were first filled with the granules followed by A2 powder, and five extra vials in the inverse filling order were similarly prepared.

The influence of granules particle size was tested by filling ten vials first with granules from the 90 µm sieve fraction, followed by A2 loading. The same procedure was followed for the 125 µm sieve fraction.

For each condition, an extra vial with dyed A2 used instead of the normal A2 powder was prepared. All the vials were mixed together in a Turbula mixer. The mixer was stopped at 1, 2, 3, 4, 5, 10, 30, 60, 90, 120 and 150 rotations, and the samples (excluding the colored ones) were measured by NIR at the different mixing times. A2 quantification was done at each time point and a concentration profile was generated.

Figure 4-1 illustrates the method followed for this study.

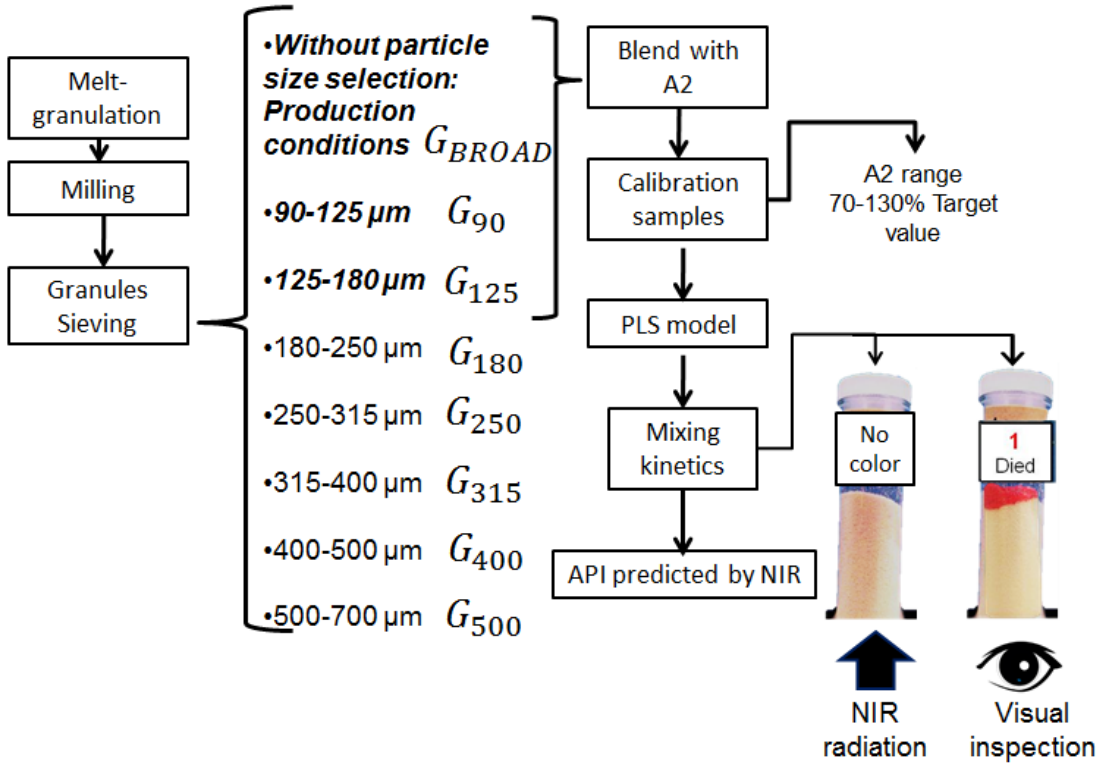

Figure 4-1 Particle size project overview.

4.4 Results and discussion

Granules characterization

The granules used in this study were formed through a melt-granulation step, in which only the polymer was melted-down and the temperature was kept under the melting point of A1. The A1 granules represented 96 % (m/m) and A2 4% (m/m) of the binary blends. Achieving a homogeneous blend of two components with a large difference in mass ratios is challenging mostly for the homogeneity of the API in lower proportion. Despite the fact that the homogeneity of the lower dose component is the critical parameter, the physical characteristics of the granules are of great importance. Table 4-1 contains the particle size and density values for each sieve fraction including G_{BROAD}, A1 (raw API before melt-granulation), and A2. The difference in densities among the formualtion ingredients can affect the physical stability of the mixture, since the heavier particles have the tendency to fall to the bottom while the lighter particles move to the top of the powder bed. In Table 4-1, the

densities of the granular sieve fractions as well as the raw APIs were within the range of 0.43 to 0.55 g/cm^3.

Bulk density and tapped density were used for the calulation of the compressibility index and Hausner ratio, which are correlated to a flow character. A1 was identified with “fair” flow, therefore A1 could present inconvinients when the fast flow inside the tableting dyes is requiered. The flow of A1 was greatly improved to “excellent” in G_{BROAD} after the melt granulation was performed. Fast or free flowing materials are desired for the tabletting process, on the other hand during a blending process it is desirable to have some cohesion in order to avoid further segregation problems. Besides, A2, did not undergo a granulation process and presented a “passable” flow behavior. The reasons for keeping A2 as small particles is that large particle populations of A2 are necessary for achieving blend homogeneity and small particles of A2 possess higher surface area; therefore dissolution is directly related to the particle size.

Table 4-1 Granules and A2 characterization

Parameter	A1	A2	G_{BROAD}	G_{90}	G_{125}	G_{180}	G_{250}	G_{315}	G_{400}	G_{500}
Sieve fraction	-	-	-	90-125 µm	125-180 µm	180-250 µm	250-315 µm	315-400 µm	400-500 µm	500-700 µm
Bulk density [g/cm^3]	0.48±0.01	0.45±0.01	0.55±0.01	0.453±0.002	0.449±0.001	0.430±0.002	0.444±0.003	0.446±0.000	0.456±0.000	0.484±0.002
Tapped density [g/cm^3]	0.58±0.01	0.57±0.01	0.58±0.01	0.486±0.000	0.473±0.003	0.459±0.004	0.460±0.003	0.472±0.000	0.483±0.003	0.506±0.004
Compressibility index	17.72±1.4	20.85±0.91	6.10±1.00	6.623±0.45	4.998±0.471	6.305±0.513	3.504±0.031	5.357±0.000	5.614±0.608	4.472±0.502
Hausner ratio	1.22±0.02	1.26±0.02	1.07±0.01	1.071±0.005	1.053±0.005	1.067±0.006	1.037±0.000	1.057±0.000	1.060±0.007	1.047±0.006
Flow character	Fair	Passable	Excellent	Excellent	Excellent	Excellent	Excellent	Excellent	Excellent	Excellent
Mean particle size d_{50} [µm]	57.34±4.45	59.40±2.77	241.44±21.67	90.14±1.35	128.23±1.49	190.30±2.71	244.51±12.6	364.86±6.22	452.62±8.27	644.12±8.20
Span	2.43±0.25	2.91±0.63	5.58 ±0.22	1.50±0.02	1.55±0.03	1.50±0.02	1.51±0.09	1.38±0.13	1.30±0.05	1.11±0.03

Particle size and shape are the most important characteristics in powder blending. Small particles have higher cohesion due to interparticular forces such as van der Waals.These forces reduce the freedom of motion that originates segregation. The mean particle size of the granules increased accordingly to their sieve fraction. Therefore, G_{500} has the bigger particle size and is expected to induce segretation of A2 particles.

Granules characterization by NIR diffuse reflectance

The particle size of a sample has a significant effect on the NIR spectrum. Particle size changes interfere with the amount of radiation scattered by the sample. Figure 4-2 shows the spectra for each of the sieve fractions.The spectra keep the same shape, but the spectrum baseline decreased with the particle size. The intensity of the reflectance signal decreased for bigger granules, since scattering of the radiation diminished and light can penetrate deeper into the powder bed.The same effect was observed in other studies (Rantanen et al., 2000; O'Neil et al., 2003), where the reflectance exhibited an inverse relationship with the particle size. The highest reflectance was obtained for particles under 90 µm; in this case the cohesion, density and porosity played an important role, thus increasing the reflectance of the incidet light. An explanation is that reflectance tends to be proportional to the surface of the particles and smaller particles have greater surface. Additionally, when the particles are smaller the incident radiation changes direction more often than with longer particles.

The spectra obtained in diffuse reflectance were transformed by means of the Kubelka-Munk equation or converted to absorbance values $(\log 1/R)$. The Kubelka-Munk equation was used assuming that the radiation was isotropically distributed, that the particles were randomly distributed and that the layer presented diffuse reflection (Kubelka, 1948). Kubelka-Munk function $f(R)$ is the ratio of the absorption (k) and scattering (s):

Equation 4-4 $$\boldsymbol{f(R) = k/s.}$$

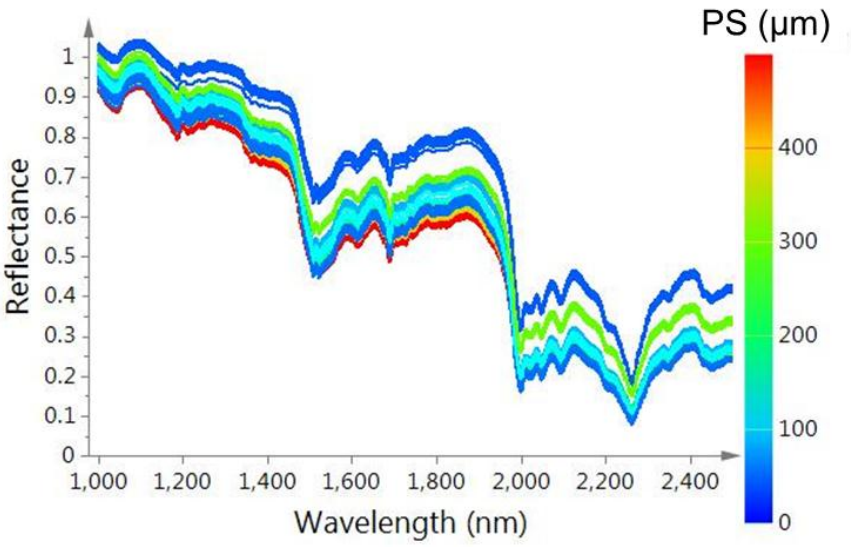

Figure 4-2 NIR reflectance spectra of granules with different mean particle size.

Figure 4-3 shows the spectra after Kubelka-Munk transform. The values of $f(R)$ increased with the particle size, therefore the ratio k/s also increased. Higher k/s values represented lower scattering, s for the bigger granules; this is in accordance with Szalay et al (2005) who observed the same trend. Smaller particles have a smaller k/s ratio, and therefore have lower absorbance and higher reflectance.

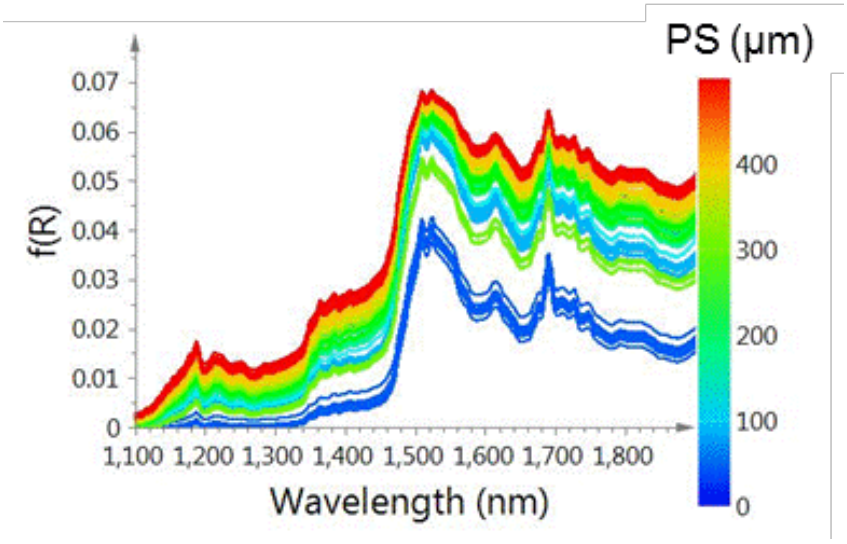

Figure 4-3 $f(R)$ for the different sieve fractions.

A PCA was carried on the $f(R)$ spectra, showing that the first principal component carried 92% of the variability associated with particle size differences (Figure 4-4). The second PC may contain the variability of chemical and physical inhomogeneities in the granules.

In this case the Kubelka-Munk conversion was tested in order to increase the lineartity of the spectral measurements with the particle size of the granules. Most of the preprocessing techniques are focused on the correction of multiplicative and additive artifacts on the spectra due to differences in particle size, shape, and particle packaging. In this study, the aim was to enhance and extract the information due to physical varibility of the spectra.

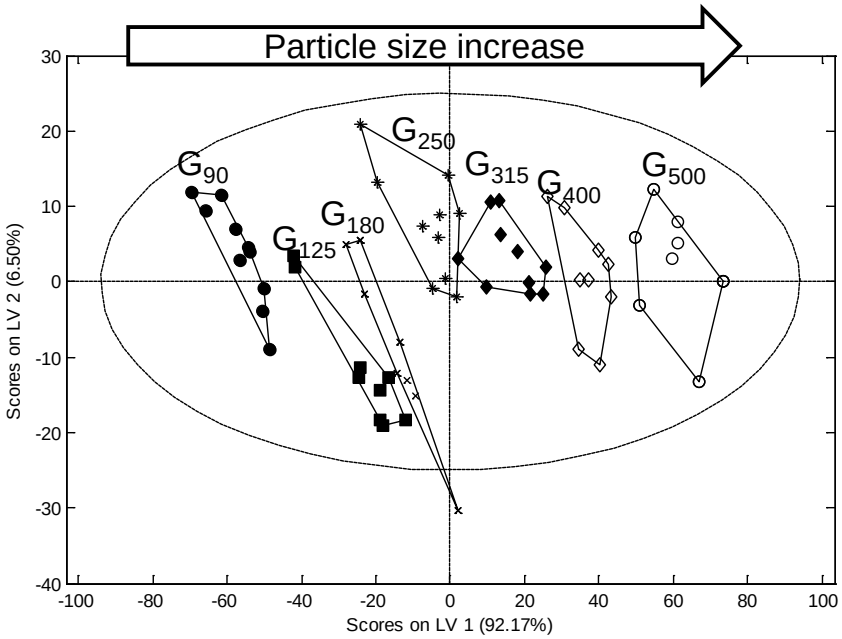

Figure 4-4 Scores plot for the $f(R)$valuescoresponding to the different sieve fractions.

A PLS model for the prediction of mean particle size was generated by matching $f(R)$ with the d_{50} values measured by laser diffraction for each of the sieve fractions. A second PLS model was generated using absorbance values instead of $f(R)$. Table 4-2 contains the description of each of the PLS models. It is clear that absorbance values gave lower RMSEP and prediction bias than $f(R)$. O'Neil et al. (2003) also found that for particle size distribution of microcrystalline cellulose, absorbance values gave the best performance and the lowest RMSEP compared with other preprocessing techniques. Out of these results, absorbance values are better suited for particle size measurements.

Table 4-2 Statistics for particle size PLS models

Parameter	PLS model for $f(R)$	PLS model Absorbance
Xcum [%]	99.98	99.97
Ycum [%]	97.46	98.17
R^2	0.969	0.983
PC	4	4
Root Mean Square Error of the Prediction, RMSEP [µm]	26.7	15.9
Prediction Bias [µm]	4.13	0.66
Wavelength [nm]	1100-1900	1100-1900

Particle size and segregation tendency

Particle beds have variable particle size populations and their behavior is difficult to predict. Difference in inter-particulate bonds, absolute size and size distribution of the particles need to be controlled if a high-quality mixture needs to be produced (Chowhan et al., 1981; Fan et al., 1970). In order to visually identify particle size incompatibilities between A1 and A2 granules, an experiment consisting of a colored tracer was carried out. The tracer consisted of A2 particles dyed with Erythrosine, producing an intense pink color. The tracer was not measured by laser diffraction nor by NIR due to changes in the refraction index as a result of the pigmentation.

SEM micrographs showed higher content of fines for A2 (Figure 4-5a) than for the tracer (Figure 4-5b). Two possibilities can produce this situation: one is a non-representative sampling and the second reason could be that dying produced a slight agglomeration of the particles.

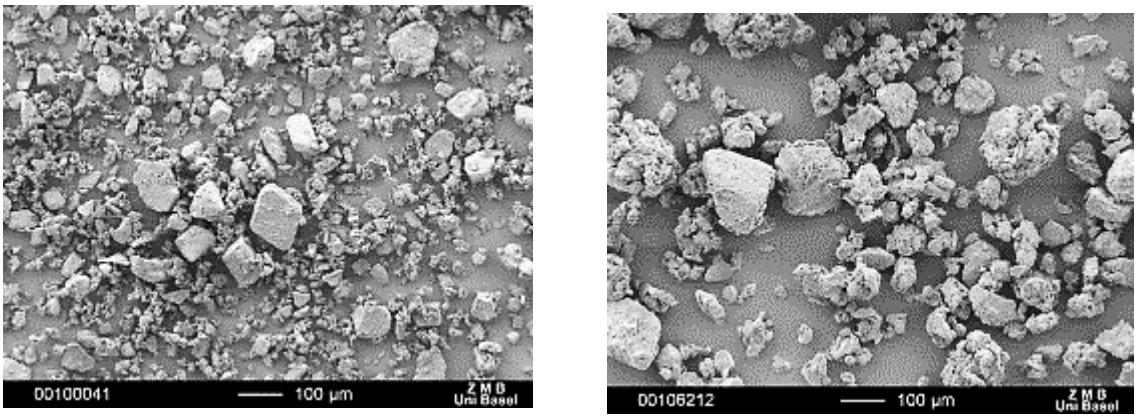

(a) *(b)*

Figure 4-5 SEM micrographs of A2 (a) and the tracer (b).

Glass vials were filled with granules and tracer, covering a total of nine different presentations of A2: A2 before the melt granulation process (physical blend between A2 and polymer), granules with a wide particle size distribution (G_{BROAD}), and granules coming from different sieve fractions: G_{90}, G_{125}, G_{180}, G_{250}, G_{315}, G_{400}, and G_{500}. Each vial was blended for 30, 60 and 300 seconds as shown in Figure 4-6. From this figure it is possible to make the next observations:

- **G_{BROAD}** shows fast and homogenous blending of the granules with the tracer. In this case a good compromise between blending and flow was achieved. The small particles form the tracer as well as from the granules fill the inter-particular voids, reducing segregation tendencies.
- **Powder before melt-granulation**: under these conditions the components did not reach the homogeneity state at 300 seconds. Here the geometry of the vial was one of the limiting factors together with high cohesion. In the case of highly cohesive particles, higher energy is needed for breaking down the clusters formed due to inter-particular attraction forces such as van der Waals and electrostatic forces (Orr and Shotton, 1973; Staniforth, 1985). Mixing is generally enhanced by slight cohesion (Sarkar and Wassgren, 2010), on the other hand, high powder cohesion may be challenging for the achievement of an homogeneous blend, like in this situation. One of the advantages that cohesive powders possess is that once the homogeneity is

achieved, these blends are very stable and resistant to segregation; nevertheless these blends are not suitable for tableting due to bad flow behavior.

- **G_{90} and G_{125}**: There was no evident segregation of the tracer. The granules and the tracer visually formed a homogeneous blend after 30 seconds of blending. The sieve fractions of G90 and G125 appeared to be compatible with A2 particle size.
- **G_{180}, G_{250}, G_{315}, G_{400}, and G_{500}**, presented segregation. In these cases the tracer could easily percolate through the intra-granular voids formed by the big particles (Fan et al., 1990). Inter-particle percolation occurred due to the different physical nature of the granules and the tracer, failure zones were formed where the tracer could easily move through the interstices. This is the main problem of free-flowing materials: their easy motion can lead to severe segregation problems.

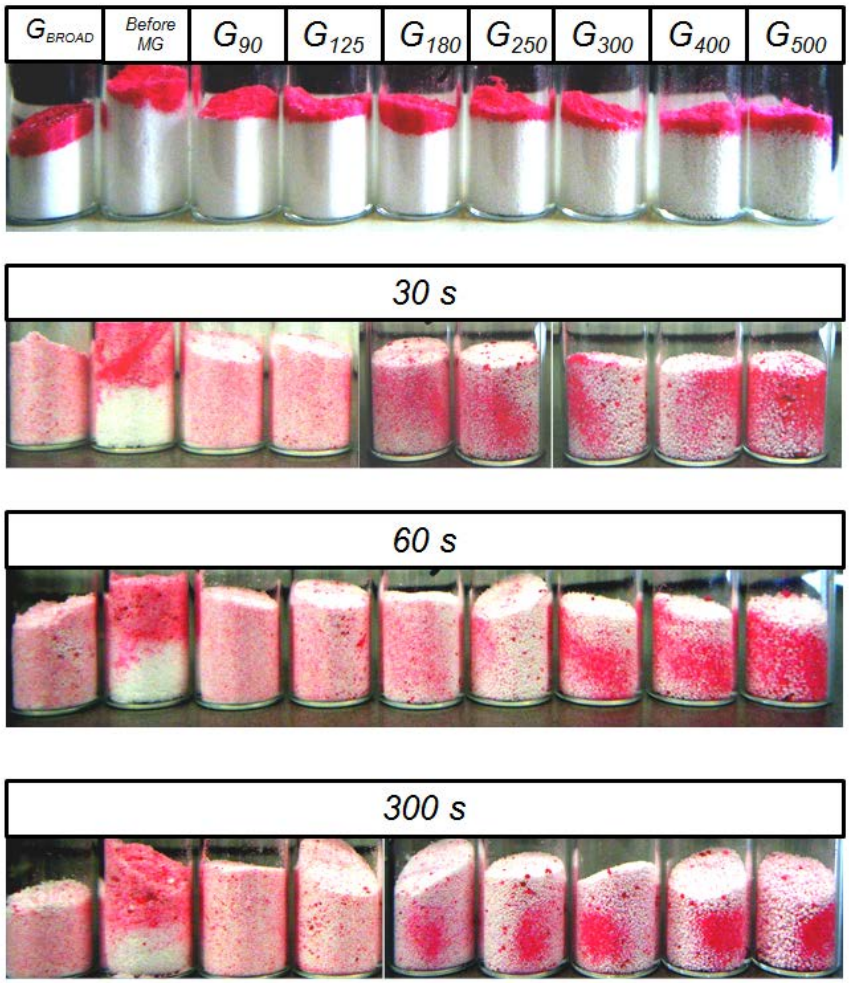

Figure 4-6 Visual evaluation of the mixing between A2-tracer and granules with different sieve fractions.

Although the experiment with the tracer is not of a quantitative nature, the information about segregation is very valuable and facilitates the selection of compatible particle size ranges. Therefore the granules sieve fraction of 90 um and 125 um and G_{BROAD} were chosen for further experimentation. Figure 4-7a shows that G_{BROAD} granules as aggregates with heterogeneous shapes and sizes. Figure 4-7b corresponds to the sieve fraction of 90-125 µm, the granules were uniform in shape and size as well as the granules from 125 to 180 µm (Figure 4-7 c).

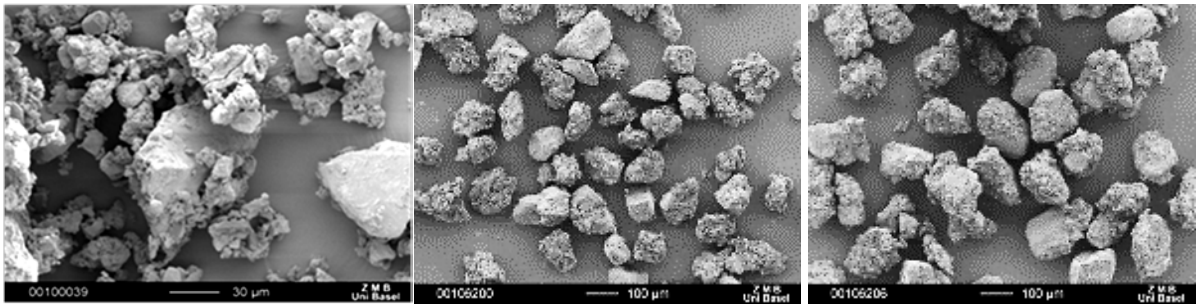

(a) (b) (c)

Figure 4-7 SEM micrographs of (a) granules without particle selection. (b) 90 µm sieve fraction and (c) 125 µm sieve fraction.

PLS model development for A2 quantification

Figure 4-8 shows the NIR spectra for A2 and G_{BROAD}. A2 has a sharp peak at 1554 nm, two extra wider peaks appear at 1200 nm and 1700 nm. These regions are rich in information for A2 and can be used for quantification purposes. In this section of the study, the chemical information is the one of interest. Therefore, the preprocessing techniques were chosen to reduce the multiplicative and additive effects caused by particle size variations. The combination of first derivative with Savitzky-Golay smoothing of 15 points was applied for baseline drift correction and for the magnification of small variations due to A2 concentration changes. After the first derivative, SNV was applied for removing the multiplicative interferences of scattering and particle size (Barnes, et al., 1989). This preprocessing combination was applied to each of the datasets; subsequently three PLS-models were

generated only differing on the granules particle size used for the binary blends. Each model was validated through an independent prediction set containing one third of the data, previously excluded from the calibration set.

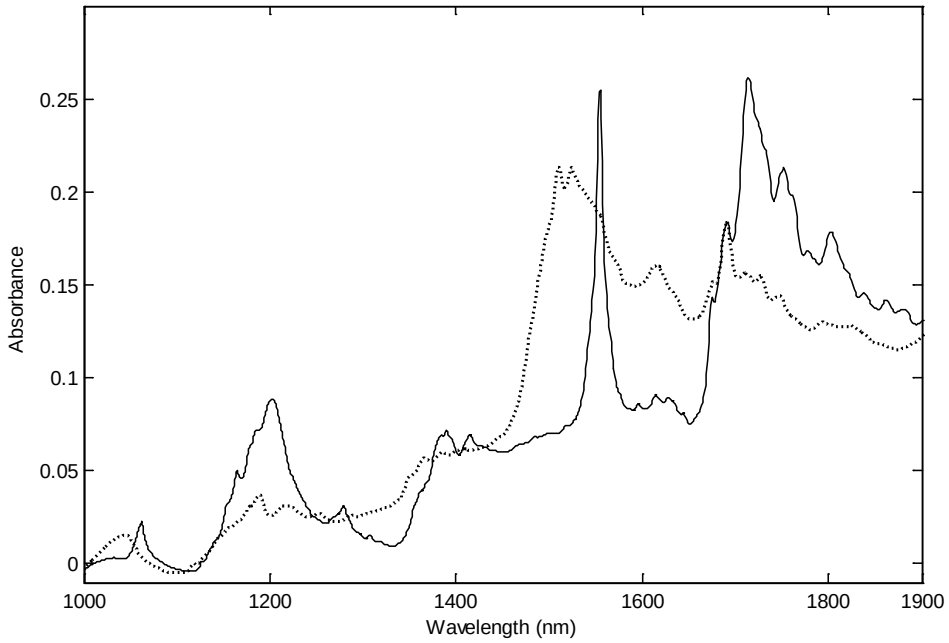

Figure 4-8 NIR spectra for the G_{BROAD} (dotted line) and A2 (continuous line).

Table 4-3 contains the relevant statistics for each of the PLS-models. All of them were computed using four principal components, which carried more than 97 % of the variability for the Y variable (A2 concentration). For each model the Root Mean Square Error of the Prediction (RMSEP) was calculated. The lowest RMSEP was found for the binary blend with G_{BROAD}, followed by G_{90} and the highest value was for G_{125} with 4.98% of the nominal value. The bias of the model followed the same trend as the RMSEP. Therefore, the best statistics were obtained for the G_{BROAD} PLS-model. This result can be associated with a better physical and chemical homogeneity of the A2-G_{BROAD} blend. The model that presented the highest bias and RMSEP was for the A2-G_{125} blend. This result could be associated with chemical inhomogeneities due to slight segregation by percolation of the A2 fine particles. Shaking of the vials was carefully avoided throughout the experiment because this mechanism of segregation is potentially influenced by vibrations.

Table 4-3 PLS-model statistics for the quantification of A2.

		Model 1	Model 2	Model 3
Granules type		G_{BROAD}	G_{90}	G_{125}
Number of latent variables		4	4	4
Xcum[a] [%]		95.54	88.27	92.89
Ycum[b] [%]		98.60	99.48	97.75
RMSEP	% Nominal	2.76	3.30	4.98
	% m/m	0.12	0.15	0.22
R^2		0.985	0.991	0.972
Prediction Bias		0.33	0.70	2.51

Influence of loading order

The blending of G_{BROAD} with A2 was studied as a function of A2 concentration changes. The quantification was performed by a PLS model developed for the A2-G_{BROAD} blend. In addition, an extra vial containing the tracer was used for visualization of the mixing process.

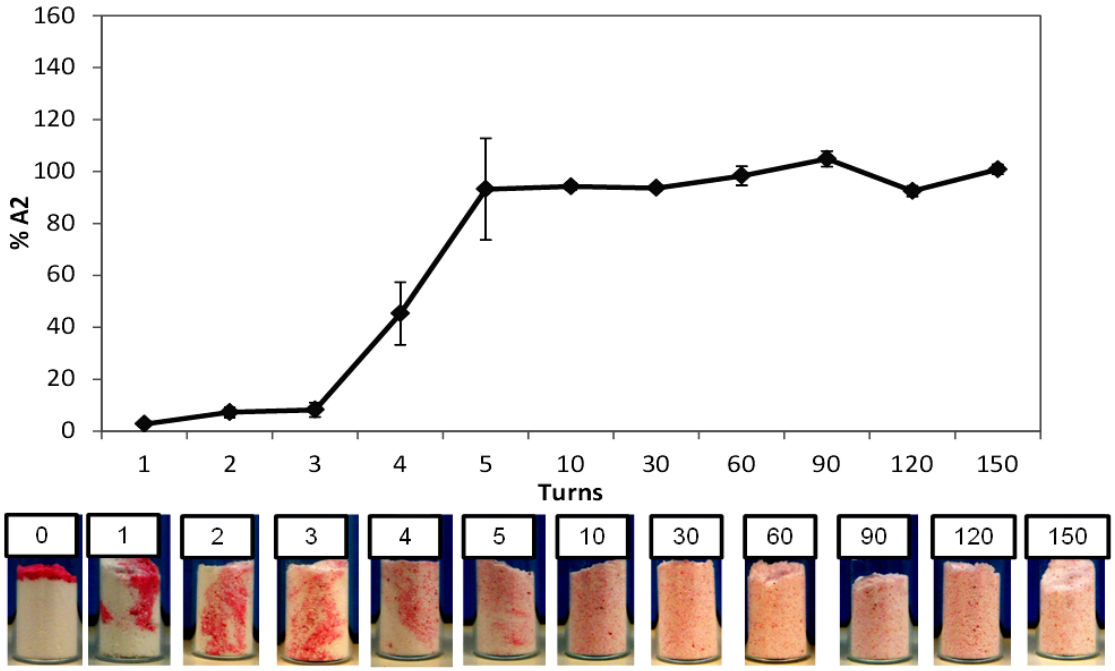

Figure 4-9 NIR predictions and influence of filling order, G_{BROAD} loaded first followed by A2. The bars represent standard error.

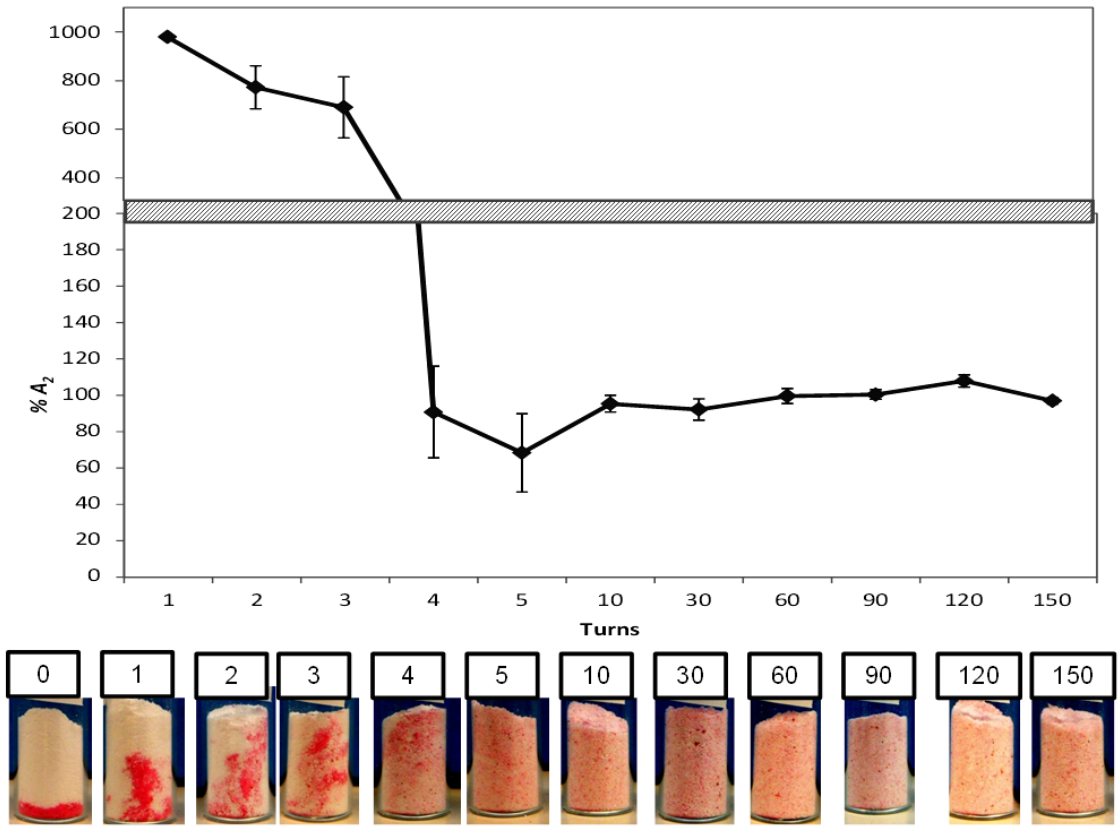

Figure 4-10 Mixing kinetics for A2 and G_{BROAD} blends followed by NIR and a visual tracer. Influence of filling order, A2 first followed by G_{BROAD}. The bars represent standard error.

Figure 4-9 shows the concentration variations for A2 at different numbers of turns. During the first three turns, it is mostly the granules that were in contact with the incident light from the NIR. The predicted level of A2 increased once the A2 particles reached the bottom of the vial where the blend was scanned. Turns 4 and 5 showed mainly convection mixing where the big aggregates of A2 were broken down and started to disperse throughout the powder bed. From ten turns onward, the blend seemed to reach homogeneity.

The filling order was inverted; A2 was loaded first followed by the granules. Figure 4-10 shows that during the first three turns, A2 was highly concentrated on the bottom of the vial, thus A2 was the main component in contact with the NIR light. Convection appeared at turns 3 to 5, showing the decrease on the A2 predicted values. From turn ten onwards, the blend stabilized.

The filling order influenced the NIR predictions during the beginning of the mixing; however, after the convection stage the predictions showed the same behavior.

Influence of granules particle size

Two different sieve fractions for the granules were selected. Figure 4-11 illustrates the mixing behavior of the A2-G_{90} blend. The mixing curve resembled the A2-G_{BROAD} blend (Figure 4-9). In both cases, during the first three turns A2 was forming an aggregate due to interparticle attractions. Once this aggregate was broken down as a result of convection mechanism, the blend stabilized.

In the case of the blend between A2 and G_{125} (Figure 4-12), the breakage of the initial A2-cluster appeared on the first two turns. This is a clear indicator of the free mobility of A2 particles among the G_{125} granules. The standard error was higher for this blend in comparison with G_{90} and G_{BROAD} blends. Despite the fact that the blend reached a stable state after 60 turns, this blend could be the most prone to exhibit segregation as a result of intergranular channels where A2 could easily flow and percolate.

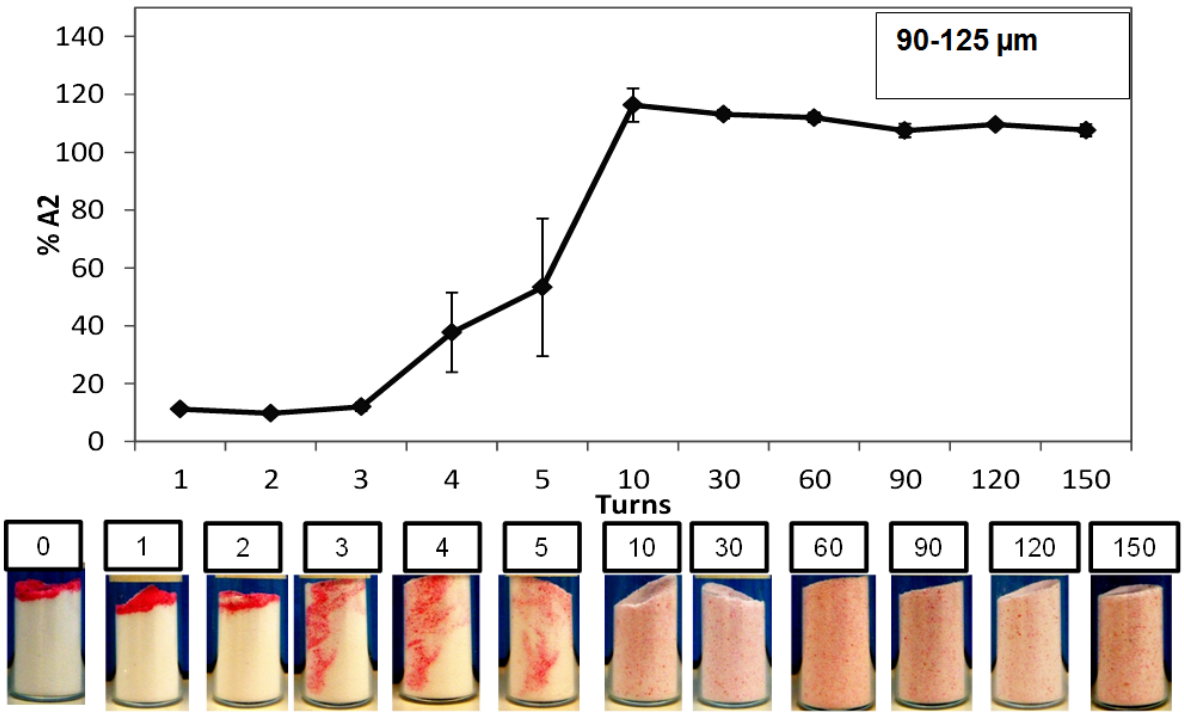

Figure 4-11 Mixing kinetics for A2 and G_{90} blends followed by NIR and a visual tracer.

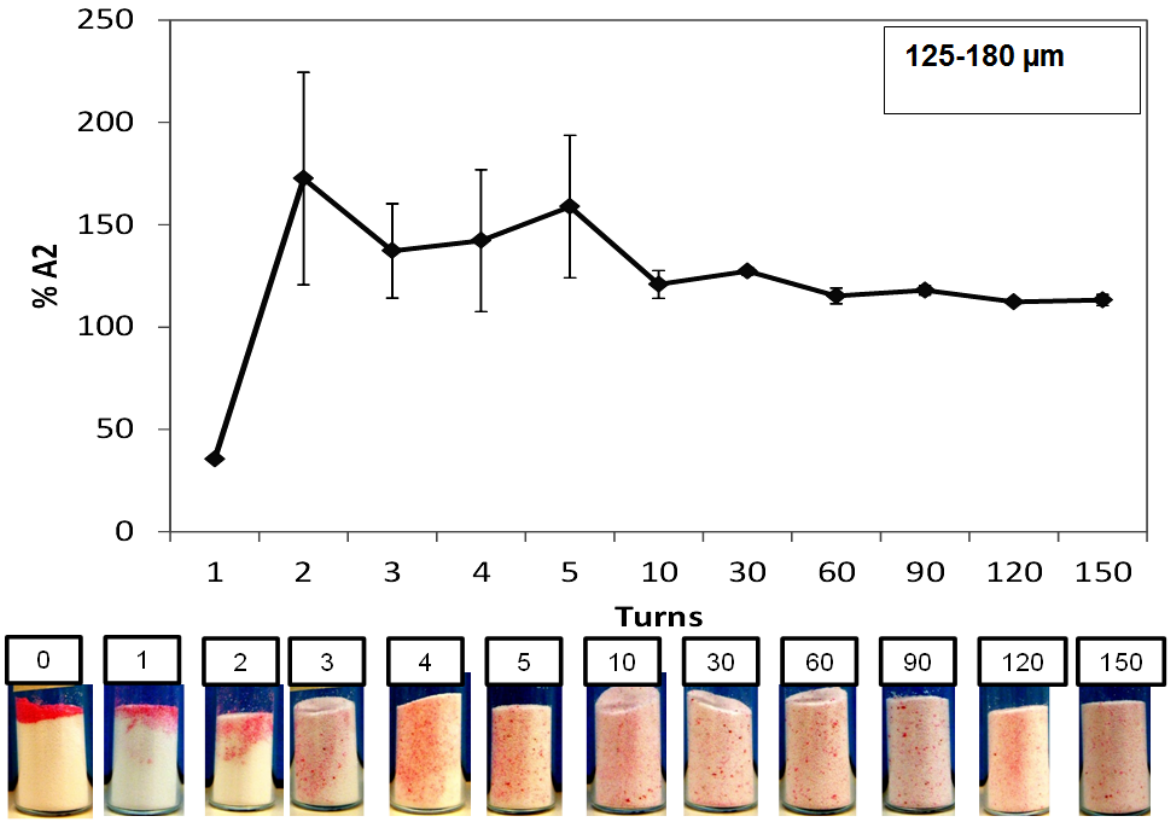

Figure 4-12 Mixing kinetics for A2 and G_{125} blends followed by NIR and a visual tracer.

4.5 Conclusions

Segregation tendencies were studied as a function of particle size incompatibilities between the blend components. The best blend performance was found for granules with a wide particle size distribution and for granules with small particle size. Big particles that exhibit free flowing behavior showed evident segregation due to percolation of the small particles.

NIR was used for mean particle size determination and for the quantification of the low dose active ingredient. NIR showed high potential for the particle size measurement of granules. By correct selection of the spectral pretreatments it was possible to extract the physical information from the NIR spectra.

The filling order showed no influence on the NIR predictions for the final blend. On the other hand, particle size was shown to influence the robustness of the final blend. Segregation

tendencies can be observed from the PLS model development in which higher RMSEP can indicate the presence of chemical and physical inhomogeneities on the calibration samples.

References

Aiache, J.-M., Beyssac, E., 2007. Powders as Dosage Forms, in: Swarbrick, J. (Ed.), Encyclopedia of Pharmaceutical Technology, 3rd Informa Healthcare USA, Inc, New York, pp. 2971-2982.

Barnes, R.J., Dhanoa, M.S., Lister, S.J., 1989. Standard Normal Variate Transformation and De-trending on Near-Infrared Diffuse Reflectance Spectra. Appl. Spectrosc. 43, 772-777

Chowhan, Z.T., Chi, L-H., Yang, I.-C., 1981. Mixing of Pharmaceutical Solids. IV. Effects of Concentration and Material Properties on Multicomponent Mixing of Cohesive Powders. Powder Tech. 29, 251-256.

Fan, L.T., Chen, S.J., Watson, C.A., 1970. Solids Mixing. Ind. Eng. Chem. 62, 53-69.

Fan, L.T., Chen, Y.-M., Lai, F.S., 1990. Recent Developments in Solids Mixing. Powder Tech. 61, 255-287.

Gamble, D.L., Barnett, C.E., 1937. Scattering in the near Infrared. A Measure of Particle Size and Size Distribution. Ind. Eng. Chem. 9, 310-314.

Geladi, P., MacDougall, D., Martens, H., 1985. Linearization and Scatter-Correction for Near-Infrared Reflectance Spectra of Meat. Appl. Spectrosc. 39,491-500.

Harnby, N., 2000. An engineering view of pharmaceutical powder mixing. PSTT, 3. 303-309.

Johnson, M.C.R., 1975. The effect of particle size upon mixture homogeneity. Pharm. Acta. Helv. 50, 60-63.

Kubelka, P., 1948. New Contributions of the Optics of Intensely Light-Scattering Materials. Part I. J. Opt. Soc. Am. 38, 448-457.

Martens, H., Stark. E.,1991. Extended multiplicative signal correction and spectral interference subtraction—new preprocessing methods for near infrared spectroscopy. J. Pharm. Biomed. Anal. 9, 625–635.

O'Neil, A.J., Jee, R.D., Moffat, A.C., 1998. The application of multiple linear regressionto the measurement of the median particle size of drugs and pharmaceutical excipients by near-infrared spectrosocpy. Analyst, 123, 2297-2302.

O'Neil, A.J., Jee, R.D., Moffat, A.C., 2003. Measurement of the percentage volume particle size distribution of powdered microcrystalline cellulose using reflectance near-infrared spectroscopy. Analyst 128, 1326-1330.

Orr, N.A., Shotton, E. 1973. The Mixing of Cohesive Powders. Chemical Engineer 269, 12-18.

Pasikatan, M.C., Steele, J.L. Spillman, C.K., Haque, E. 2001. Near infrared reflectance spectroscopy for online particle size analysis of powders and ground materials. J. Near Infrared Spectrosc. 9, 153-164.

Rantanen, J., Räsänen, E., Tenhunen, J., Känsäkoski, M., Mannermaa, J.-P., Yliruusi, J., 2000. In-line moisture measurement during granulation with a four-wavelength near infrared sensor: an evaluation of particle size and binder effects. Eur. J. Pharm. Biopharm. 50, 271-276.

Rees, J.E., 1977. Mixing of particulate solids to ensure homogeneity of dosage forms: The need for a critical approach to pharmaceutical process development. Boll. Chim. Farm. 116, 445-462.

Sarkar, A., Wassgren, C., 2010. Continuous blending of cohesive granular material. Chem. Eng. Sci. 65, 5687-5698.

Staniforth, J.N., 1985. Ordered Mixing or Spontaneous Granulation? Powder Tech. 45, 73-77.

Szalay, A., Antal, I., Zsigmond, Z., Marton, S., Erős, Regdon, G., Pintye-Hódi, K., 2005. Study on the Relationship between Particle Size and Near Infrared Diffuse Reflectance Spectroscopic Data. Part. Part. Syst. Charct. 22, 219-222.

Train, D., 1959. Mixing of Pharmaceutical Solids: The General Approach. J. Am. Pharmaceut. Assoc. 49, 265-271.

United States Pharmacopeia 35/ National Formulary 30, 2012. General Chapter <1174> Powder Flow. The United States Pharmacopeial Convention, Rockville, MD, USA, pp. 801-804.

Yalkowsky, S.H., Bolton, S., 1990. Particle Size and Content Uniformity. Pharmaceut. Res. 7, 962-966.

Zhang, Y., Johnson, C., 1997. Effect of drug particle size on content uniformity of low-dose solid dosage forms. Int. J. Pharm. 154, 179-183.

5 Batch Mixing

Martinez, L., Peinado, A., Liesum, L., 2013. In-line quantification of two active ingredients in a batch blending process by near infrared spectroscopy: Influence of physical presentation of the sample. Int. J. Pharm. 451, 67-75.

Graphical Abstract

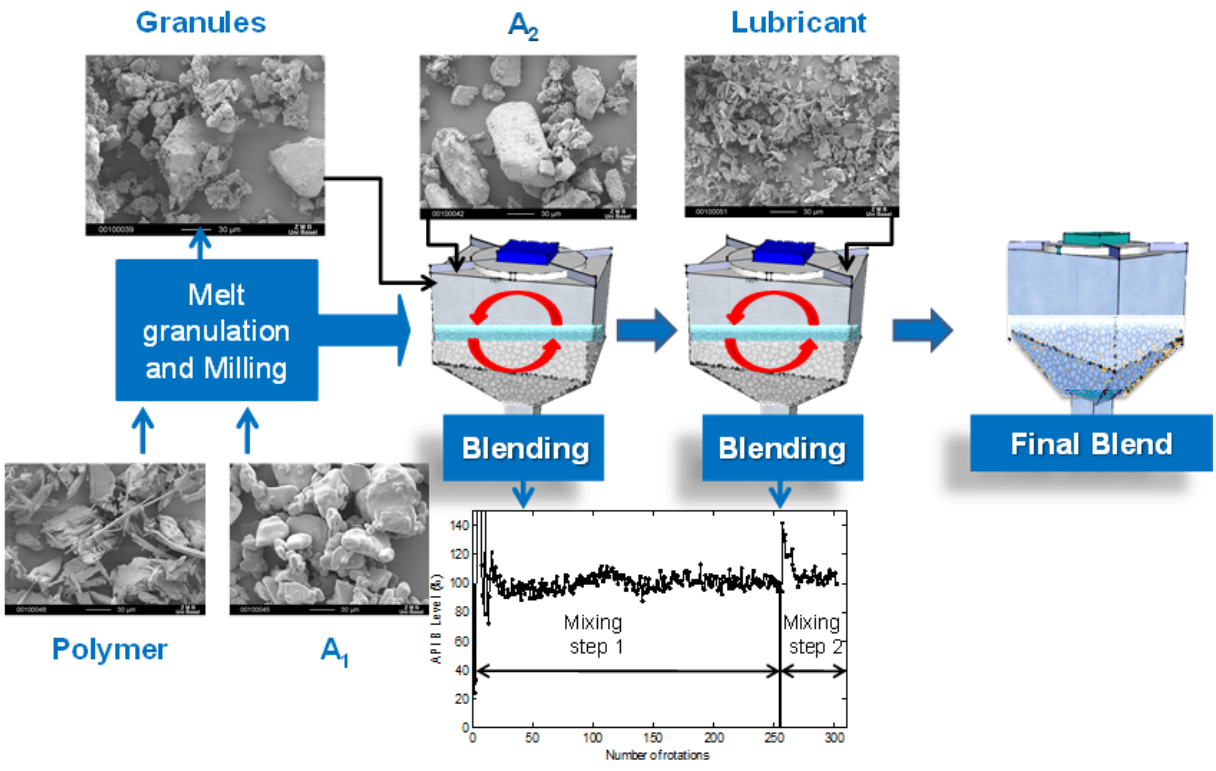

Abstract

The aim of this study was to apply near-infrared (NIR) spectroscopy to the simultaneous in-line monitoring of two active pharmaceutical ingredients (APIs) in a pharmaceutical batch blending process. The formulation under study consisted of a high load API, one polymer, a second API and one lubricant. The API of interest corresponded to 4% (m/m) of the formulation. Additionally, the effects of the presentation of high load active on the spectral data were evaluated. For this purpose, the high load active was blended either as a cohesive powder or as a free flowing material. For improving the flow behavior of the high load active a melt-granulation (MG) step was performed.

The NIR spectra of the high load API before and after MG showed that the polymer wavelength absorption band was the most affected, this wavelength range was also associated with the water band region. Thus, these frequencies carried information from the process and could be influenced by the water content.

For the APIs quantification, independent partial least squares (PLS-1) models for each API were generated. Furthermore, a PLS-2 model was also developed for the simultaneous quantification of each API. The PLS models were used for the in-line blend uniformity monitoring of both APIs.

Keywords

PAT, blending, NIR, melt-granulation, off-line calibration, PLS2

5.1 Introduction

Solid dosage forms are the most accepted forms by the patients and dominant on the pharmaceutical market. The manufacturing process of tablets typically involves several unit operations such as blending, granulation, tableting, and coating, all of which can have critical influences on the final quality of the pharmaceutical form. Therefore, a scientific understanding of the pharmaceutical formulation and the manufacturing process is of crucial importance. Process monitoring is an additional tool to guarantee a high and predefined quality standard and furthermore offers the possibility to react at any stage of the process if any parameters drift from the normal operating range. Near-infrared (NIR) spectroscopy holds great potentials for monitoring pharmaceutical manufacturing processes in-line and for end-product analytics. NIR spectroscopy has gained a broad range of applications in various industries such as fuels, food, and feed, and attracted attention during recent years also from the pharmaceutical side, from both the industry and the health authorities. This has brought up the process analytical technology initiative launched by the FDA (FDA, 2004). However, the pharmaceutical industry is tightly regulated and therefore the implementation of NIR needs careful risk assessment due to the fact that predictions are obtained by statistical correlations based on established assays rather than being a direct assay. Thus the establishment of comprehensive methodologies is needed for NIR quantification, which is specific for powders and solid dosage forms, with the aim of minimizing effects originating from the physical properties (Blanco et al., 2010; Ely et al., 2008; Saeed et al., 2009).

In the present study, NIR spectroscopy is implemented to the blending operations of the manufacturing process of an immediate release formulation containing two active pharmaceutical ingredients (API) and several process steps including melt granulation (MG), milling, and blending see Fig. 1. One API (A_1) is included in a polymeric matrix by MG while A_2 is incorporated to the formulation after MG.

In the present study melt granulation was performed using a twin-screw melt extruder. Hot-melt extrusion (HME) is a technique used increasingly in the pharmaceutical industry in which the drug is homogeneously embedded in a polymeric matrix and subsequently processed for shaping, such as milling. HME is commonly applied for controlling drug release (Fukuda et al., 2006; McGinity et al., 2007) to cope with solubility limitations of poorly water soluble drugs (Miller et al., 2007). Even though the equipment for MG and HME can be the same, in HME the materials are heated above their melting temperature while in MG temperatures are below the melting point of the API but higher than the melting point of the polymer. The important advantage of both techniques over other methods is the fact that the extrusion process (also in the melt-granulation modality) is an industrially feasible single step process without the use of solvents (Breitenbach 2002; Follonier et al., 1994; Follonier et al. 1995). Among the disadvantages are the use of heat and the occurrence of shear forces on the material due to the screw extrusion step (Qi et al., 2008). NIR (Rohe et al., 1999) and Raman spectroscopy (De Beer et al., 2011; Tulumuri et al., 2008) has been applied to monitor the extrusion process and for drug quantification of extruded formulations, respectively.

A full understanding of the physical state of the APIs in the formulations is of significant importance because: on the one hand, stability and dissolution behavior can be affected (Qi et al., 2008) and, on the other hand, robust calibration models must be developed since NIR spectra contain both chemical and physical information. Therefore, preprocessing techniques and wavelength selection ranges should be carefully chosen to extract the chemical information that is mainly correlated with the API concentration.

Blending of powders is an essential unit operation in the manufacture of a wide range of solid dosage forms and is considered as critical when a formulation contains a small amount of API. Inadequate blending during the production sequence of solid dosage forms can result in insufficient quality of the final product. Hence, a scientific understanding of the blending process and the critical parameters are very important to achieve homogenous blends. In

most cases, the materials to be mixed are particulate materials of different size, density, morphology and cohesiveness and thus tend to segregate (Muzzio et al., 1997). Blending can be defined as a combination of three different mechanisms occurring during the process, such as convective, shear and diffusive mixing. Convective mixing is the movement of large groups of particles, the exchange of particles across the shear zones produces shear mixing, and random motion of particles at small scale corresponding to diffusive mixing (Alexander and Muzzio, 2002; Bridgwater, 1994; Manjunath, et al., 2004). Blending performance is largely dependent on the physical characteristics of the material (Bellamy et al., 2008; Chaudhuri et al., 2006; Venables and Wells, 2001; Virtanen et al., 2007) and the process conditions (Sudah, et al., 2002).

In quality assurance, the resulting blend uniformity (BU) is critical to ensure compliant content uniformity and dissolution rate behavior of the final product. Conventional blend uniformity (BU) involves stopping the blender on a fixed time basis, collecting samples usually by thief sampling, and performing an off-line analysis using chromatographic methods. Conventional BU analysis is time consuming, labor intensive, prone to induced segregation during sampling, and homogeneity determination is focused on the active pharmaceutical ingredient (API) level in a static way. Application of NIR as an on-line monitoring tool can avoid the drawbacks of the conventional method. Assessment of homogeneity by NIR however is a common challenge for BU determination and different procedures are described in literature: principal component analysis (Cuesta-Sanchez et al., 1995; El-Hagrasy, et al., 2001; Varanese et al., 2010), principal component scores distance analysis (Puchert et al., 2011), bootstrap error-adjusted single-sample technique (Wargo and Drennen, 1996), mean square of differences (Blanco et al., 2002) and moving block of standard deviation (MBSD) (Sekulic et al., 1996; Sekulic et al., 1998). Sekulic and coworkers determined the end-point of the blending process qualitatively by the MBSD method that consists of selecting a set of consecutive spectra (block or window size) then the standard deviation for the absorbance at the selected wavelength range is calculated, followed by the mean standard deviation computation of that set. Mean standard deviation is plotted against

time, subsequently the spectral set is shifted by one time unit and the calculations are repeated.

Several strategies have been developed for the acquisition of calibration samples for the quantification of the API in a blending process. Some strategies involved stopping the blender at different time points and acquiring calibration samples by thief sampling (Wargo and Drennen, 1996). However, thief sampling can disturb the blend (Muzzio et al., 1997). Berntsson et al., (2002) prepared off-line samples for a binary mixture and performed a quantitative monitoring of powder blending. Shi et al. (2008) proposed to monitor the blending process at the top and side of the blender with two NIR sensors for a better process monitoring. Karande et al. (2010) exemplifies the complexity in acquiring representative calibration samples. They acquired the samples in static and dynamic modes, showing that the better predictions were obtained when the dynamic samples were employed. Sulub et al. (2009) used an off-line static calibration set for developing a partial least squares (PLS) model for on-line prediction of one API at almost 30% (m/m) drug load. The off-line PLS model was transferred to a production site.

In this study the aim was to apply near-infrared (NIR) spectroscopy to the simultaneous in-line monitoring of two active pharmaceutical ingredients (APIs) in a pharmaceutical batch blending process. The formulation under study consisted of a high load API, one polymer, a second API, and one lubricant. Additionally, the effects of the presentation of high load active on the spectral data were evaluated. For this purpose, the high load active was blended either as a cohesive powder or as a free flowing material. For improving the flow behavior of the high load active a melt-granulation (MG) step was performed, resulting on the active ingredient embedded in a polymeric matrix. Moreover, it was possible to study the influence that MG exerted on the physical and spectroscopic properties of the blends. Further, the quantification of both APIs was achieved by developing independent PLS models for each API and by the APIs simultaneous quantification through a PLS-2 model.

5.2 Materials and Methods

The target formulation consisted of 96% (m/m) of a granular material. The granules contained one high load API (A_1) and one cellulose based polymer, a second API (A_2) corresponding to 4% (m/m) of the formulation, and one lubricant (1% m/m).

The morphological characterization was performed by scanning electron microscopy (SEM) (ESEM XL 30 FEG, Philips, The Netherlands) at an applied voltage of 10 kV and magnifications of 100-2000 times. The sample preparation included placing the powder on carbon adhesive, followed by gold plating.

The average particle size was measured using a laser diffraction system (Mastersizer S long bed, Malvern, Worcestershire, UK). The lens range was within the particle size range of 4.2-3500 µm. The samples were dispersed through a dry powder feeder and the measurements were carried out 5 times. Obscuration value was kept between 10-30% and residual under 1%. The analysis was set in “polydisperse” mode. The mean and median diameters and the span values were recorded.

For the flow character determination, approximately 100 g of powder were poured in a volumetric cylinder and the unsettled apparent volume was measured, then the sample was tapped until no volume changes occurred. The final volume was recorded and bulk (ρ_{bulk}) and tapped (ρ_{tapped}) densities were computed. The compressibility index and the Hausner ratio of the A_1 before and after the MG process were determined following the procedure given in the USP 35.

Melt granulation

The A_1 was combined with the cellulose based polymer in the ratio of 10:1, the powders were fed into a twin screw extruder (Leistritz Extrusionstechnik GmbH, Nuremberg, Germany), the extruder temperatures ranged from 20 to 135 °C, under the melting point of the A_1 (222°C), and the screw speed was set at 90 rpm. The extruded product was milled in a Frewitt

hammer mill (Fribourg, Switzerland) with knives forward at 2100 rpm and the screen size was fixed at 1000 µm. The resulting product is referred to A_{MG} on the manuscript.

Blending and NIR instrumentation

All measurements were obtained using a SentroPAT Blend Uniformity TL, NIR spectrometer (Sentronic GmbH, Dresden, Germany) based on a micro-electromechanical system, equipped with an onboard computer, two tunable laser sources, and Indium Galium Arsenide detector. Spectra acquisition was done in reflectance mode over the wavelength range of 1350-1800 nm at 1 nm intervals.

The bin blender was loaded first with $A_{MG,}$ then the second drug (A_2) was charged, followed by a first mixing step of 250 revolutions. The blender was stopped and the lubricant was loaded and a second blending step of 50 revolutions was performed. The rotational speed for both blending steps was 10 rpm. For on-line measurements the spectrometer was mounted on the top of the bin blender (Figure 5-1) and the in-line data acquisition was triggered by the position of the NIR spectrometer, with a trigger angle of -45° to + 45°, corresponding to the moment in which the powder was in contact with the spectrometer lid. One spectrum per turn was obtained and the data were wireless-transmitted from the SentroPAT spectrometer to a computer in close proximity.

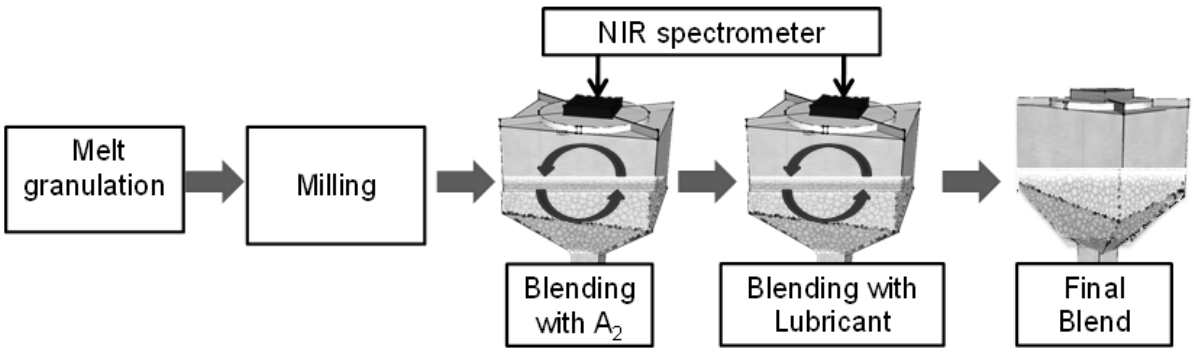

Figure 5-1 Process flow chart with emphasis on the blending steps monitored by NIR.

Off-line calibration samples

The calibration set was designed to mimic incomplete blending in which the components were in varying amounts. A_1 was blended either as its pure form or as a granule (A_{MG}). A_{MG} kept a constant ratio within A_1 and the polymer. A_2 was varied from 50-150% of the API target. The amount of A_1 was restricted to 95% to 105% of its target value, since it is the dominant component of the blend and variations of its concentration were expected to be minimal. Thirteen calibration samples with a total weight of 15 ± 0.3 g were prepared by accurately weighing all components and mixed (Turbula type T2C, W. Bachofen, Switzerland) for 5 minutes. Each sample was placed over the spectrometer lid scanned for a period of 2 minutes. The resulting compositions of the samples are shown in Table 5-1.

Table 5-1 Constituent concentrations of the target formulation for the off-line calibration set.

Blend	A_1 Presentation	A_1 [% Nom]	A_2 [% Nom]	Polymer [% Nom]	Lubricant [% Nom]
B1	A_{MG}	101.4	69.6	101.5	105.5
B2 [v]	PB	101.3]	73.4	105.3	53.4]
B3	PB	105.4]	80.2	57.4	85.0
B4	A_{MG}	100.9	81.2	100.9	105.5
B5	A_{MG}	100.3	92.8	100.4	105.5
B6 [v]	PB	98.3	93.8	123.7]	72.4
B7 [v]	PB	102.9	98.6	74.5	63.2
B8	A_{MG}	100.0	100.0	100.0	100.0
B9	PB	96.4	105.2	129.6	139.5
B10	PB	95.2	109.9	146.0	71.7
B11 [v]	A_{MG}	99.5	110.2	99.6	105.5
B12	A_{MG}	99.0	121.8	99.1	105.3
B13	PB	102.3	130.5	65.4	55.5

PB=Physical Blend
[v] Validation samples

Spectral pretreatment and PLS-model building

Different combinations of preprocessing techniques were tested for reducing the spectral variability associated to the physical characteristics of the samples. Under the scattering correction methods; standard normal variate (SNV) was selected since it corrects variations in particle size and density (Barnes et al., 1989). Second derivative with the Savitzky Golay (SG) algorithm (Savitzky and Golay, 1964) with a window size of 15 points were used in order to remove additive effects by correcting baseline drifts (Rinnan et al., 2009). The pretreated spectra were matched with the reference values of each API value and independent PLS models for A_1 and A_2 were generated. The PLS models were externally validated using the calibration samples 2,6,7, and 11 (previously excluded from the calibration set), the validation set was predicted and the determination coefficient (R^2), the root mean square error of the prediction (RMSEP) and the prediction bias were computed.

As a second approach for the simultaneous quantification of both APIs, a PLS-2 model was generated. The PLS-2 model included the nominal values (Table 5-1) of A_1, A_2, polymer, lubricant, and the physical presentation of A_1. The presentation of A_1 within the blend was handled as a covariate; A_{MG} was matched with 1 and PB with -1. The model was externally calibrated with the same samples as for the PLS-1 models.

The software used for the chemometrical analysis was Matlab (The Mathworks Inc.) version 2009Ra with PLS_toolbox (Eigenvector Research Inc.) version 6.2.1.

PLS-models application

The PLS-models were applied to monitor the evolution of the formulation components in real scale batches in a production site. The blend uniformity was followed by the moving block of standard deviation computed over the wavelength range of 1500-1600 nm, with a window of 10 points according to the method described by Sekulic et al. 1996.

The average of the predicted concentrations for each API corresponding the last 10 turns was compared to the content uniformity of the average of 10 tablets for each batch. The content uniformity for each API was achieved by a validated HPLC method.

5.3 Results and Discussion

Effect of MG on the physical properties of the A_1

SEM micrographs of the formulation components are shown in Figure 5-2. A_1 particles (Figure 5-2a) got heterogeneous size distribution and cohesiveness was present on the particles surface. A_1 particles stuck together, fine powder was present in the surface of the big particles. The cellulose based polymer (Figure 5-2b) had a fibrous and needle shaped aspect. After the melt granulation between A_1 and the polymer, the resulting product was milled. In Figure 5-2c, the milled granules (A_{MG}) showed crushed aggregates that physically differed from the original components. In addition, the amount of fine powder stuck on the surface of the clusters reduced compared to A_1. A_2 particles (Figure 5-2d) were mainly oblong; they resulted in heterogeneous particle size distribution and less fine powder stuck to its surface compared to A_1. Lubricant (Figure 5-2e) was present as fine powder. Table 5-2 shows the particle size distribution and flow characterization for A_2 and for A_1 before and after MG process. The particle size for A_1 increased from 66 to 463 µm after the MG process was performed and the granulated form was obtained. The span values showed a wider particle size distribution for A_{MG} compared to the pure A_1 form. According to the compressibility and Hausner indices, the flow character of A_1 improved from fair to excellent. Thus the granules of A_1 improved the flow performance of the formulation.

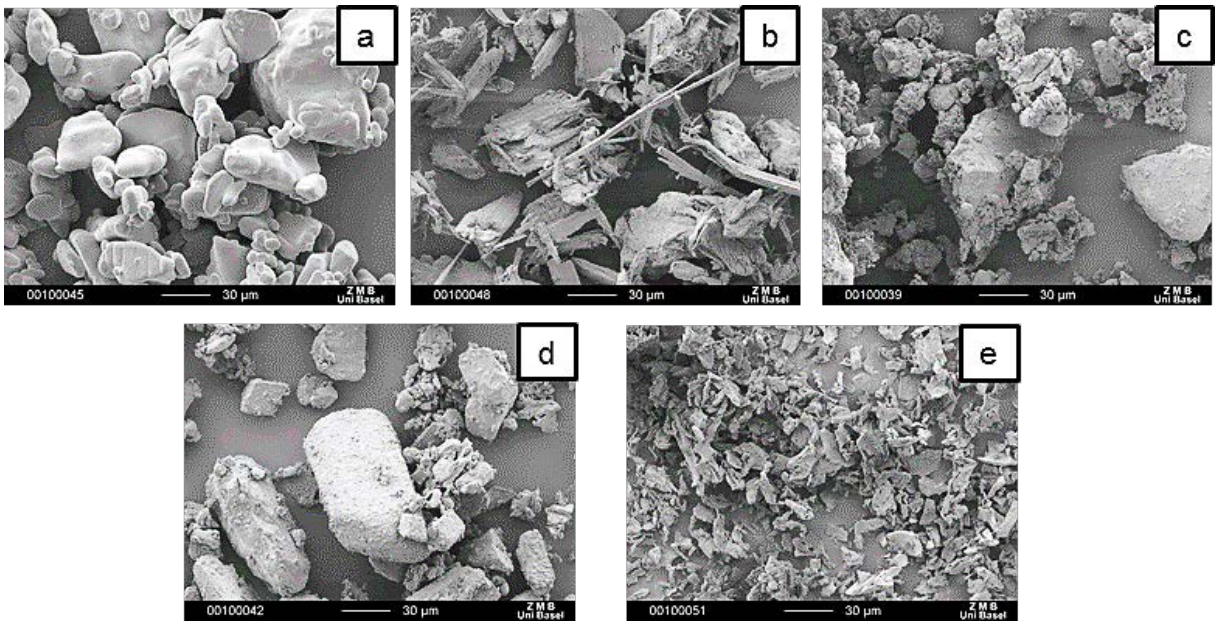

Figure 5-2 SEM micrographs of the different powders used: A_1 (a); cellulose based polymer (b); A_{MG} (c); A_2 (d), lubricant (e).

Table 5-2 Powder characterization.

Parameter	**A_1**	**A_{MG}**	**A_2**
Bulk density [g/cm^3]	0.48	0.55	0.45
Tapped density [g/cm^3]	0.58	0.58	0.57
Compressibility index	17.72	6.10	20.85
Hausner index	1.22	1.07	1.26
Flow character	Fair	Excellent	Passable
Median diameter [µm]	57.34	241.44	-
Mean diameter [µm]	65.52	463.07	-
Span*	2.43	5.58	-

* Span measures the width of the distribution and is calculated as:$[d(0.9) - d(0.1)]/d(0.5)]$

Effect of the MG on the NIR spectra

Figure 5-3a contains the NIR spectra of the four pure components of the formulation scanned under static conditions. A_1 broad absorption band at 1525 corresponds to the first overtone of the NH stretching for the primary amine of A_1. At 1554 nm A_2 has a characteristic peak, at

these frequencies both excipients presented low absorbance. The evaluation of the spectroscopic effect of the physical presentation of A_1 was fundamental since this correlates with the melt granulation process influence on the formulation. Figure 5-3b shows the spectral characteristics of two blends containing the same components and only varying the presence of A_1 either as a physical blend with the polymer (before MG) or in its granular state (after MG). The standard deviation computed from both spectra (Figure 5-3c), showed a high variability under 1500 nm. These frequencies corresponded to the absorption band of cellulose. The broad band at 1450 contained information of the hydrogen-bonded and is associated with the free water band, and the visible changes within the NIR spectra are due to changes in hydrogen bonding (Shenk et al., 2001). During melt granulation, the polymer passed through a glass transition temperature. This wavelength region carried the information of the process, and was therefore excluded from the chemometric analysis.

The wavelength region over 1500 nm (Fig. 3b) presented a baseline shift emanating mainly from particle size, particle shape, and density variations among the samples. The spectra do not exhibit new peaks nor peak shifts. Saerens et al. (2012) identified the appearance of peak shifts in NIR spectra taken during a extrusion process due to the interactions of the polymer with the drug, and the shifts were intensified when the extrusion process was performed over the melting point of the drug. In our study the temperature of the twin-screw extruder was kept under the melting point of A_1 thereby explaining the absence of peak shifts for the frequencies over 1500 nm.

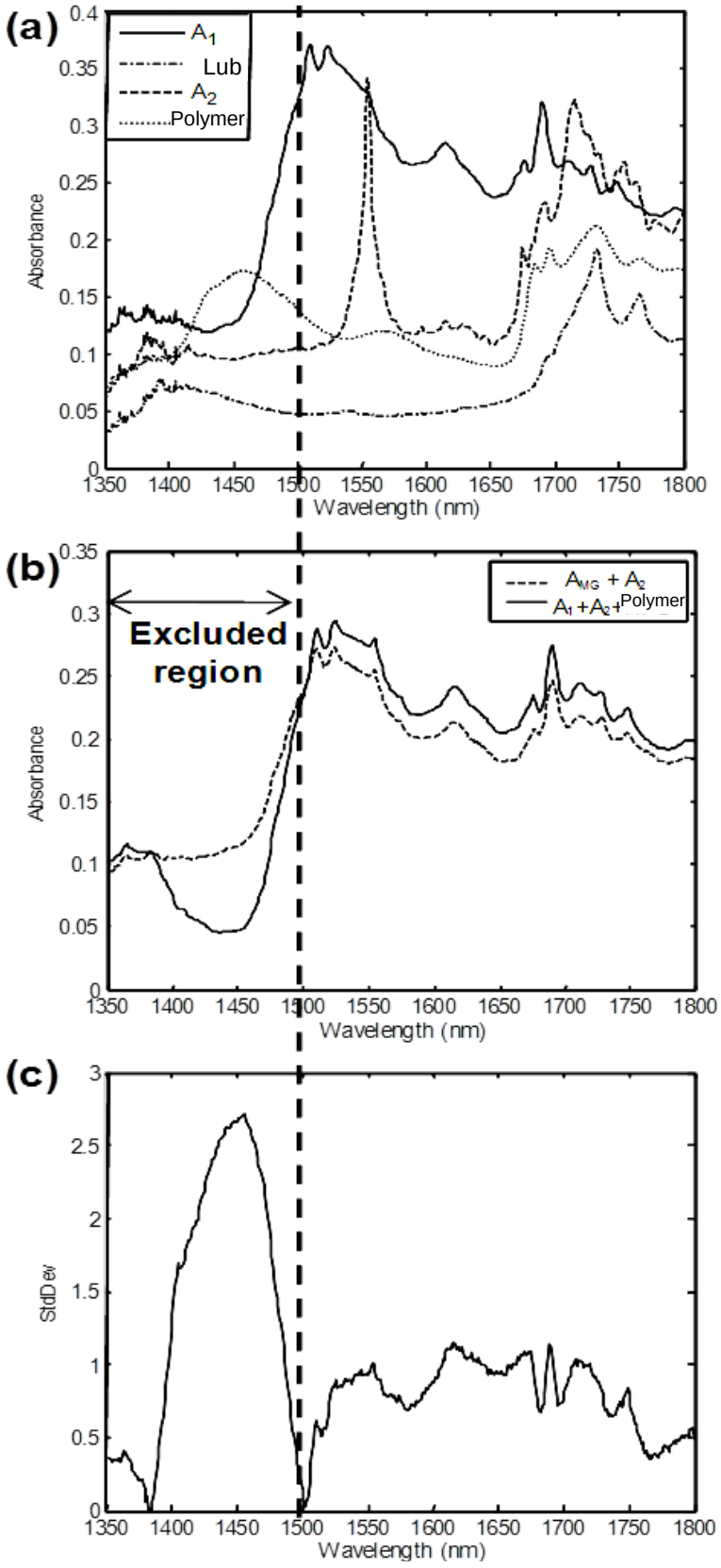

Figure 5-3 (a) Spectra of the formulation ingredients, (b) spectral comparison of two blends, with their standard deviation (c). First blend A_1, A_2, and the cellulose based polymer and the second blend A_{MG} and A_2. The pointed lined shows the excluded frequencies.

Model development

PLS-1 models for each API were computed. The wavelength range of 1350-1500 nm was excluded from the calibration wavelength region because this area was highly influenced by the information of the MG process. The preprocessing technique chosen for the reduction of the scattering due to physical influence on the calibration spectra was SNV with second derivative. In addition, for the PLS-1 model for A_1, the wavelength range of 1546 to 1562 nm was excluded; these excluded frequencies were highly correlated with the concentration changes of A_2.

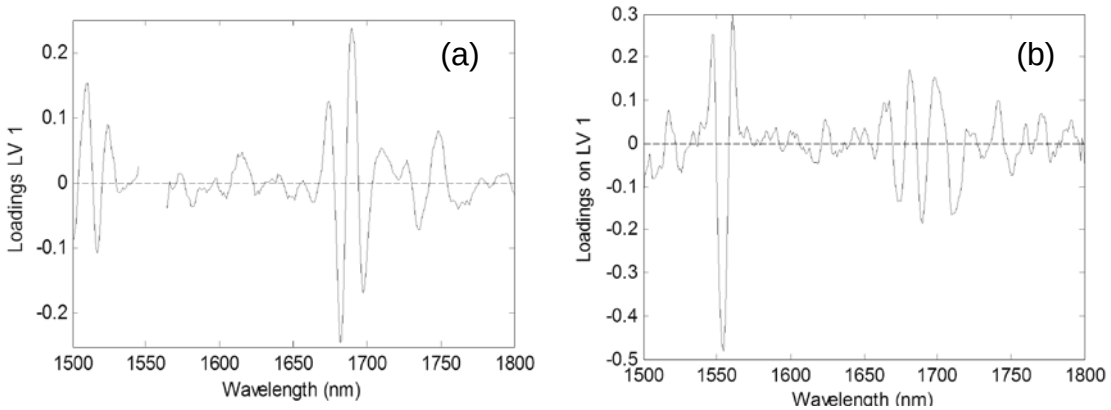

Figure 5-4 First component loadings for A1 PLS-1 model (a) and A2 PLS-1 model (b).

Figure 5-4 contains the first loading for each API PLS-1 models. Loadings were used as a reference parameter for each PLS model, hence the loadings were compared with the second derivative of each API (Figure 5-5). A_1 and A_2 second derivative preprocessed spectra showed similarity with the loadings of the first principal component of their respective PLS models.

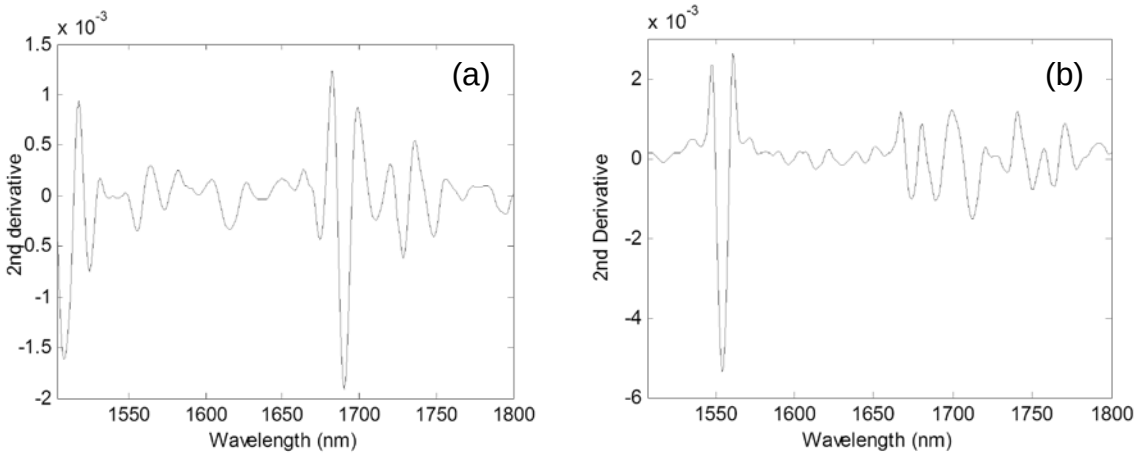

Figure 5-5 Second derivative for A1 (a) and A2 (b) spectra.

The variance captured by the PLS-2 model for each Y variable (Figure 5-6a) showed that the first principal component mainly accounted for the presentation of A_1, either as granules or as a physical blend. This is in agreement with the loading structure in Figure 5-6b as it resembles to the second derivative spectrum of A_1 whereas the second latent variable (Figure 5-6c) carried the variability correlated to the concentration of the APIs and the polymer with a protruding peak at 1554 nm corresponding to A_2 (Figure 5-6d). The loadings for the first two latent variables accounted for the variability of both APIs and the influence of the lubricant and polymer can be detected.

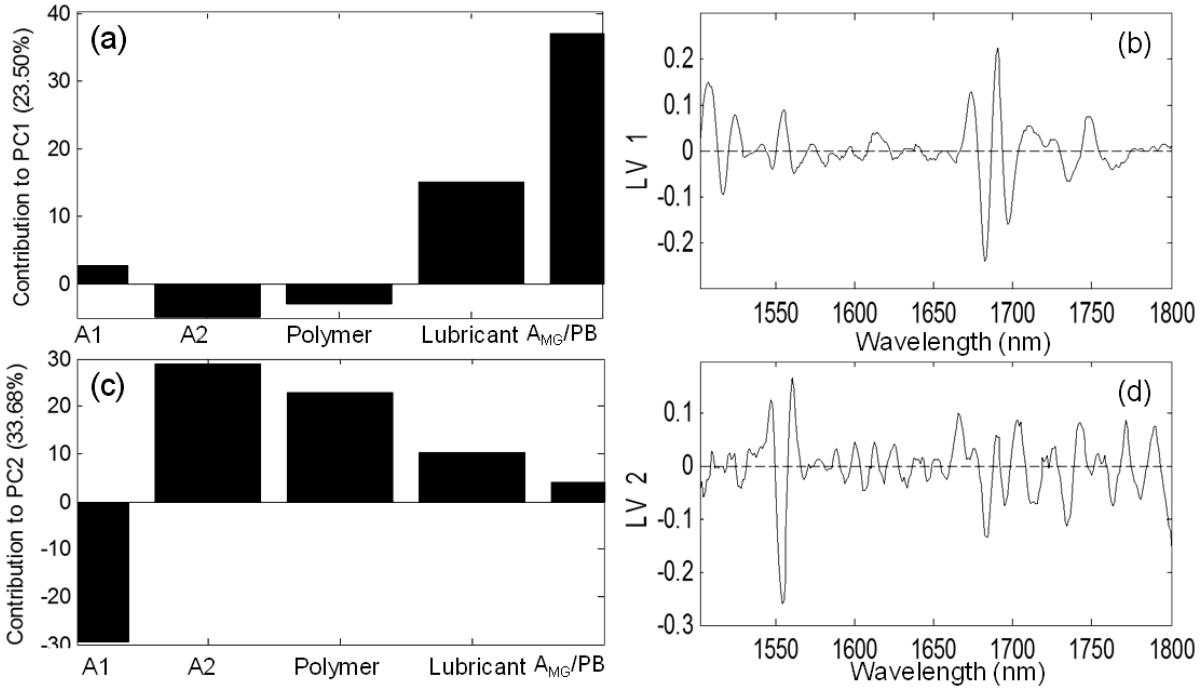

Figure 5-6 Variance captured for each variable on the first (a) and second (c) components for the PLS-2 model. Loadings for the first (b) and second latent variables (d).

The main statistics for each PLS model are summarized on Table 5-3. From the results, it can be seen that the PLS-2 model requiered more latent variables for explaining almost the same variability as the PLS-1 models. Given that A_1 is a high load active and A_2 accounted only for 4% (m/m) of the formulation, the RMSECV and RMSEP were given in percentage of the target level and in mass percentage in order to be able to compare the performance of the different PLS models. The statistics for A_1 were better for the PLS-1 model. These results could be explained due to wavelength selection for the PLS-1 model in which the frequencies correlated to the second API were excluded, thus the wavelength region was more selective for A_1. A_2 prediction errors for PLS-1 and PLS-2 models were within the same range.

Table 5-3 Main statistics obtained for the calibration and validation of PLS-1 and PLS-2 models.

		PLS-1 model		PLS-2 model	
		A_1	A_2	A_1	A_2
Number of latent variables		3	3	5	
Xcum[a] [%]		97.23	97.26	98.42	
Ycum[b] [%]		99.17	98.22	98.95	
RMSECV	[% Nominal]	0.255	2.486	0.261	1.566
	[% m/m]	0.220	0.107	0.225	0.067
RMSEP	[% Nominal]	0.428	2.261	0.843	2.296
	[% m/m]	0.369	0.097	0.726	0.099
R^2		0.987	0.981	0.969	0.990
Prediction Bias		0.214	-0.877	0.386	-1.916
Preprocessing technique		SNV+SGS (15 pt) 2nd Derivative	SNV+SGS (15 pt) 2nd Derivative	SNV+SGS (15 pt) 2nd Derivative	
Wavelength range [nm]		1502-1545, 1563-1800	1502-1800	1502-1800	

[a] Cumulative variance captured by the model for the X variables.
[b] Cumulative variance captured by the model for the Y variables.

BU monitoring

The NIR spectrometer was coupled over the inspection window placed on the lid of the bin blender. This configuration enabled proper in-line spectral acquisition for an industrial blending process. The measurements were triggered according to the position of the blender collecting one measurement per rotation. The spectral data was fitted into the PLS-1 and PLS-2 models, allowing the prediction of the target level for each API. The continuous monitoring of the blending process gave an insight into the behavior of each of the active ingredients. Figure 5-7a shows the predicted A_1 values for batch1. The concentration of A_1 varied at the beginning of both mixing steps due to the addition of the second active and the lubricant. Alexander et al. (2004) mentioned the importance of the loading order of the blend components in a bin blender. In our study the granules were loaded first and they accounted

for 94.7 % (m/m) of the formulation load. Under these conditions the A_2 granules performed as the filler of the formulation. The high load and the excellent flow behavior of the granules resulted in fast mixing and minimal variations on the predicted A_1 level. A visual inspection showed that A_1 reached an equilibrium state of blend homogeneity before A_2. Figure 5-7b corresponds to the predicted concentration of A_2. In the beginning of the mixing process the blend was in a segregated state with A2 on the top of the mixture. The high variability at early blending stage corresponded to the convective mixing, followed by the diffusive blending over 30 revolutions for the first mixing step.

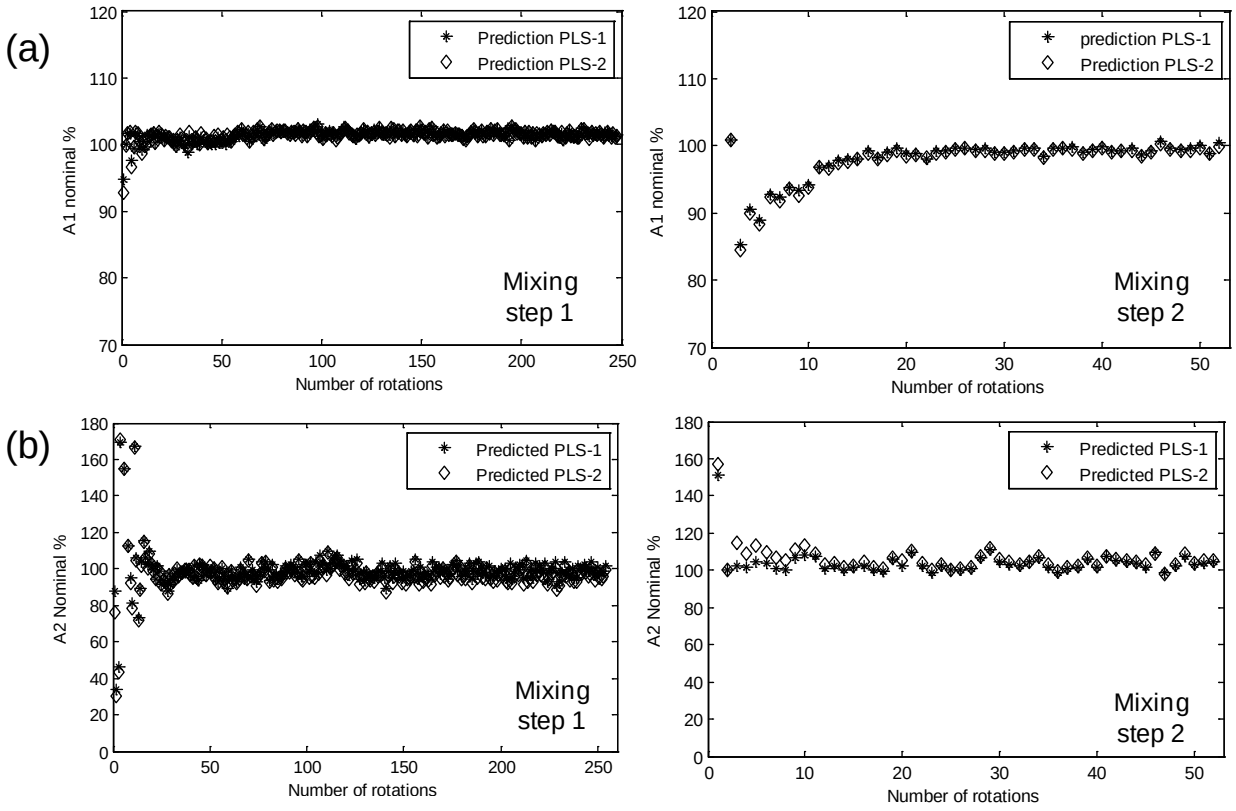

Figure 5-7 PLS predicted values of A1 (a) and A2 (b) corresponding to first and second mixing steps for a randomly selected batch.

In order to avoid over lubrication, which could result in dissolution problems, lubricant was added in a second mixing step. The second mixing stage was the previous operation before compaction of the blends and it was chosen for the determination of the relative standard deviation (RSD). The RSD of the predicted values for each API at the second mixing step was computed. The RSD was calculated through the standard deviation of the predicted

values of each API presiding over a range of five rotations and subsequently divided by their average. The RSD limit was established at 5%. Liew at al., (2010) successfully applied the RSD for the homogeneity determination of cohesive blends. They observed that the lubricant tended to distribute uniformly. Figure 5-8 shows that the RSD was lower for A_1 compared to A_2. The RSD values were under the 5% established limit for the predictions of PLS-1 and PLS-2 models.

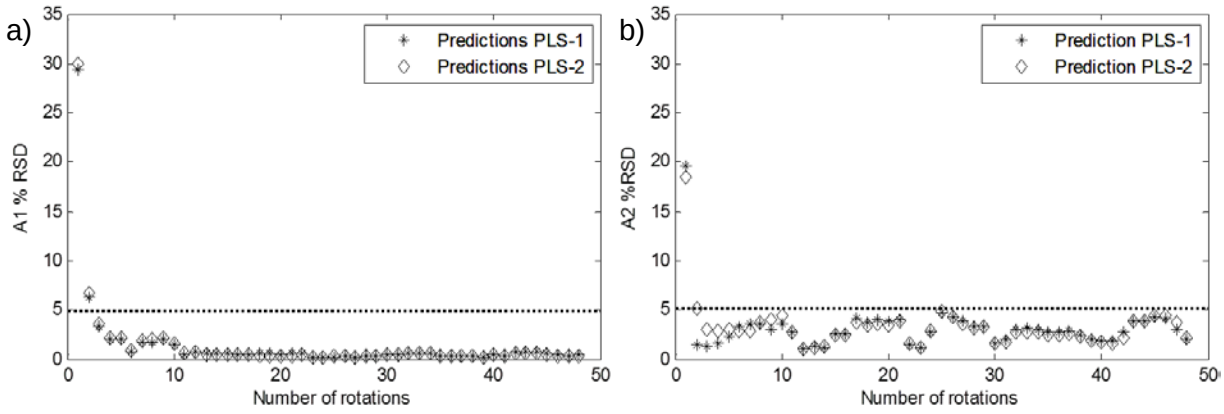

Figure 5-8 RSD for the second mixing step of (a) A1 and (b) A2.

The MBSD was calculated with a window of 10 spectra over the wavelength range of 1500 to 1800 nm using the SNV and second derivative pretreated spectra of both blending steps. Figure 5-9 shows the MBSD behavior; a clear decrease on the MBSD values at zero to twenty rotations corresponed to the inhomogeneous state of the blend, in which A_2 spectral features were dominating. The same situation appeared at the early stage of the second mixing step with the adition of the lubricant. The addition of the lubricant disturbed the equilibrium of the blend followed by the recovery of the steady state after 20 rotations.

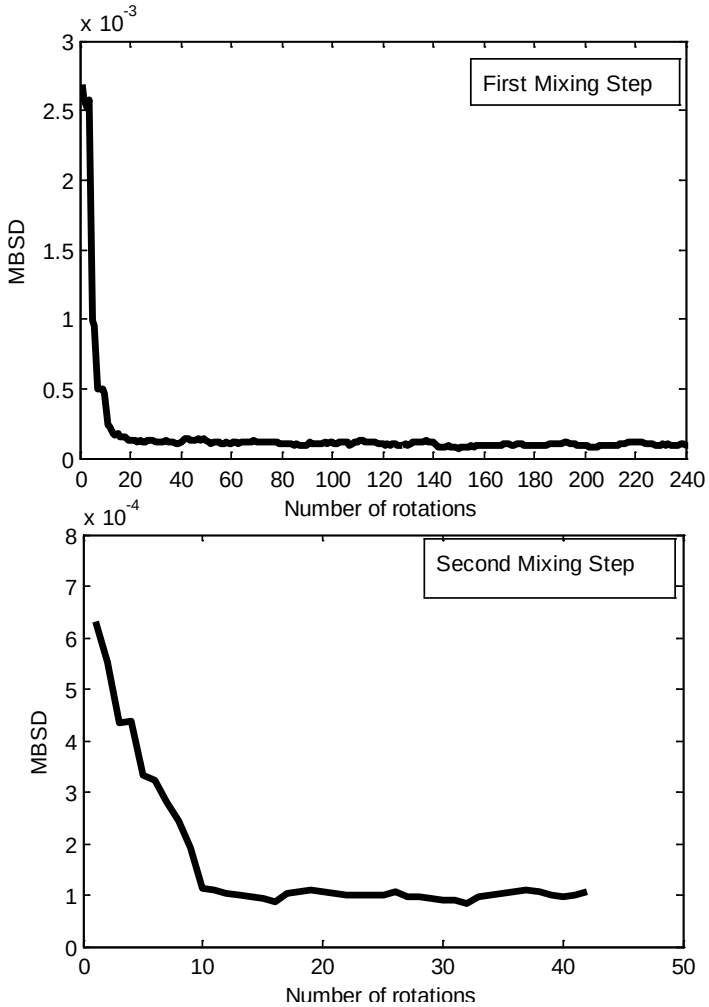

Figure 5-9 MBSD for both mixing steps.

Finally, the independent PLS-1 models were applied to the monitoring of 5 production batches acquiered one year after the development of the calibration models. The average predicted values for the last ten revolutions corresponding to A_1 and A_2 are given in Table 5-4. The NIR predicted results were confirmed by HPLC content uniformity analsysis of the manufactured tablets. These results probe the feasability of monitoring a complex formulation in which high physical variability was incorporated into the model. Overall, the off-line calibration models showed to be a fast methodology for the simultaneous quantification of two active ingredients in a 20:1 mass ratio.

Table 5-4 BU results from the average of the last ten revolutions and CU average of ten tablets.

Batch Number	CU HPLC A_1 [% Nom]	PLS-1 A_1 [% Nom]	CU HPLC A_2 [% Nom]	PLS-1 A_2 [% Nom]
1	100.2±1.0	99.7±0.5	99.6±1.7	103.3±2.7
2	100.7±0.6	99.7±0.2	100.1±1.2	98.5±2.7
3	99.8±1.0	98.8±0.3	99.4±1.3	96.8±2.3
4	99.6±0.7	97.6±0.5	98.8±0.6	103.5±1.8
5	99.9±1.0	98.1±0.4	98.7±1.3	100.8±1.5

5.4 Conclusions

The experiments conducted in this study indicate that melt granulation improved the flow behavior of A_1 by increasing the particle size and reducing the amount of fine powders. The NIR spectra of the A_1 before and after MG showed that the polymer wavelength absorption band was the most affected during the melt granulation and milling processes. This wavelength range was also associated with the water band region. Thus, these frequencies carried information from the process and could be influenced by variations in the water content on the blends.

The loadings showed better selectivity for the PLS-1 models; however the root mean square error and the APIs predictions were of a comparable magnitude.

A_1 reached an equilibrium state of blend homogeneity before A_2 due to concentration differences of the formulation. The addition of the lubricant disturbed the equilibrium of the blend followed by the fast recovery of the steady state of A_1.

The loadings showed better selectivity for the PLS-1 than for the PLS-2 models; however the RMSEP and the APIs predictions were within the same range.

Blend uniformity monitoring by NIR gave a deeper insight into the mixing behaviour of both actives. Furthermore, the method described is suggested to be extended to the monitoring of

blending time of lubricant in the formulation in order to avoid overlubrication problems. Finally, the MBSD and the RSD could be used as a basis for the blend end point determination.

Acknowledgements

The authors would like to thank the Zentrum Mikroskopie of the University of Basel for the SEM micrographs and Theo Baumgartner for collecting the production spectra.

References

Alexander, A.W., Muzzio, F.J., 2002. Batch Size Increase in Dry Blending and Mixing, in: Levine, M. (Ed.), Pharmaceutical Process Scale-Up, Marcel Dekker, New York, pp. 115-132.

Alexander, A., Sudah, O., Arratia, P., Goodridge, C., Alani, L., Muzzio, F., 2004. Characterization of the Performance of Bin Blenders Part 2 of 3: Free-Flowing Mixtures. Pharm. Technol. 28, 56-68.

Barnes, R.J., Dhanoa, M.S., Lister, S.J., 1989. Standard Normal Variate Transformation and De-trending on Near-Infrared Diffuse Reflectance Spectra. Appl. Spectrosc. 43, 772-777.

Bellamy, L.J., Nordon, A., Littlejohn, D., 2008. Effects of particle size and cohesive properties on mixing studied by non-contact NIR. Int. J. Pharm. 361, 87-91.

Berntsson, O., Danielsson, L.-G., Lagerholm, B., Folestad, S., 2002. Quantitative in-line monitoring of powder blending by near infrared reflection spectroscopy. Powder Tech. 123, 185-193.

Blanco, M., Eustaquio, A., Gonzalez, J.M., Serrano, D., 2000. Identification and quantitation assays for intact tablets of two related pharmaceutical preparations by reflectance near-infrared spectroscopy: Validation of the procedure. J. Pharm. Biomed. Anal. 22, 139-148.

Blanco, M., González-Bañó, R., Bertran, E., 2002. Monitoring powder blending in pharmaceutical processes by use of near infrared spectroscopy. Talanta 56, 203-212.

Blanco, M., Peguero, A., 2010. Influence of physical factors on the accuracy of calibration models for NIR spectroscopy. J. Pharm. Biomed. Anal. 52, 59-65

Breitenbach, J., 2002. Melt extrusion: from process to drug delivery technology. Eur. J. Pharm. Biopharm., 54, 107-117.

Bridgwater, J., 1994. Chapter 10 Mixing, in: Chulia, D., Deleuil, M., Pourcelot, Y. (Eds.), Powder Technology and Pharmaceutical Processes, Elsevier, Amsterdam, pp. 347-357.

Chaudhuri, B., Mehrotra, A., Muzzio, F.J., Tomassone, M.S., 2006. Cohesive effects in powder mixing in a tumbling blender. Powder Tech. 165, 105-114.

Cuesta-Sánchez, F., Toft, J., van der Bogaert, B., Massart, D.L., Dive, S.S., Hailey, P., 1995. Monitoring powder blending by NIR spectroscopy. Fresenius J. Anal. Chem. 352, 771-778.

De Beer, T., Burggraeve, A., Fonteyne, M., Saerens, L., Remon, J.P., Vervaet, C., 2001. Near infrared and Raman spectroscopy for the in-process monitoring of pharmaceutical production processes. Int. J. Pharm. 417, 32-47.

El-Hagrasy, A.S., Morris, H.R., D'Amico, F., Lodder, R.A., Drennen III, J.K., 2001. Near-Infrared Spectroscopy and Imaging for the Monitoring of Powder Blend Homogeneity. J. Pharm. Sci. 90, 1298-1307.

Ely, D.R., Thommes, M., Carvajal, M.T., 2008. Analysis of the effects of particle size and densification on NIR spectra. Colloids A. Physicochem. Eng. Asp. 331, 63-67.

FDA, 2004. Guidance for Industry: PAT – A Framework for Innovative Pharmaceutical Development, Manufacturing, and Quality Assurance. http://www.fda.gov/downloads/Drugs/GuidanceComplianceRegulatoryInformation/Guidances/ucm070305.pdf, accessed December 2011.

Follonier, N., Doelker, E., Cole, E.T., 1994. Evaluation of hot-melt extrusion as a new technique for the production of polymer-based pellets for sustained release capsules containing high loadings of freely soluble drugs. Drug Dev. Ind. Pharm. 20, 323-1339.

Follonier, N., Doelker, E., Cole, E.T., 1995. Various ways of modulating the release of diltiazem hydrochloride from hot-melt extruded sustained release pellets prepared using polymeric materials. J. Control Rel., 36, 243-250.

Fukuda, M., Peppas, N.A., McGinity, J.W., 2006. Properties of sustained release hot-melt extruded tablets containing chitosan and xanthan gum. Int. J. Pharm. 310, 90-100.

Karande, A.D., Liew, C.V., Heng, P.W.S., 2010. Calibration sampling paradox in near infrared spectroscopy: A case study of multi-component powder blend. Int. J. Pharm. 395, 91-97.

Liew, C.V., Karande, A.D., Heng, P.W.S., 2010. In-line quantification for drug and excipients in cohesive powder blends by near infrared spectroscopy. Int. J. Pharm. 386, 138-148.

Manjunath, K., Dhodapkar, S., Jacob, K., 2004. Solids Mixing, Part B: Mixing of Particulate Solids in the Process Industries, in: Paul, E.L., Atiemo-Obeng, V.A., Kresta, S.M., (Eds.), Handbook of Industrial Mixing: Science and Practice, John Wiley & Sons, Inc, New Jersey, pp. 924-985.

McGinity, J.W., Repka, M.A., Koleng, J.J., Zhang, F., 2007. Hot-Melt Extrusion Technology, in: Swarbrick, J. (Ed.), Encyclopedia of Pharmaceutical Technology, 3rd Informa Healthcare USA, Inc, New York, pp. 2005-2020.

Miller, D.A., McConville, J.T., Yang, W., Williams III, R.O., McGinity, J.W., 2007. Hot-melt extrusion for enhanced delivery of drug particles. J. Pharm. Sci. 96, 361-376.

Muzzio, F.J., Robinson, P., Wightman, C., Brone, D., 1997. Sampling practices in powder blending. Int. J. Pharm. 155, 153-178.

Puchert, T., Holzhauer, C.-V., Menezes, J.C., Lochmann, D., Reich, G., 2011. A new PAT/QbD approach for the determination of blend homogeneity: Combination of on-line NIRS with PC Scores Distance Analysis (PC-SDA). Eur. J. Pharm. Biopharm. 78, 173-182.

Qi, S., Gryczke, A., Belton, P., Craig, D.Q.M., 2008. Characterization of solid dispersions of paracetamol and EUDRAGIT® E prepared by hot-meltextrusion using thermal, microthermal and spectroscopic analysis. Int. J. Pharm. 354, 158-167.

Rinnan, Å, van der Berg, F., Engelsen, S., 2009. Review of the most common pre-processing techniques for near-infrared spectra. Trends Anal. Chem. 28, 1201-1222.

Rohe, T., Becker, W., Kölle, S., Eisenreich, N., Eyerer, P., 1999. Near infrared (NIR) spectroscopy for in-line monitoring of polymer extrusion processes. Talanta 50, 283-290.

Saeed, M., Saner, S., Oelichmann, J., Keller, H., Betz, G., 2009. Assessment of Diffuse Transmission Mode on Near-Infrared Quantification – Part I: The press effect on Low-Dose Pharmaceutical Tablets. J. Pharm. Sci. 98, 4877-4886.

Saerens, L., Dierickx, L., Quinten, T., Adriaensens, P., Carleer, R., Vervaet, C., Remon, J.P., De Beer, T., 2012. In-line NIR spectroscopy for the understanding of polymer-drug interaction during pharmaceutical hot-melt extrusion. Eur. J. Pharm. Biopharm. doi:10.1016/j.ejpb.2012.01.001

Savitzky, A., Golay, M.J.E., 1964. Smoothing and Differentiation of Data by Simplified Least Squares Procedures. Anal. Chem. 36, 1627-1639.

Sekulic, S.S., Ward II, H.W., Brannegan, D.R., Stanley, E.D., Evans, C., Sciavolino, S.T., Aldridge, P.K., 1996. On-Line Monitoring of Powder Blend Homogeneity by Near-Infrared Spectroscopy. Anal. Chem. 68, 509-513.

Sekulic, S.S., Wakeman, J., Doherty, P., Hailey, P.A., 1998. Automated system for the on-line monitoring of powder blending processes using near-infrared spectroscopy Part II. Qualitative approaches to blend evaluation. Pharm. Biomed. Anal. 17, 1285-1309.

Shenk, J.S., Workman, J., Westerhaus, M.O., 2001. Application of NIR Spectroscopy to Agricultural Products, in: Burns, D.A, Ciurczak, E.W. (Eds), Handbook of Near-Infrared Analysis, Marcel Dekker, Inc. New York, pp. 419-474.

Shi, Z., Cogdill, R.P., Short, S.M., Anderson, C.A., 2008. Process characterization of powder blending by near-infrared spectroscopy: Blend end-points and beyond. J. Pharm. Biomed. Anal. 47, 738-745.

Sudah, O.S., Coffin-Beach, D., Muzzio, F.J., 2002. Effects of blender rotational speed and discharge on the homogeneity of cohesive and free-flowing mixtures. Int. J. Pharm. 247, 57-68.

Sulub, Y., Wabuyele, B., Gargiulo, P., Pazdan, J., Cheney, J., Berry, J., Gupta, A., Shah, R., Wu, H., Khan, M., 2009. Real-time on-line blend uniformity monitoring using near-infrared reflectance spectrometry: A noninvasive off-line calibration approach. J. Pharm. Biomed. Anal. 49, 48-54.

Tulumuri, V.S., Kemper, M.S., Lewis, I.R., Prodduturi, S., Majumdar, S., Avery, A. A., Repka, M. A., 2008. Off-line and on-line measurements of drug-loaded hot-melt extruded films using Raman spectroscopy. Int. J. Pharm. 357, 77-84.

United States Pharmacopeia 35/ National Formulary 30, 2012. General Chapter <1174> Powder Flow. The United States Pharmacopeial Convention, Rockville, MD, USA, pp. 801-804.

Vanarase, A.U., Alcalà, M., Jerez-Rozo, J. I., Muzzio, F.J., Romañach, R.J., 2010. Real-time monitoring of drug concentration in a continuous powder mixing process using NIR spectroscopy. Chem. Eng. Sci. 65, 5728-5733.

Venables, H.J., Wells, J.I., 2001. Powder Mixing. Drug Dev. Ind. Pharm. 27, 599-612.

Virtanen, S., Antikainen, O., Yliruusi, J., 2007. Uniformity of poorly miscible powders determined by near infrared spectroscopy. Int. J. Pharm. 345, 108-115.

Wargo, D.J., Drennen, J.K., 1996. Near-infrared spectroscopic characterization of pharmaceutical powder blends. J. Pharm. Biomed. Anal. 14, 1415-1423.

6 Continuous mixing

This work was presented at the FIP World Congress of Pharmacy and Pharmaceutical Sciences, Amsterdam, 2012. Awarded the Best Young Pharmacist Presentation of the Industrial Pharmacy Section.

Martinez, L., Peinado, A., Liesum, L., Betz, G. 2013. Use of near-infrared spectroscopy to quantify drug content on a continuous blending process: Influence of mass flow and rotation speed variations. Eur. J. Pharm. Biopharm.
http://dx.doi.org/10.1016/j.ejpb.2013.01.016

Graphical abstract

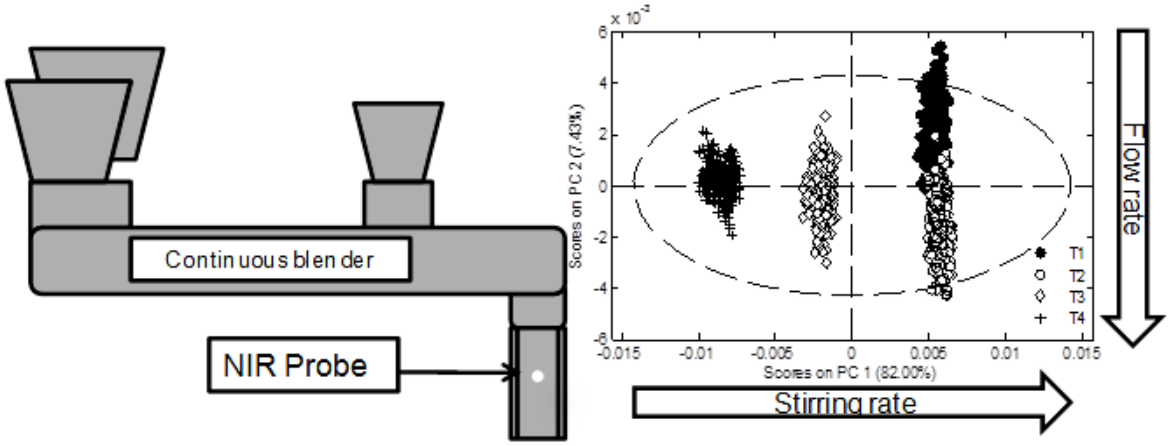

Abstract

The aim of this study was to develop a quantitative near-infrared (NIR) method which monitors the homogeneity of a pharmaceutical formulation coming out of a continuous blender. For this purpose, a NIR diode array spectrometer with fast acquisition parameters was selected. Additionally, the dynamic aspects of a continuous blending process were studied; the results showed a well-defined cluster for the steady-state, and the paths for the start-up and emptying stages were clearly identified. The end point of the start-up was detected by moving block of standard deviation, residual standard deviation, and principal component analysis, giving consistent results.

A partial least square (PLS) model was generated for the quantification of the drug, with a standard error of prediction of 0.2% m/m. The PLS model was successfully applied for monitoring the drug level at the outlet of a continuous blender. Furthermore, the PLS model was tested under different flow and stirring rates. Flow and stirring rate variations caused different powder flow dynamics, which were reflected on the NIR measurements. Therefore, the PLS-model was sensitive to changes on mass flow and rotation speeds.

Keywords

PAT, continuous blending, NIR, PLS, homogeneity, moving solids, moving block of standard deviation

6.1 Introduction

Blending of powders is an essential unit operation in a wide range of industries such as pharmaceutical, food, cosmetics, or construction materials. Powder mixing is a central and extremely important unit operation that is practiced to a great extent whenever particulate materials are processed. In the pharmaceutical industry, blending is involved in the manufacture of solid dosage forms, which includes tablets, capsules, and granules. Hence, it is fundamental to have a correct control strategy for powder blending.

Mixing of solids is the process by which two or more components (active ingredients and excipients) are randomized (Fan et al., 1970). Lacey (1954) suggested three possible mixing mechanisms for particulate material: convective, shear and diffusive mixing. Convective mixing involves the transfer of neighbor particles from one location to another, comprising the movement of large masses of particles; diffusive mixing is the distribution of particles over a freshly developed surface with random motion at small scale; and the exchange of particles across the shear zones corresponds to shear mixing (Alexander & Muzzio, 2002; Bridgwater, 1994; Manjunath et al., 2004; Staniforth, 1982; Williams, 1972,). Blending performance is largely dependent on the physical characteristics of the material (Bellamy et al., 2008; Chaudhuri et al., 2006; Venables & Wells, 2001; Virtanen et al., 2007) and the process conditions (Sudah, et al., 2002).

Mixing operations of particulate solids in the pharmaceutical industry are carried out batchwise even when the previous or further process steps are continuous. Hence, the handling and storage of the blended product can lead to segregation problems. An alternative to batch mixing is continuous blending. Continuous blending aims to continuously feed and blend the ingredients thus the resulting blend is ready for the next unit operation (Manjunath et al, 2004; Weinekötter & Gericke, 2006). Continuous blending when connected to the following unit operation offers several advantages such as continuity of production, reduction of the intermediate handling resulting in lower segregation, less storage space,

high production capacity, easier scale-up, faster product availability (Pernenkil & Cooney, 2006; Manjunath et al, 2004; Weinekötter & Gericke, 2006; Williams & Rahman, 1970).

The mixing of powders gains more and more economical importance, since the mixing process adds value to the product and incorrect blend uniformity can lead to out of specification products. Rees (1977) emphasized the importance of building quality into the product during development and manufacturing processes instead of relying and waiting for the control test of the final product. This statement clearly refers to the Quality by Design (QbD) context described by the ICH Q8 (R2) (2009), where the quality of the final product cannot be tested in the product, but rather should be built-in by design. The FDA's Process Analytical Technology (PAT) initiative (2004) also promotes the process understanding by encouraging the pharmaceutical industry on the implementation of new technologies and by predesigning the quality of the final product. One of the most widespread PAT tools is Near-Infrared (NIR) spectroscopy, which is a fast and non-invasive analytical technique that is suitable for the real-time monitoring of a blending process. Another characteristic of NIR spectroscopy is that the sample does not require previous treatment and can be measured as it is. Given that, this vibrational technique is sensitive to physical and chemical attributes (Blanco et al., 2000; Saeed et al., 2009), the resulting spectra need to be properly analyzed in order to focus the study to the quality attribute of interest.

NIR has been mostly applied to the quantification of API (Berntsson, et al., 2002; El-Hagrasy et al., 2001; Sulub, et al., 2009) and excipients (Liew, et al., 2010; Wu, et al., 2009) in batch mixing, but few has been done on the monitoring of continuous blending processes. There are several techniques described in the literature for assessing blend uniformity on a batch mixing process using NIR: principal component analysis (El-Hagrasy et al., 2001), principal component scores distance analysis (Puchert et al., 2011), bootstrap error-adjusted single-sample technique (Wargo & Drennen, 1996), mean square of differences (Blanco et al., 2002), caterpillar algorithm (Flåten et al., 2012) and moving block of standard deviation (MBSD) (Sekulic et al., 1996, 1998). Assessing blend uniformity in a batch process is based

on the determination of the blending end-point, on the other hand in continuous blending it is of great importance to determine when the process has reached a steady-state as well as the homogeneity of the blend. A common continuous mixing process can be divided into three sections: start-up, steady-state and emptying. In this study, we decided to choose PCA, MBSD, and relative standard deviation (RSD) for the steady-state identification.

One of the challenges of measuring a blending process is that the powders are under continuous movement, thus the different moving dynamics (different physical presentation of the sample) can interfere with the acquisition of reliable results. Andersson et al. (2005), examined moving solids with a NIR Fourier transform spectrometer, pointing out that powder speed influenced the quality of the resulting spectra, later studies (Benedetti et al., 2007; Ropero et al., 2009) showed the feasibility of measuring flowing powders. Koller et al. (2011) followed the blending process in a bladed mixer by NIR, concluding that fill level had a strong influence on the mixing dynamics. Besides the dynamic nature of the measurement, the inhomogeneities due to the performance of the blender as well as the powder properties are critical (Marikh, et.al, 2005; Portillo et al., 2010; Sarkar & Wassgren, 2010; Sudah, et al., 2002).

Weinekötter & Gericke (2000) studied the powder fluctuations at the outlet of the blender; they periodically disturbed the continuous feeding of the powder and observed the ability of the blender to buffer these disruptions. Kehlenbeck (2006) applied NIR spectroscopy for the in-line monitoring of a continuous mixing process of calcium carbonate and maize starch, the blend flowed over the probe followed by a cleaning step with compressed air. The spectra acquisition by the Fourier transform spectrometer was challenged by the movement of the sample that could cause false results. Vanarase et al. (2010) developed a quantification model for the real-time monitoring of a continuous blending process of acetaminophen, showing promising results for the industrial implementation of NIR as a PAT tool. Besides, the complexity of powder flow makes necessary to further study the process parameters that could influence the reliability of a multivariate model for a continuous blending process.

In this study, we will present and discuss some results concerning to the influence that mass flow rate and stirring rate variations exerted on NIR diffuse reflectance measurements. Subsequently, we developed an analytical method for the in-line quantification of the drug content using NIR and chemometrics tools. We focused the study into the identification of the parameters that may interfere with the accuracy of the NIR results and the range of applicability of the multivariate model. Furthermore we identified the different phases present on the continuous blender: star-up, steady-stage and emptying. Overall, this study explores the potential usage of a continuous blender combined with a NIR in-line process control for a pharmaceutical product.

6.2 Materials and methods

Continuous blending

The formulation under consideration contains two actives, one polymer and one lubricant. One granular ingredient containing a high dose active corresponded to 95 % (m/m). Subsequently, the granules were blended with the active of interest (A1). A1 represented 4% (m/m) of the formulation, while the lubricant accounted for 1% (m/m). The study was focused on monitoring the lower dose active, A1, given that the absence of the high load active would be gravimetrically evident. The physical characteristics and flow behavior of A1 and the granules are given in Table 6-1. The average particle size was measured using a laser diffraction system (Mastersizer S long bed, Malvern, Worcestershire, UK). The lens range was within the particle size range of 4.2-3500 µm. The samples were dispersed through a dry powder feeder and the measurements were carried out 5 times. Obscuration value was kept between 10-30% and residual under 1%. The Hausner index corresponds to the ratio formed by tapped and bulk densities.

Table 6-1 Properties of the A1 and granules containing a second active, A2.

	Granules	A1
Bulk density [g/cm^3]	0.55±0.01	0.45±0.01
Tapped density [g/cm^3]	0.58±0.01	0.57±0.01
Hausner index	1.07±0.01	1.26±0.02
Flow character	Excellent	Passable
Mean particle size d_{50} [µm]	241.44±21.67	59.40±2.78
Span*	5.58±0.22	2.91±0.63

* Span measures the width of the distribution and is calculated as $[d(0.9) - d(0.1)]/d(0.5)$

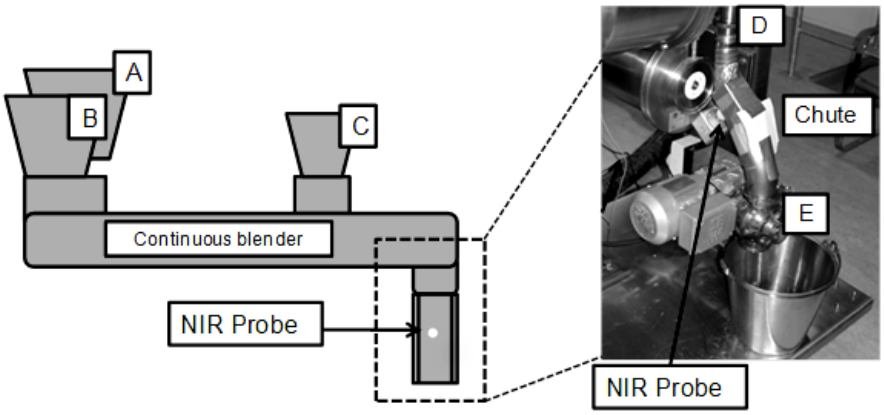

Figure 6-1 Experimental set-up. A, B, and C correspond to the granules, A1, and lubricant feeders respectively. D is the outlet of the blender and E refers to a rotary valve.

The granules, A1, and the lubricant were mixed in a continuous blender with Modulomix technology (Hosokawa Micron BV, NL) where the stirring speed was varied (400, 700, and 1000 rpm). The materials were fed through a twin screw loss-in-weight feeder (K-tron). Two classes of feeders were used: a KT35 for higher feed rate of the granules and a KT20 for the low concentration materials such as A1 and the lubricant. The granules and the A1 were mixed over the full length of the continuous blender while the lubricant inlet position was chosen to be at the last third of the blender, for avoiding over lubrication of the formulation (Figure 6-1).

Table 6-2 contains the process settings for four trials designed to evaluate the influence of the flow rate and stirring rate. Spectral data were collected for each trial at the outlet of the continuous blender as shown on Figure 6-1.

Table 6-2 Process settings for the continuous blending trials.

	Continuous blending trial			
	T1	**T2**	**T3**	**T4**
Flow rate [kg/h]	52.8	126.7	79.2	79.2
Granules Feed rate [kg/h]	50.0	120.0	75.0	75.0
API Feed rate [kg/h]	2.3	5.5	3.4	3.4
LubricantFeed rate [kg/h]	0.5	1.2	0.8	0.8
Stirring rate [rpm]	1000	1000	700	400
Trial duration [min]	5	5	5	5

NIR instrumentation

For the measurements of the flowing powder a NIR probe was mounted at the outlet of the continuous blender (Figure 6-1). The NIR equipment consisted of a SentroPAT FO spectrometer (Sentronic GmbH, Dresden, Germany) with a diode array detector, the data acquisition was performed through a diffuse reflectance probe SentroProbe DR LS (Sentronic GmbH, Dresden, Germany) with tungsten halogen bulbs as light source. The blends were scanned through the sapphire window of the probe, the NIR measurements were triggered automatically once the powder started to slide over the probe. Spectra acquisition was done in diffuse reflectance mode over the wavelength range of 1100-2200 nm at 1 nm intervals. One spectrum was obtained through the average of 60 scans and the scan time was 0.012 s.

Calibration samples and PLS-model building

In order to reproduce the physical conditions of the flowing powder bed, the calibration blends were blended directly at the continuous blender and scanned at the outlet of the blender. The rotation speed for the calibration samples was 1000 rpm, which corresponds to high shear inside the blender. Throughout the blending, the A1 level was varied according to the designed experiment (Figure 6-2); each concentration level was run for two minutes. The calibration spectra were selected from the steady state of each concentration subset. The feed rate for A1 varied from 0.9 to 4.3 kg/h for covering a concentration range of 25 to 125 % of the target value (1.1 to 5.4% m/m).The granules and lubricant feed rate were kept constant at 75 kg/h and 0.8 kg/h respectively.

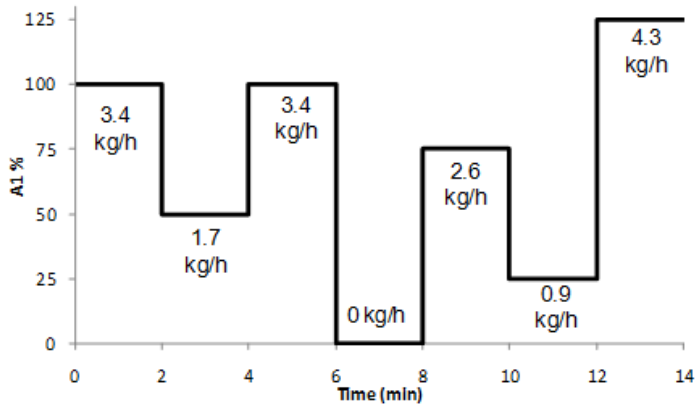

Figure 6-2 A1 level variation for the calibration samples including A1 feed rates.

The calibration spectra were chosen from the steady zone of each A1 level, with a total of 220 spectra. The resulting calibration spectra were preprocessed in order to remove spectral variation that was not correlated to A1 variations as well as to enhance the spectral selectivity for A1. Under the scattering correction methods; standard normal variate (SNV) was selected since this preprocessing technique reduces the multiplicative interferences of scattering and particle size (Barnes et al., 1989). Second derivative with the Savitzky Golay (SG) algorithm (Savitzky & Golay, 1964) were used in order to remove additive effects by correcting baseline drifts (Rinnan et al., 2009).

The wavelength range selected corresponded to 1535-1800 nm, these frequencies were highly correlated with A1 level variations. The pretreated spectra were matched with the gravimetric reference values of A1 and a PLS model was generated using random subsets cross-validation. The random subsets cross-validation considered 10 data splits and each subset was generated by random selection, such that no single object is in more than one test set, this procedure was repeated as much as 5 iterations.

The software used for the chemometrical analysis was Matlab (The Mathworks Inc.) version 2009Ra with PLS_toolbox (Eigenvector Research Inc.) version 6.2.1.

PLS-models application

The PLS-model was applied to the monitoring of a long duration trial of 25 minutes. The settings for this trial were the same as for the calibration samples: high stirring rate (1000 rpm), medium feeding rate for the lubricant (0.8 kg/h), A1 (3.4 kg/h) and the granules (75 kg/h), corresponding to the medium inflow rate.

NIR spectroscopy is well-known for containing physical and chemical information of the samples. Physical properties of the powder bed such as particle packaging and void distribution can be influenced by the process parameters, consequently, the NIR spectra and PLS model's predictions may be influenced as well. In a continuous blending process, the rotation speed and the mass flow rate can be defined by the operator, thus these parameters were selected for testing the influence that may have on the measured NIR spectra. The process settings are given on Table 6-2 and the spectral data were collected for each trial at the outlet of the continuous blender as shown on Figure 6-1.

Blending stages identification

The start-up, steady-state and emptying phases were identified by PCA, MBSD, and RSD. PCA was used for data exploration and extraction of relevant information by identification of similarities on the data. This is done by the projection of the large data space into a smaller

space that is easier to analyze (Geladi, 2003). PCA in this study was used for the detection of clusters and gradients originated during the continuous blending process, which could be associated to the different blending stages. PCA was performed on mean-centered spectra for T1, T2, T3 and T4 trials, over the wavelength range of 1535-1800 nm.

The MBSD analysis was performed on the preprocessed spectra of each trial. The wavelength range was 1535 to 1800 nm and the preprocessing combination was SNV, SG (15 pts) with 2nd derivative, the same techniques as for the one used for the development of the calibration model. The MBSD method consisted on selecting a set of 15 consecutive spectra then the standard deviation for the pretreated absorbance values at the selected wavelength range was calculated. Subsequently, the mean standard deviation of that set was computed. Mean standard deviation is plotted against the time, subsequently the spectral set was shifted by one time unit and the calculations were repeated. A full description of the MBSD technique can be found in Sekulic et al. 1996.

The relative standard deviation (RSD) is a mixing index widely used in industry. The RSD of the NIR predicted values for A1 were computed. The RSD was calculated through the standard deviation of the predicted values presiding over a range of 15 predictions and subsequently divided by their average, the values are shifted on one unit time and the calculations are repeated, resulting in a moving RSD.

Sampling

At the outlet of the blender samples were taken manually for T1, T2, and T3 at 30, 60, 120, 180, and 300 seconds. The long duration trial was sampled at 15, 30, 45, 60, 90, 120, 300, 600, and 1500 seconds. The sampling was performed to the flowing powder, taking approximately 3 g per time point. Subsequently A1 quantification of each sample was performed off-line by a validated HPLC method. The results from HPLC were compared with the average of ten predicted NIR concentrations of the corresponding time range.

6.3 Results and Discussion

Calibration model development

The single component NIR spectra for the granules and A1 were measured off-line (Figure 6-3). A1 is characterized by a narrow and intense peak at 1554 nm and a broader absorption band at 1710 nm. The wavelength region selected for the chemometric analysis was 1535 to 1800 nm corresponding to the absorbance frequencies of A1.

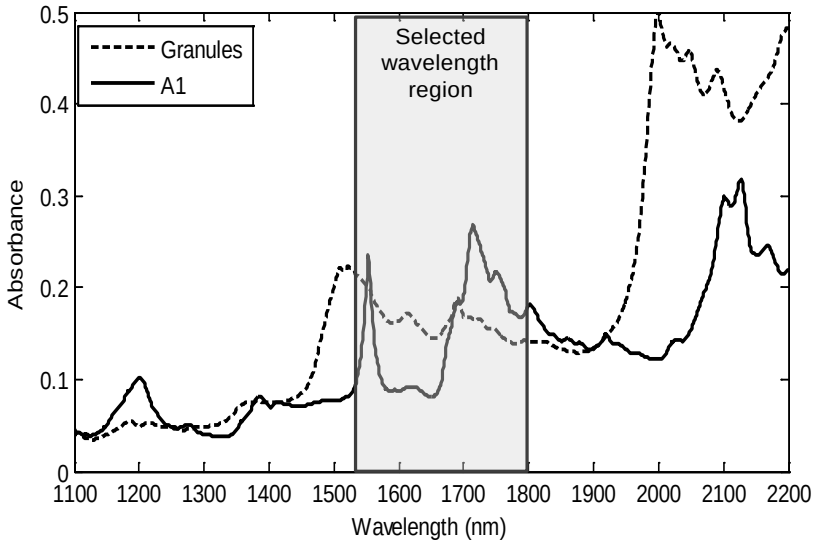

Figure 6-3 Raw spectra for A1 and granules containing a second API. The gray area corresponds to the selected wavelength region.

Certainly, the selected frequencies showed to be highly correlated with A1 level variations as shown in Figure 6-4 close-ups, this is reflected on the scores plot in Figure 6-5 in which well-defined clusters for each A1 level were presented. The scores plot shows that the first principal component covered 93.15% of the spectral variability, associated with the chemical information brought by the A1 concentration changes. Proving that the preprocessing combination of SNV and SG (15pt) second derivative corrected most of the physical variability of the calibration samples, while the wavelength range selected was correlated with A1 level variations.

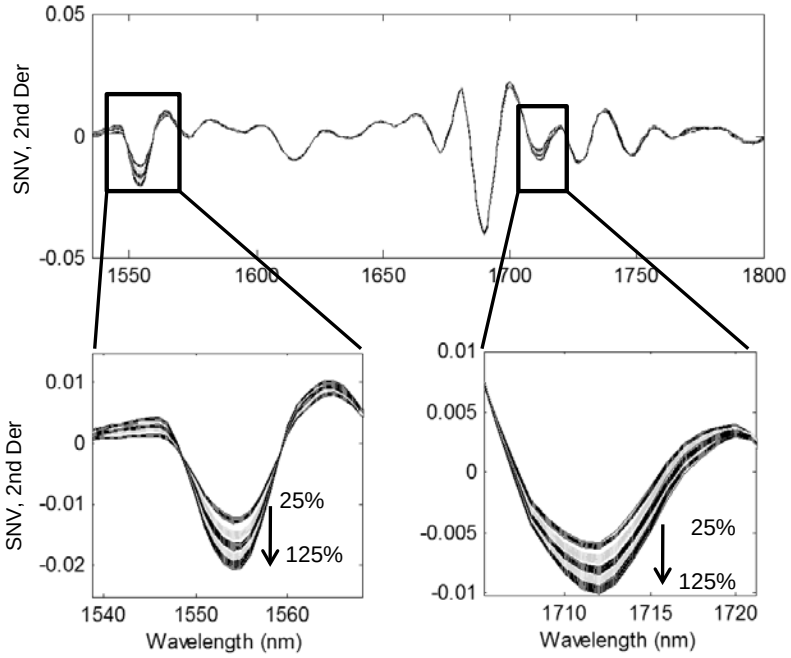

Figure 6-4 Preprocessed calibration spectra at the selected wavelength range, including two close-ups at A1 absorbance frequencies.

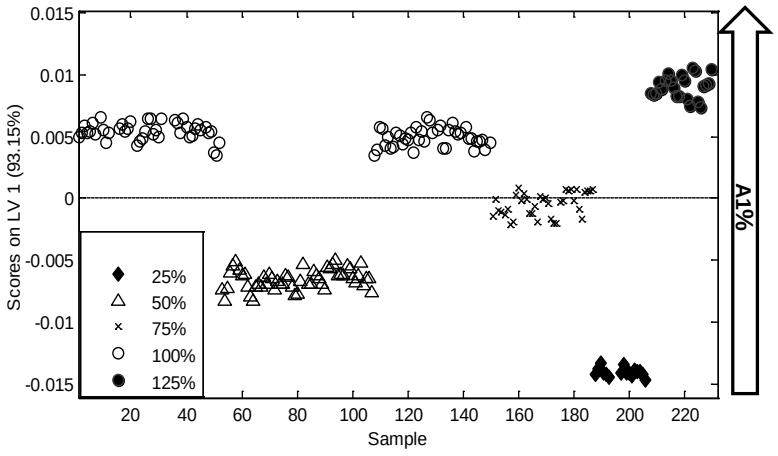

Figure 6-5 Scores plot for the calibration set preprocessed spectra at the selected wavelength region (1535-1800 nm).

The PLS model parameters are displayed in Table 6-3. The PLS model was generated with one principal component, which successfully carried out the quantitative information for A1 and showed better robustness when applied to independent data sets. The root mean square error of the cross validation (RMSECV) was 4.7% of A1 target value equivalent to an error of 0.2% m/m, indicating that the NIR model has an acceptable bias.

Table 6-3 Description of A1 PLS model.

Parameter		PLS-model Statistics
Number of principal components		1
Xcum[a] [%]		93.15
Ycum[b] [%]		97.56
RMSECV	[% Nominal]	4.7
	[% m/m]	0.2
R^2		0.975
Preprocessing technique		SNV, SG 2nd Derivative (15pt)
Wavelength range [nm]		1535-1800

[a] Cumulative variance captured by the model for the X variable (spectral data).
[b] Cumulative variance captured by the model for the Y variable (A1 % target value).

Results from the long duration trial

The quantification of the compound of interest in a blending process has been restricted to the analysis of samples retrieved from the outlet of the continuous blender on a regular time basis (Gao et al., 2011; Portillo et al., 2009). Recent work (Vanarase et al. 2010) showed the feasibility of real-time monitoring of a continuous blending process by NIR. In a PAT framework, the continuous quality assurance is achieved by a continuous monitoring of a process (FDA, 2004), therefore in this study, the continuous blending of a pharmaceutical formulation was monitored continuously and the quantification of A1 was made through the one principal component PLS-model.

A continuous blending trial with a total duration of 25 minutes was in-line monitored by NIR. The objective of this trial was to simulate a real production condition in order to evaluate the robustness of the PLS-model. The blending settings for the trial were the same as for the calibration samples: high stirring rate (1000 rpm), medium feeding rate for the lubricant, A1 and the granules, corresponding to the medium inflow rate.

The high throughput of a continuous blender requires a system that can react fast in order to identify deviations from the process specifications. The high sampling frequency of the NIR allowed constant monitoring of the blending process as shown in Figure 6-6. The predicted concentrations for A1 and the RSD values were acquired every second. High RSD values were observed at the beginning of the process, which was associated to the start-up phase. The start-up phase corresponded to the time that the blender required to reach a constant hold-up mass, thus reaching a steady-state among the inlet and outlet flow rates. The RSD vales presented some fluctuations above 5% these fluctuations might be associated with chemical inhomogeneities as well as bulk variations of the powder bed. Figure 6-7 shows the HPLC values for the samples retrieved at different time points, A1 concentrations varied within the range of 90 to 110%.

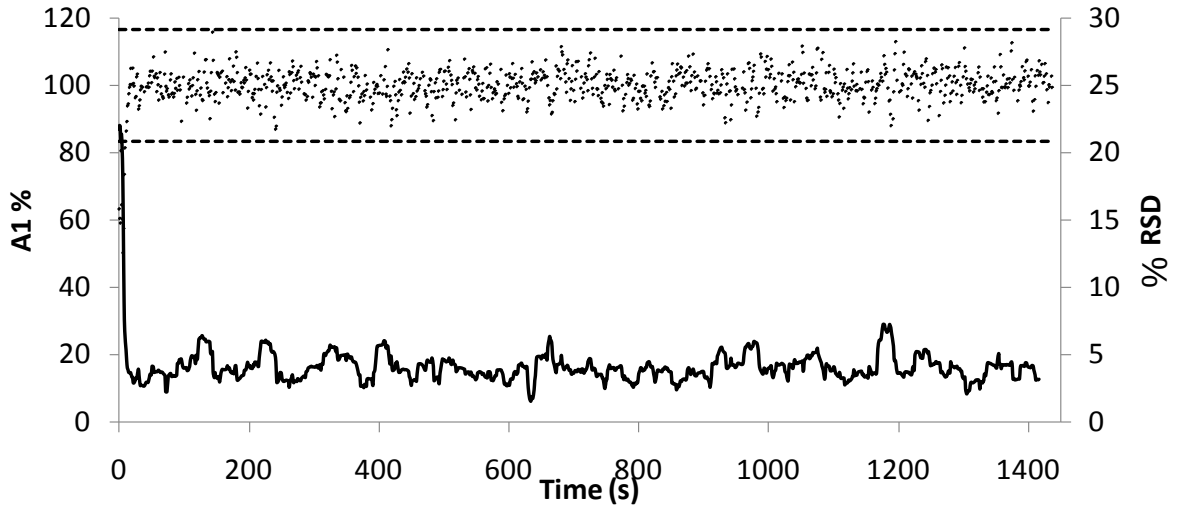

Figure 6-6 Results from the long duration trial each point corresponds to one NIR prediction, and the dotted line represents ±3 SD while the continuous line is the RSD.

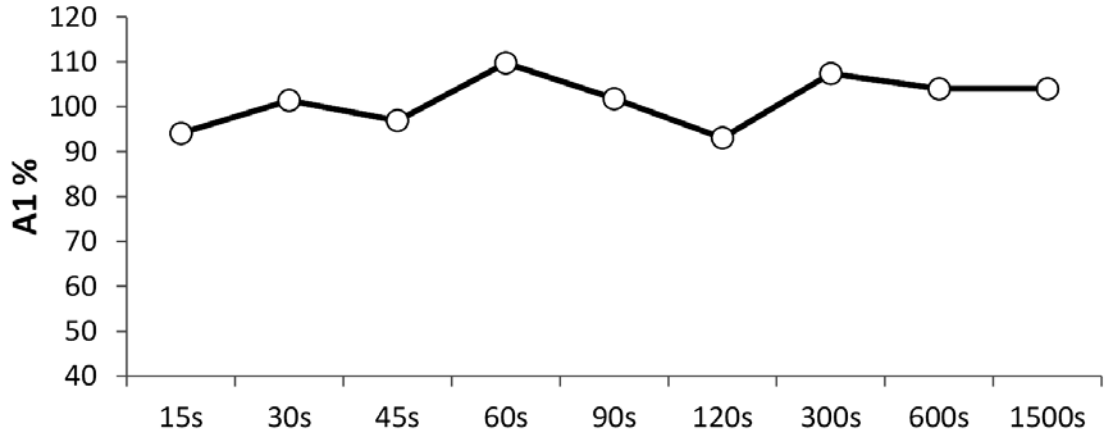

Figure 6-7 Off-line HPLC results for the samples retrieved form the continuous blender at different time points.

Influence of stirring and flow rate variations

The trials were designed in order to test the influence that the feeding rate and stirring rate exerted on the A1 concentrations calculated by the PLS model. The one principal component PLS-model was used to predict the A1 concentration on four different trials, with different process parameters of flow rate and rotation speed but leading to the same expected level of A1 (100% of the nominal value). Figure 6-8 contains the predicted NIR concentrations for the four different continuous mixing trials. T2, T3 and T4 concentrations were at the target concentration of 100%. These trials corresponded to the medium and high flow rate (79.2 and 126.7 kg/h) and three rotation rates (400, 700 and 1000 rpm), indicating that the PLS model was robust enough to cushion changes due to rotation speed changes. However, this was not the case for the T1 trial which was under predicted by almost 20%. T1 corresponded to the lowest flow rate (52.8 kg/h) and the PLS model was developed for an inflow rate ranging from 75 to 80 kg/h. This is directly reflected on the different amount of powder that passed through the probe at the same scan time. Even though the HPLC results for T1 indicate that the off-line samples varied within the range of 90 to 110% (Figure 6-9). Therefore, a reduction on the mass flow over the probe had a major influence on the PLS predictions. This might be a result of the decrease in the interaction between the NIR incident light and the particles, thus less mass equals less particles and more voids. In addition, a

higher flow rate may generate a more stable powder bed with less physical variations of density and particle packaging. Therefore the PLS model cannot be applied for the blend uniformity monitoring of inflow rates lower than the calibration range. Consequently, the development of a PLS model must consider the final flow rate conditions.

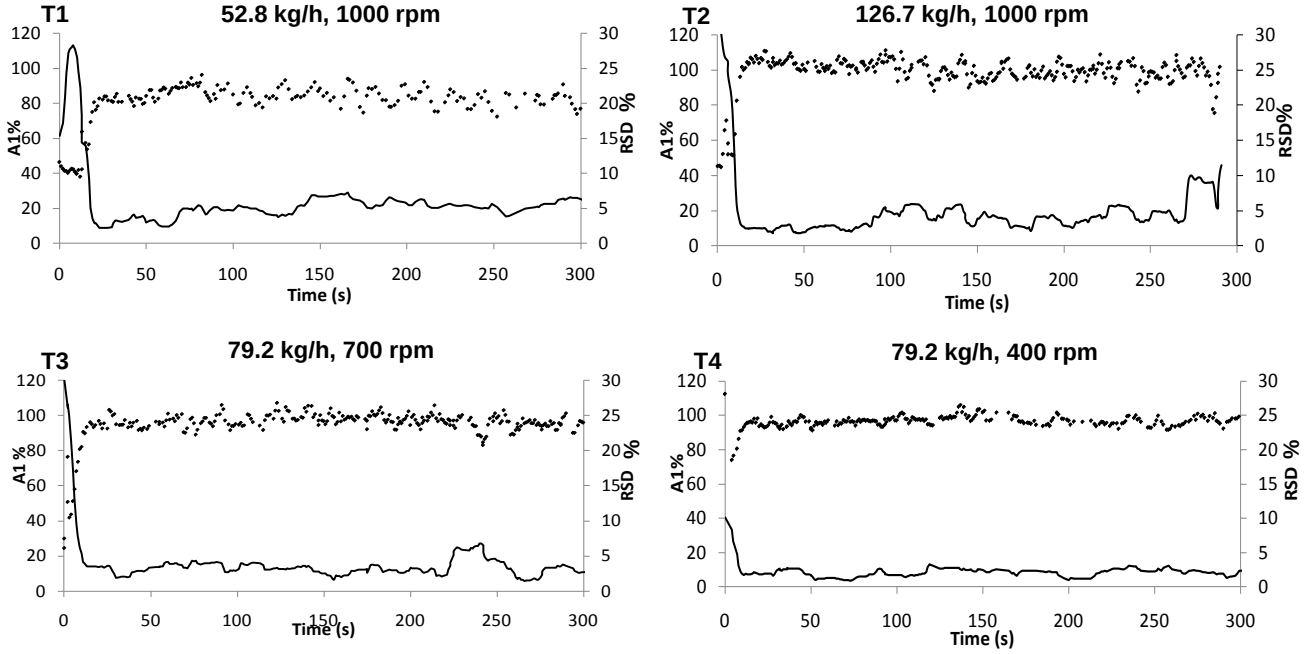

Figure 6-8 Predicted NIR values (♦) with RSD (continuous line) for the four trials at different flow rates and stirring rates.

Figure 6-8 depicts the RSD for each of the continuous blending trials. All the trials presented high RSD values at the beginning of the process, corresponding to the start-up period followed by the steady-state. RSD is an indicator of the uniformity of the blend; lower RSD values are correlated with better blend uniformity. On Figure 6-8 it can also be seen that as the rotation rate diminished the fluctuations on the predictions as well as the RSD trend were more stable. Given that the flow dynamics on the chute changed at different stirring rates, a better sample presentation to the NIR probe was obtained at 400 rpm. RSD values for T1 were over 5% indicating poor blend uniformity; this could be associated with the lack of predictability of the PLS model, thus RSD was not the indicated estimator for this trial. T2 corresponded to the trial with high inflow rate and high rotation rate. The RSD results showed that under these process conditions, the predicted concentrations showed more fluctuations

compared to T3 and T4. In accordance with the work of Gao et al. (2011) who describe higher variability on the residence time distribution curve for higher feeding rates, due to large fill levels and less homogeneous dispersion in the axial direction. T4 accounted for the lowest RSD values and was blended at the lowest stirring rate (400 rpm), resulting in a higher residence time. According to Williams & Rahman (1970) and Portillo et al. (2009) examinations, the influence of the rotation rate on the quality of the blend, shows that better content uniformity was achieved at lower rotation rates. This explanation is suggested for the lower fluctuation of the T4 trial in comparison with the other blending trials.

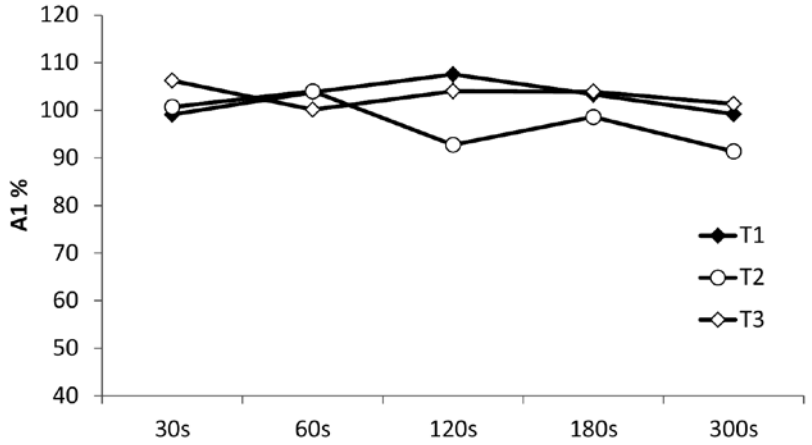

Figure 6-9 HPLC results for the retrieved samples for trials T1, T2, and T3.

Influence of stirring and flow rates studied by PCA

A principal component analysis was performed in order to find differences among the continuous blending trials. The start-up and emptying stage were removed and only the steady state spectra from each trial were selected. The same wavelength range and preprocessing techniques as for the PLS model were applied. Roggo et al. (2005) applied PCA successfully for the identification of different pharmaceutical process influence on spectroscopic results, showing the high value of this technique for process understanding. PCA was chosen as a useful qualitative tool for the identification of dissimilarities within the trials. We used this unsupervised classification method to identify the effect of the different continuous blender settings on the samples. Figure 6-10 shows the scores plot for the

preprocessed spectral data of the four continuous blending trials, in which the first principal component accounted for 82% of the spectral variability showing three clusters that were associated with the three different stirring rates. The loadings related to the first principal component are shown on Figure 6-11a. Loadings are difficult to interpret, however spectral signatures related to the presence of both actives can be detected. T3 and T4 were the trials with similar inflow rate though they differed on the rotation rate. Once the process reached the steady state the inflow and outflow rates were similar and did not vary with stirring rate changes, in agreement with Ammarcha et al. (2011). These results prove that NIR was sensitive to the different powder dynamics and particle packaging at the outlet of the continuous blender associated with the different stirring rates. This preprocessing combination was sensitive to stirring rate changes; hence the spectral preprocessing is fundamental in order to focus the analysis on the variable of interest. Previous efforts have shown that NIR spectroscopy could be used to identify physical variability as well as particle segregation on flowing blends (Barajas et al., 2007).

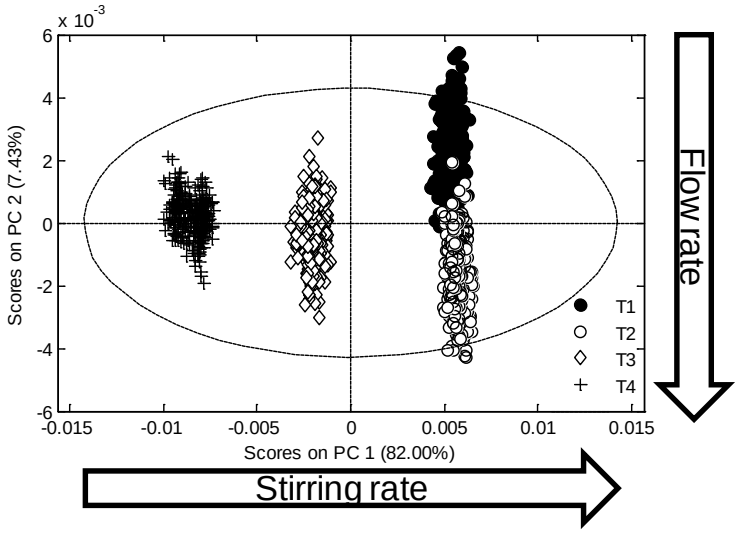

Figure 6-10 Scores plot for the four different continuous blending trials. The arrows indicate the increasing direction of stirring and flow rates.

The second principal component was linked with flow rate variations. The loadings in Figure 6-11b show the presence of a peak correlated to A1. Presumably the flow rate could interfere with the amount of powder sampled by the probe, in accordance with the under predicted

values for T1, in which less amount of powder was flowing over the probe per unit time. As Ropero et al. (2009) illustrates, the reflected radiation carried the information of the flow rate changes associated with the number of particles that interact with the NIR radiation.

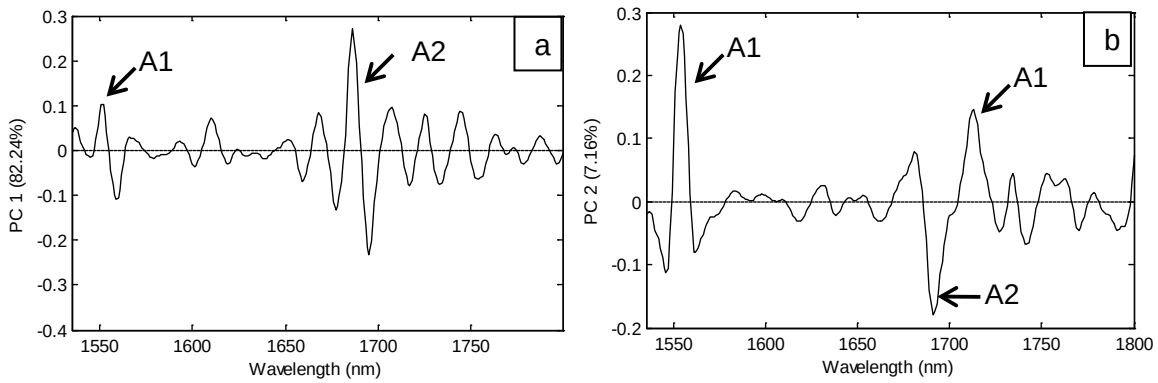

Figure 6-11 Loadings for the first and second principal components.

Steady-state determination

For the identification of the steady-state of each trial we applied three different qualitative approaches: PCA, MBSD and RSD. A continuous blending process is commonly divided into three phases, start-up, steady stage, and emptying (or shut down).,Each process step could be distinguished on a score plot. Figure 6-12 illustrates the score plot for each trial; the scores for the start-up and emptying were connected for showing the path that the blend followed. In all the cases a well-defined cluster for the steady or homogeneous state was observed. The results are encouraging for the application of PCA as a qualitative tool for the end point of the start-up determination. Subsequently, the pretreated spectra were used for the homogeneity determination by the MBSD with a 15 point window. MBSD was introduced by Sekulic et al., (1996, 1998) for the homogeneity determination of batch blending. We have chosen this technique due to its simplicity and fast application on the blend uniformity monitoring. Furthermore, MBSD is independent of a quantitative model like PLS and therefore does not require predicted values as RSD. On Figure 6-13, T1 and T2 showed higher MBSD values in addition to the presence of more fluctuations compared to T3 and T4; this was in accordance with the RSD of the predicted NIR values which also showed more

inconsistency for T1 and T2 trials. The different performances of the trials might be associated with several factors related to the variations on the physical presentation of the sample to the NIR probe, as well as factors associated with the blender performance.

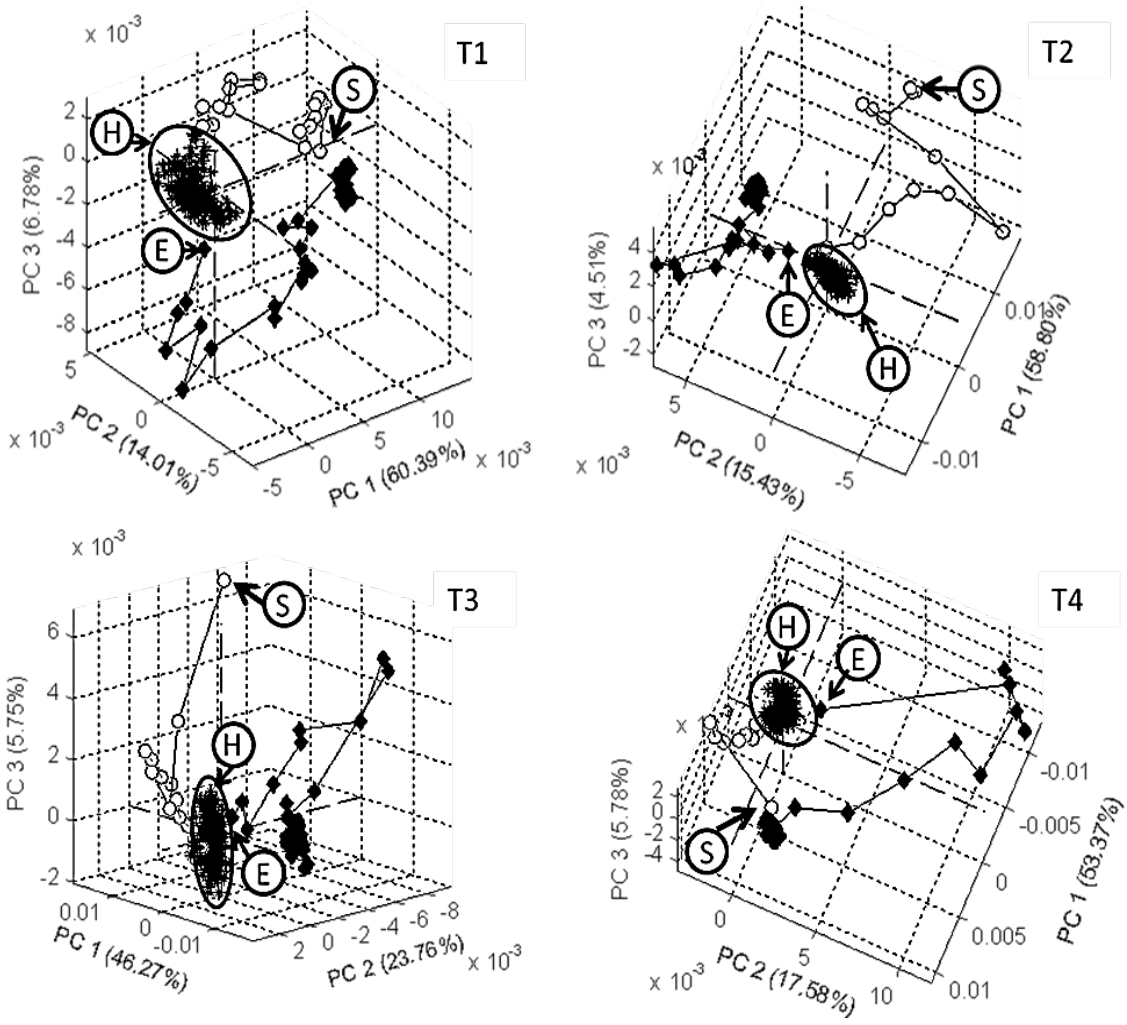

Figure 6-12 PCA for each trial. (○) start-up stage, (*) steady stage and (♦) emptying. S indicates the first measured sample. H corresponds to the homogeneous blend and E to the emptying stage corresponding to the first sample that is out of the homogeneous cluster. The plots were rotated for visualization purposes.

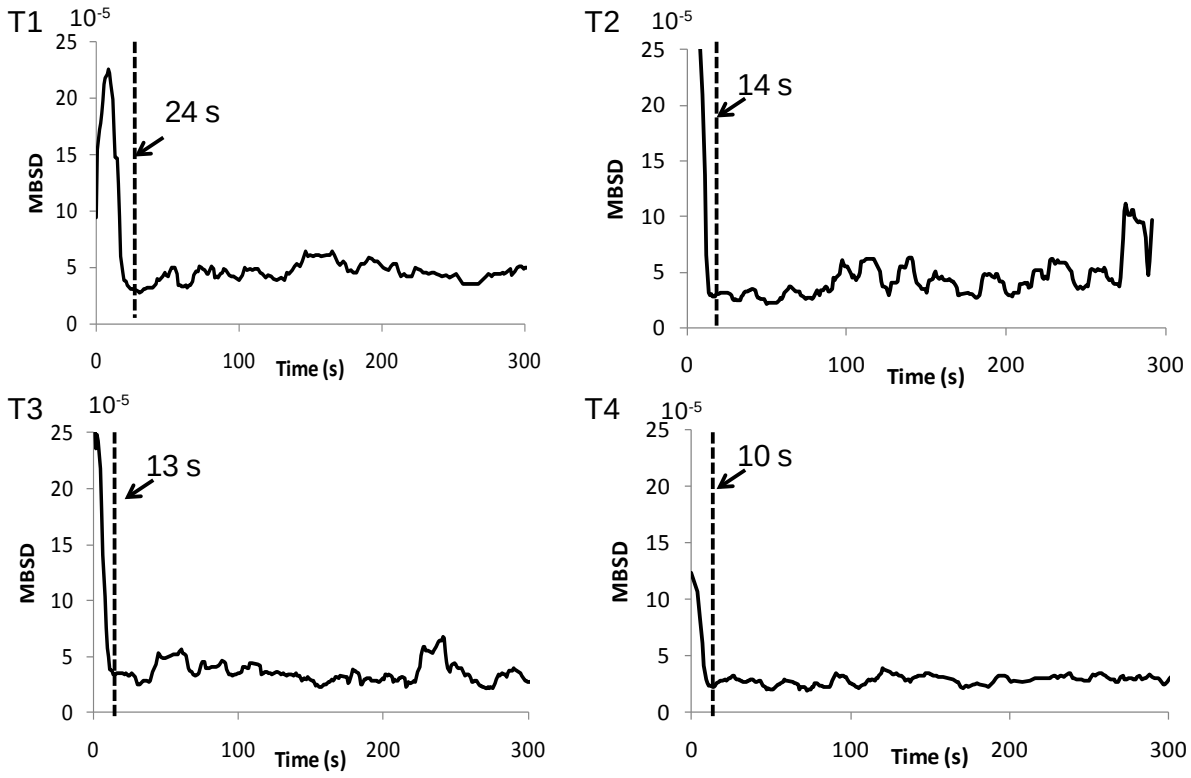

Figure 6-13 MBSD for each trial. The dotted line indicates the end of the start-up stage.

The start-up period refers to the time that the continuous mixer required to reach a constant hold-up mass. Subsequently the process was considered to have reached a steady state. The start-up times calculated from PCA, MBSD, and RSD for each trial are given in Table 6-4, where all the trials gave small start-up times due to the high rotation rates applied (400-1000 rpm). All three methods gave similar results for the start-up times, showing that T1 needed the longest (23 s) for achieving the steady state. This trial had the lowest inflow rate, consequently it required a few extra seconds for reaching the hold-up mass. This is in accordance with Ammarcha et al. (2011) and Marikh et al. (2005) who studied the hold-up mass as a function of the flow rate, noticing that as the inflow rate increases and the stirring rate decreases, the hold-up mass increases, thus influencing the start-up time. Furthermore, the mass associated with the start-up period was calculated by multiplying the average start-up time by the inflow rate of each trial. Even though T1 required the highest start-up time, T2 was the trial that needed more mass (457 g) in order to reach the steady-state. The start-up mass on a continuous blender needs to be determined since this amount represents a non-

homogeneous blend and when the outlet of the blender is directly connected to a tabletting machine, this could lead to out of specification product.

Table 6-4 Start-up end point determination.

	Method				
Trial	**PCA**	**MBSD**	**RSD**	**Average time**	**Start-up mass ***
	[s]	**[s]**	**[s]**	**[s]**	**[g]**
T1	22	24	23	23	337
T2	12	14	14	13	457
T3	13	13	13	13	286
T4	12	10	12	11	242

* Start-up mass= (average time* flow rate)

6.4 Conclusion

This paper described the development of an in-line PLS model for the quantification of the API in a continuous blending process for a pharmaceutical formulation. The PLS model was successfully applied for the monitoring of a continuous blending process under real production conditions and no statistically significant difference was found between the off-line HPLC results and the in-line NIR predicted values. The influence of the inflow rate and stirring rate on the quality of the blend was studied by PCA and RSD, showing that lower stirring rates reduced the fluctuations at the outlet of the blender, while low feed rates were not accurately predicted by the PLS model. Hence, if high variations on the feeding rate of the ingredients are expected, this variability should be included in the PLS-model in order to increase robustness. All the trials showed three stages on the PCA: start-up, steady-state and emptying. PCA, MBSD and RSD showed consistent results for the determination of start-up and end point, thus indicating when the steady-state or homogenous blend began.

This work constitutes a proof of concept on the feasibility of using NIR for the real-time monitoring of a continuous blending process of a pharmaceutical formulation.

Acknowledgements

We sincerely acknowledge Lukas Doulakas and Neil McDowall who added many useful discussions to this project.

References

Alexander, A.W., Muzzio, F.J., 2002. Batch Size Increase in Dry Blending and Mixing, in: Levine, M. (Ed.), Pharmaceutical Process Scale-Up, Marcel Dekker, New York, pp. 115-132.

Ammarcha, C., Gatumel, C., Dirion, J.L., Cabassud, M., Mizonov, V., Berthiaux, H., 2011. Predicting bulk powder flow dynamics in a continuous mixer operating in transitory regimes. Adv. Powder Technol. doi:10.1016/j.apt.2011.10.008

Andersson, M., Svensson, O., Folestad, S., Josefson, M., Wahlund, K.-G., 2005. NIR spectroscopy on moving solids using a scanning grating spectrometer-impact on multivariate process analysis. Chemometr. Intell. Lab. Syst. 75, 1-11.

Barajas, M.J., Rodriguez-Cassiani, A., Vargas, W., Conde.C., Ropero, J., Figueroa, J., Romañach, R.J., 2007. Near-Infrared Spectroscopic Method for Real-Time Monitoring of Pharmaceutical Powders During Voiding. Appl. Spectrosc. 61, 490-496.

Bellamy, L.J., Nordon, A., Littlejohn, D., 2008. Effects of particle size and cohesive properties on mixing studied by non-contact NIR. Int. J. Pharm. 361, 87-91.

Benedetti, C., Abatzoglou, N., Simard, J.-S., McDermott, L., Léonard, G., Cartilier, L., 2007. Cohesive, multicomponent, dense powder flow characterization by NIR. Int. J. Pharm. 336, 292-301.

Berntsson, O., Danielsson, L.-G., Lagerholm, B., Folestad, S., 2002. Quantitative in-line monitoring of powder blending by near infrared reflection spectroscopy. Powder Tech. 123, 185-193.

Blanco, M., González-Bañó, R., Bertran, E., 2002. Monitoring powder blending in pharmaceutical processes by use of near infrared spectroscopy. Talanta 56, 203-212.

Blanco, M., Peguero, A., 2010. Influence of physical factors on the accuracy of calibration models for NIR spectroscopy. J. Pharm. Biomed. Anal. 52, 59-65

Bridgwater, J., 1994. Chapter 10 Mixing, in: Chulia, D., Deleuil, M., Pourcelot, Y. (Eds.), Powder Technology and Pharmaceutical Processes, Elsevier, Amsterdam, pp. 347-357.

Chaudhuri, B., Mehrotra, A., Muzzio, F.J., Tomassone, M.S., 2006. Cohesive effects in powder mixing in a tumbling blender. Powder Tech. 165, 105-114.

El-Hagrasy, A.S., Morris, H.R., D'Amico, F., Lodder, R.A., Drennen III, J.K., 2001. Near-Infrared Spectroscopy and Imaging for the Monitoring of Powder Blend Homogeneity. J. Pharm. Sci. 90, 1298-1307.

FDA, 2004. Guidance for Industry: PAT – A Framework for Innovative Pharmaceutical Development, Manufacturing, and Quality Assurance. http://www.fda.gov/downloads/Drugs/GuidanceComplianceRegulatoryInformation/Guidances/ucm070305.pdf, accessed March 2012.

Flåten, G.R., Ferreira, A.P., Bellamy, L., Frake, P., 2012. PAT within the QbD Framework: Real-Time End Point Detection for Powder Blends in a Compliant Environment. J. Pharm. Innov. 7, 38-45.

Gao, Y., Vanarase, A., Muzzio, F., Ierapetritou, M., 2011. Characterizing continuous powder mixing using residence time distribution. Chem. Eng. Sci. 66, 417-425.

Kehlenbeck, V., 2006. Continuous dynamic mixing of cohesive powders. PhD thesis Technische Universität München, Germany.

Koller, D.M., Posch, A., Hörl, G., Voura, C., Radl, S., Urbanetz, N., Fraser, S.D., Tritthart, W., Reiter, F., Schlingmann, M., Khinast, J.G., 2011. Continuous quantitative monitoring of powder mixing dynamics by near-infrared spectroscopy. Powder Tech. 205, 87-96.

Liew, C.V., Karande, A.D., Heng, P.W.S., 2010. In-line quantification for drug and excipients in cohesive powder blends by near infrared spectroscopy. Int. J. Pharm. 386, 138-148.

Manjunath, K., Dhodapkar, S., Jacob, K., 2004. Solids Mixing, Part B: Mixing of Particulate Solids in the Process Industries, in: Paul, E.L., Atiemo-Obeng, V.A., Kresta, S.M., (Eds.), Handbook of Industrial Mixing: Science and Practice, John Wiley & Sons, Inc, New Jersey, pp. 924-985.

Marikh, K., Berthiaux, H., Mizonov, V., Barantseva, E., 2005. Experimental study of stirring conditions taking place in a pilot plant continuous mixer of particulate solids. Powder Tech. 157, 138-143.

Portillo, P.M., Ierapetritou, M.G., Muzzio, F., 2009. Effects of rotation rate, mixing angle, and cohesion in two continuous powder mixers- A statistical approach. Powder Tech. 194, 217-227.

Portillo, P.M., Vanarase, A.U., Ingram, A., Seville, J.K., Ierapetritou, M.G., Muzio, F.J., 2010. Investigation of the effect of impeller rotation rate, powder flow rate, an cohesion on powder flow behavior in a continuous blender using PEPT. Chem. Eng. Sci. 65, 5658-5668.

Puchert, T., Holzhauer, C.-V., Menezes, J.C., Lochmann, D., Reich, G., 2011. A new PAT/QbD approach for the determination of blend homogeneity: Combination of on-line NIRS with PC Scores Distance Analysis (PC-SDA). Eur. J. Pharm. Biopharm. 78, 173-182.

Roggo, Y., Jent, N., Edmond, a., Chalus, P., Ulmschneider, M., 2005. Characterizing process effects on pharmaceutical solid forms using near-infrared spectroscopy and infrared imaging. Eur. J. Pharm. Biopharm. 61, 100-110.

Ropero, J., Beach, L., Alcalà, M., Rentas, R., Davé, R.N., Romañach, R.J., 2009. Near-infrared Spectroscopy for the In-line Characterization of Powder Voiding Part I: Development of the Methodology. J. Pharm. Innov. 4. 187-197.

Saeed, M., Saner, S., Oelichmann, J., Keller, H., Betz, G., 2009. Assessment of Diffuse Transmission Mode on Near-Infrared Quantification – Part I: The press effect on Low-Dose Pharmaceutical Tablets. J. Pharm. Sci. 98, 4877-4886.

Sarkar, A., Wassgren, C., 2010. Continuous blending of cohesive granular material. Chem. Eng. Sci. 65, 5687-5698.

Sekulic, S.S., Ward II, H.W., Brannegan, D.R., Stanley, e.D., Evans, C., Sciavolino, S.T., Aldridge, P.K., 1996. On-Line Monitoring of Powder Blend Homogeneity by Near-Infrared Spectroscopy. Anal. Chem. 68, 509-513.

Sekulic, S.S., Wakeman, J., Doherty, P., Hailey, P.A., 1998. Automated system for the on-line monitoring of powder blending processes using near-infrared spectroscopy Part II. Qualitative approaches to blend evaluation. Pharm. Biomed. Anal. 17, 1285-1309.

Sudah, O.S., Coffin-Beach, D., Muzzio, F.J., 2002. Effects of blender rotational speed and discharge on the homogeneity of cohesive and free-flowing mixtures. Int. J. Pharm. 247, 57-68.

Sulub, Y., Wabuyele, B., Gargiulo, P., Pazdan, J., Cheney, J., Berry, J., Gupta, A., Shah, R., Wu, H., Khan, M., 2009. Real-time on-line blend uniformity monitoring using near-infrared reflectance spectrometry: A noninvasive off-line calibration approach. J. Pharm. Biomed. Anal. 49, 48-54.

United States Pharmacopeia 35/ National Formulary 30, 2012. General Chapter <1174> Powder Flow. The United States Pharmacopeial Convention, Rockville, MD, USA, p.p. 801-804.

Vanarase, A.U., Alcalà, M., Jerez-Rozo, J. I., Muzzio, F.J., Romañach, R.J., 2010. Real-time monitoring of drug concentration in a continuous powder mixing process using NIR spectroscopy. Chem. Eng. Sci. 65, 5728-5733.

Venables, H.J., Wells, J.I., 2001. Powder Mixing. Drug Dev. Ind. Pharm. 27, 599-612.

Virtanen, S., Antikainen, O., Yliruusi, J., 2007. Uniformity of poorly miscible powders determined by near infrared spectroscopy. Int. J. Pharm. 345, 108-115.

Wargo, D.J., Drennen, J.K., 1996. Near-infrared spectroscopic characterization of pharmaceutical powder blends. J. Pharm. Biomed. Anal. 14, 1415-1423.

Weinekötter, R., Gericke, H., 2006. Mixing of solids. Springer, Dordrecht, pp. 81-97.

Williams, J.C., Rahman, M.A., 1970. The continuous mixing of particulate solids. J. Soc. Cosmetic Chemists 21, 3-36.

Wu, H., Tawakkul, M., White, M., Khan, M.A., 2009. Quality-by-Design (QbD): An integrated multivariate approach for the component quantification in powder blends. Int. J. Pharm. 372, 39-48

7 NIR in a powder stream

Part of this work was presented at the FACSS (Federation of Applied Spectroscopy Societies) conference in Reno Nevada, 2011.

Graphical abstract

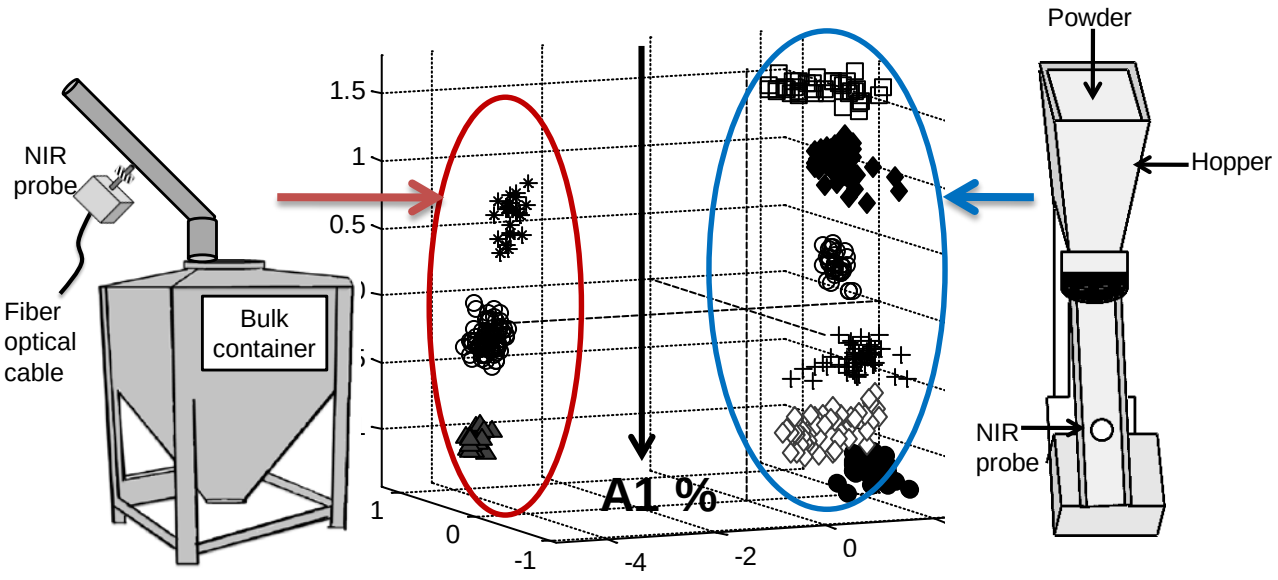

Abstract

Near Infrared (NIR) spectroscopy is a powerful analytical tool that can be used for the measurement of particulate material without previous sample preparation. Spectral NIR data contain chemical and physical information from the samples; therefore a quantitative NIR model needs to be focused on the quality attribute of interest, such as active pharmaceutical ingredient (API) concentration. The aim of this study was to use NIR spectroscopy for the development of an in-line quantitative model of an API in a powder stream. Calibration samples with different API concentrations levels were measured by NIR under flow conditions in a lab-scale set-up. The complexity of the powder flow in a powder stream could not be fully reproduced in the lab-scale set-up. Therefore the calibration set was merged with selected spectral data acquired in powder stream formed during the filling of an industrial bulk container (IBC). The combination of both spectral data sets was performed in order to integrate the unaccounted variability due to different powder flow dynamics. . The preprocessing techniques, orthogonal signal correction, combined with second derivative and standard normal variate, proved to focus the analysis into the API concentration by reducing physical and flow variations effects on the spectra. Finally the partial least squares model with a prediction error of 0.2% (m/m) was applied for the prediction of unknown samples during the bulk container filling. The NIR predictions showed good results when compared to their corresponding time-point HPLC analysis.

Keywords

PAT, NIR, PLS, homogeneity, moving solids, powder stream, Orthogonal Signal Correction

7.1 Introduction

NIR spectroscopy is a versatile tool that has gained lot of attention from the pharmaceutical industry as well as from the health authorities. The FDA launched the process analytical technology (PAT) initiative (2004), which encourages the pharmaceutical industry to improve process understanding, increase research into new technologies for process control (i.e. NIR) in order to monitor critical parameters that could potentially affect the quality of the product.

NIR is a versatile tool that has been applied in a wide range of pharmaceutical unit operations as drying (Peinado et al., 2011), blending (Cuesta et al., 1995; Sekulic et al., 1996; Blanco et al., 2002; Sulub et al., 2011), compaction (Saeed, et al., 2009), and more applications reviewed by Reich (2005) and Roggo et al.,(2007). The major advantages of NIR spectroscopy are that it is non-destructive and the immediate delivery of results, also the technology has improved and the diode array spectrometers allow the fast acquisition of spectral data. Therefore, NIR can be used to characterize powders under flowing conditions (Benedetti et al., 2007), hence is possible to monitor a powder stream as the one existing during the filling of an IBC. The granular flow in an inclined chute has a complex behavior (Ahn et al., 1991; Santomaso & Canu, 2001), in which the granular material is surrounded by air thus impacting the solid fraction (density). Random motion of the particles, physical and chemical inhomogeneties, and velocity and flow rate fluctuations, are the main challenges that in-line monitoring of a powder stream faces.

NIR spectroscopic data contain information related to physical and chemical properties of the sample. Andersson et al. (2005) showed how the dynamic conditions of the sample have a strong impact on the quality of the data acquired by a Fourier Transform spectrometer; the quality of the measurements can be improved by using diode array equipment hereafter avoiding the wavelength scanning. Diode array technology has already been tested by Vanarase et al. (2010), for the monitoring of a continuous blending process of a blend containing acetaminophen as active ingredient. The advantages of using NIR spectroscopy

for the in-line monitoring of powder stream is that the powder (or pharmaceutical blend) is analyzed without disrupting the process, the sampling stage is eliminated, and the high rate of measurements performed. Hersey (1970) mentioned, all sampling operations can lead to some degree of segregation, the number of samples is important and the more samples taken the smaller the error. Thus NIR is a promising PAT tool for the monitoring of a powder flow in a powder stream.

The complexity of the granular flow in a chute as well as the kinematic, physical and chemical information contained in the NIR spectroscopic data pushes to a careful analysis of the results, where chemometrics has a key role for the successful development of a multivariate model.

Before the development of a partial least squares (PLS) regression, it is valuable to mathematically pretreat the data in order to correct additive and multiplicative effects, thus reducing irrelevant variability due to physical influences and to enhance the chemical response on the spectroscopic data. The NIR data are commonly corrected by a differentiation and/or normalization step. Standard normal variate (SNV) is a mathematical pretreatment introduced by Barnes et al (1989). SNV reduces the influence of scattering and particle size by calculating the standard normal variation at each wavelength and removing slope variations on an individual sample basis. A popular differentiation method is the one proposed by Savitzky Golay (1964), this method includes a smoothing step, first derivative removes baseline while second corrects for baseline and detrend. Another preprocessing technique is the orthogonal signal correction (OSC), which corrects NIR spectra, by subtracting the variability on the **X**- calibration matrix that is orthogonal to the **Y**-matrix, this method was suggested for reducing differences between spectrometers during model transfers (Sjöblom et al., 1998). OSC minimizes the variability that is not referred to the y values (concentration of the analyte), has been applied for reducing the differences between the spectra of production and lab-scale samples (Blanco et al., 2001).

In the present work, near-infrared spectroscopy was used for the monitoring of an IBC filling. The API level was predicted through a PLS regression model, the model was developed by with synthetic samples obtained at lab-scale and samples acquired during the IBC filling. Different preprocessing approaches including SNV, differentiation and OSC were employed in order to correct the differences between both set-ups. Finally the model was used for the prediction of unknown spectra during an IBC filling.

7.2 Materials and methods

Powder characterization

The formulation under consideration contains two actives, one polymer and one lubricant. One active (A2) was agglomerated in a ratio of 10:1 with the polymer. Subsequently, the granules were blended with another active (A1). A1 represented 4% (m/m) of the formulation, while the lubricant accounted for 1% (m/m). The study was focused on the monitoring of the lower dose active, A1.

Experimental set-up

For the measurements of the flowing powder a NIR probe was mounted on a chute (Figure 7-1), the inclination of the chute was 54° to the vertical. This angle allowed the continuity of the powder flow without undesirable powder jams. The blends were filled into a hopper with a capacity of 100 cm^3, which was attached to the chute.

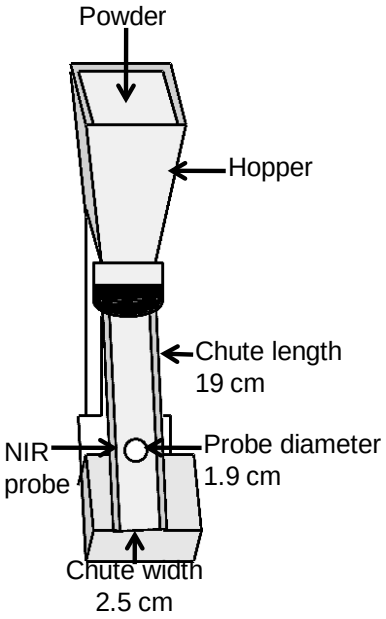

Figure 7-1 Experimental set-up for the off-line calibration samples.

We used a SentroPAT FO spectrometer (Sentronic GmbH, Dresden, Germany) that includes a diode array detector and acquires the data by a fiber optical connector from the diffuse reflectance probe SentroProbe DR LS (Sentronic GmbH, Dresden, Germany). The probe has tungsten halogen bulbs as the light source. The blends were flowed from the hopper and were measured through the sapphire window of the probe. The probe diameter was 1.9 cm, with an illuminated spot with a diameter of 5 mm (D). The NIR measurements were triggered automatically when the powder slid over the probe. Spectra acquisition was done in reflectance mode over the wavelength range of 1100-2200 nm at 1 nm intervals. A single spectrum was acquired with a scan time (t_{scan}) of 0.007 s and a total number (n) of 60 single spectra were automatically averaged and saved as an average spectrum. The NIR penetration depth (h) was assumed to be 0.1 cm. The blend bulk density (ρ_{bulk}) was 0.55 g/cm^3. The velocity of the powder (v) was 57 cm/s. This velocity value corresponded to the length of the chute divided by the time that the powder needed for sliding over the chute. The time was measured by video recording the powder flow over the chute. Subsequently frame by frame video analysis was performed. Finally the sampled mass (m) corresponding to 0.658 g was estimated by Equation 7-1.

Equation 7-1 $\boldsymbol{m = Dvh(\rho_{bulk})(t_{scan})n}$

The value of 658 mg was compared with the computed sample mass excluding the temporal variables of scan time and powder velocity. In this case the volume of powder over the illuminated spot was calculated and multiplied by the total scans, then correlated with the bulk density for the mass calculation by Equation 7-2. Thus the sampled mass corresponded to 648 mg.

Equation 7-2 $\boldsymbol{m = \pi(D/2)^2 h(\rho_{bulk})n}$

The estimated sampled mass by Equation 7-1 and 8-2 was in the same order of magnitude for these powder flow conditions corresponding to less than one unit dose of the product under study.

Calibration samples and PLS-model building

The calibration samples were prepared by varying the concentration range of 70 to 130 % of A1 target value, the lubricant concentration was kept constant at 1% m/m, and each calibration blend of 500 g was mixed for 10 minutes (Turbula type T50A, W. Bachofen, Switzerland) at 32 rpm. Each calibration blend was emptied from the hopper (Figure 7-1) and the calibration spectra were acquired as the material flowed down the chute. The spectra were chosen from the steady stage of each run, with a total of 300 spectra.

Three extra calibration samples corresponding to blends with 75, 100, and 125% nominal API value were measured by NIR during the filling of the bulk container (Figure 7-2). For the spectral data acquisition during the filling of the bulk container a second SentroPAT FO spectrometer was used with a scanning time set to 0.012 s and a total of 60 single spectra were averaged. All the spectral data were selected under steady flow conditions, therefore the spectra corresponding to the beginning and at the end of each run were discarded since they were not representative of normal operating conditions. The mass flow rate was 79 kg/h.

The calibration set contained 120 spectra selected from the normal operating conditions over the three concentration levels.

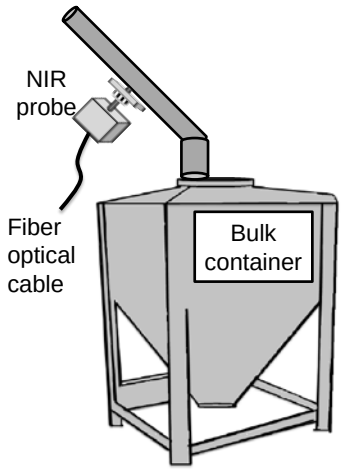

Figure 7-2 NIR measurements during the filling of a bulk container

The wavelength range selected corresponded to 1150-1900 nm since these frequencies were highly correlated with A1 level variations. Subsequently, the spectra were mathematically pretreated by standard (SNV) correction, Savitzky-Golay (11pt) with second derivative and orthogonal signal correction. The pretreated spectra were matched with the gravimetric reference values of A1 and a PLS model was generated. Validation was done through an independent vatidation set corresponding to one third of the spectra, previously excluded from the calibration dataset.

The software used for the chemometrical analysis was for principal component analysis, Matlab (The Mathworks Inc.) version 2009Ra with PLS_toolbox (Eigenvector Research Inc.) version 6.2.1. For the PLS regression model Simca P+ version 12.0 (Umetrics AB) was used.

PLS-model application

The PLS-model was applied to the monitoring of the continuous powder flow during 25 minutes, under the target flow rate of 79 kg/h. At the outlet of the pipe, samples were retrieved at 15, 30, 45, 60, 90, 120, 300, 600, 900, and 1500 seconds. The sampling was performed on the flowing powder, taking approximately 3 g per time point. Subsequently A1

quantification of each sample was performed off-line by a validated HPLC method. The results from HPLC were compared with the average of ten predicted NIR concentrations at the corresponding time range.

7.3 Results and Discussion

Figure 7-3 shows the NIR spectra for the granules and for A1. The wavelength range selected was 1150-1900 nm and was used for further chemometric analysis.

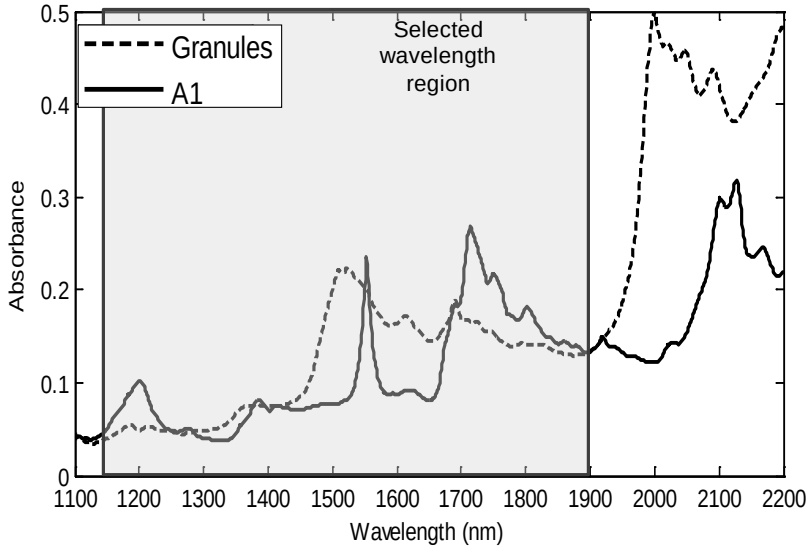

Figure 7-3 Raw spectra for A1 and the granules containing a second active. The grey area corresponds to the selected wavelength region.

The calibration model was developed for the quantification of A1 under flowing conditions in a powder stream. The raw NIR spectra from the calibration set (Figure 7-4a) showed scattering due to the difference on particle size and particle packaging on the chute, such as quantity and distribution of voids. Dahm & Dahm (2007) studied the effect of voids and particle size on the remitted light from a scattering material, thus the importance to mathematically correct the spectral information in order to focus the analysis on the chemical attributes. These multiplicative and additive effects are due to the physical variability encountered on the particulate material and were reduced by second derivative and SNV as the preprocessing techniques (Figure 7-4b). Second derivative was used in order to remove

additive effects by correcting baseline drifts (Rinnan et al., 2009); the differentiation was linked with a smoothing algorithm by the Savitzky Golay procedure (Savitzky & Golay, 1964). SNV as shown by Barnes et al. (1989) removes the multiplicative interferences of scattering and particle size. After performing this combination of mathematical pretreatments, the spectral differences were attenuated (Figure 7-4b).

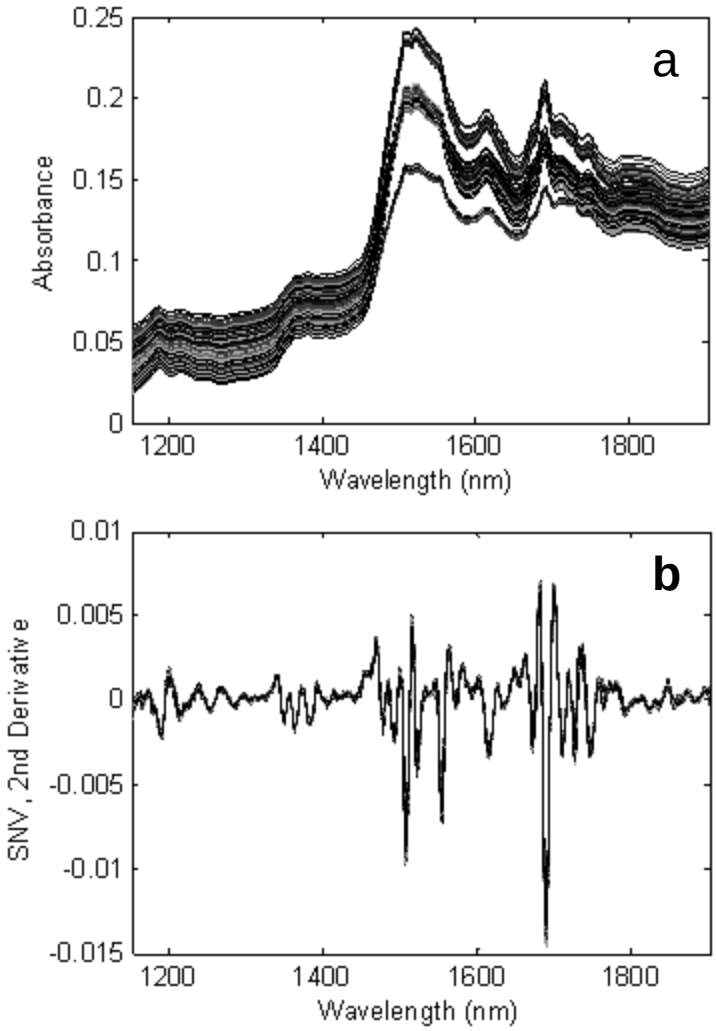

Figure 7-4 (a) Raw calibration spectra (b) SNV and 2nd derivative preprocessed spectra.

Before developing a quantitative model for the prediction of a chemical attribute, such as the API concentration level, it is useful to analyze the information contained in the spectral data by an unsupervised technique, such as PCA. PCA is helpful for the identification of patterns or trends in the data (Cowe & McNicol, 1985, Wold, et al., 1987). Figure 7-5 displays the scores plot with the first three principal components for the calibration samples after second

derivative and SNV pretreatment for the selected wavelength range. The first PC accounted for 86.55% of the variability contained in the spectral data. The first PC divided the scores in two main clusters (A) and (B) which were related to the two different experimental designs. Thus, even after applying the different mathematical pretreatments, the spectral differences were reduced, but not fully corrected. This difference between the lab-scale and the ones acquired during the filling of the bulk container was attributed to the different dynamics of the powder flow inside both chutes. As Roberts (2003) highlighted, chutes in industrial applications involves rapid or accelerated flow conditions in which a thin flow is present (thickness of the powder bed is less than the width of the chute), thus the flow dynamics can vary according to the chute design and the process conditions. In our case the flow rate was within the same magnitude for both experimental designs, on the other hand, different particle packaging, different NIR equipments, and different particle speed were the main factors that accounted for the presence of clusters (A) and (B) on Figure 7-5. This is in agreement with Karande et al. (2010), who mentioned that the laboratory synthesized calibration samples are highly accurate but they do not fully represent the samples under the actual processing parameters. Farrell et al., (2012) also showed how to improve the prediction model performance by using a lab prepared set of samples and including samples from production, this was done in order to bring into the model the unaccounted variability from the synthetic sample set. Thus, one strategy is to collect process samples that contain the process signature and to combine them with the synthetic lab samples to provide a higher variability of the component of interest, in this case A1 concentration. The A1 concentration was contained in the second PC, which carried 8.57% of the spectral variability. On the second PC, the different sub-clusters associated to the concentration variations of A1, were clearly identified.

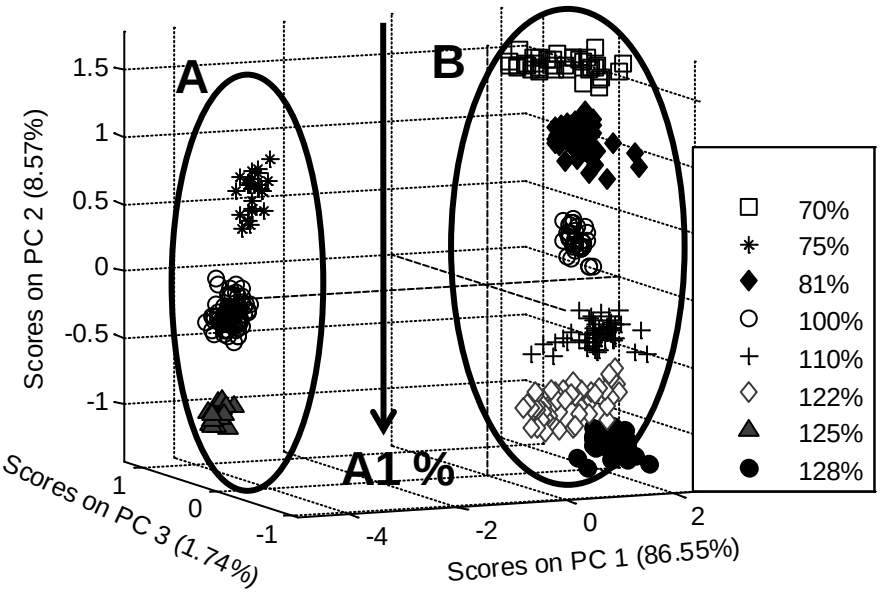

Figure 7-5 Scores plot showing two clusters (A) refers to the calibration samples acquired during the filling of the bulk container and (B) to the off-line calibration samples from the lab-scale samples.

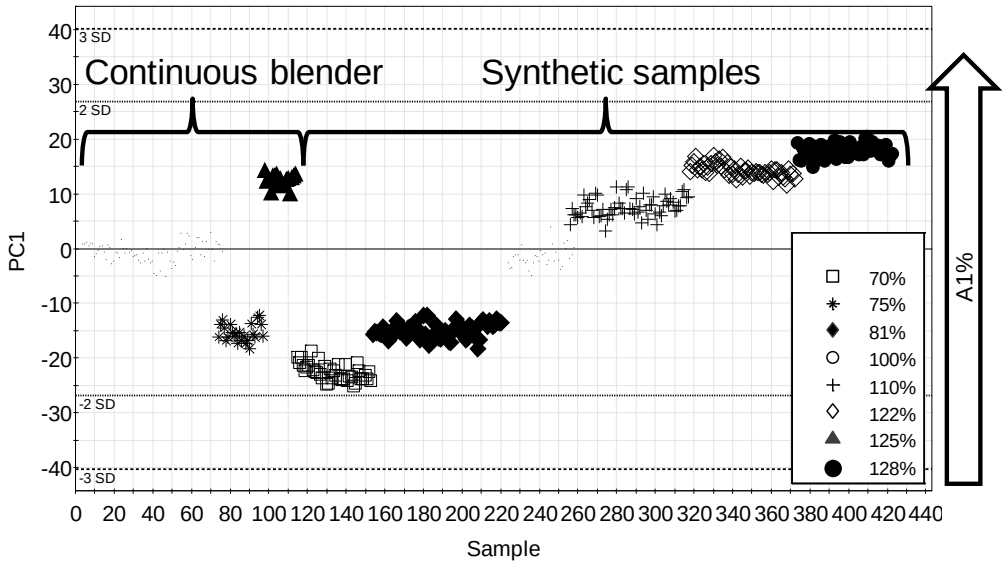

Figure 7-6 Scores plot after OSC.

Methods such as SNV proposed by Barnes (1989) or multiplicative scattering projection proposed by Geladi et al., (1985) and Martens & Stark (1991), do not use orthogonal projections to correct multiplicative effects, therefore the removal of the remaining undesirable systematic variation on the spectral data was performed by OSC. OSC corrects the spectral data (**x**) by removing the information that is orthogonal to response **y** (A1 concentration). The method was first introduced by Wold et al (1998) for the correction of

NIR spectra; while Sjöblom et al (1998) evaluated the OSC as well as the combination of second derivative followed by OSC, showing that low RMSEP values were obtained by this sequence of mathematical pretreatments. Thus the decision to apply the OSC to the differentiated and SNV corrected spectra. By a PCA analysis shown in Figure 7-6, we confirmed that by including the OSC preprocessing, the difference between the two experimental set-ups was corrected and that now only one principal component was explaining the A1 concentration changes. The preprocessed spectra were mean centered before the multivariate calibration and a PLS regression model was generated. The validation was performed by the prediction of one third of the spectra previously excluded from the calibration model. The main statistics for the A1 PLS model are summarized in Table 7-1. The PLS model was developed with one component and the captured variability of **y** was 0.976 and that the RMSEP was 3.6 % of the nominal A1 value which is equivalent to 0.2 % (m/m) error.

Table 7-1 Main statistics obtained for the A1 PLS model.

Parameter		**PLS-model Statistics**
Number of principal components		1
Xcum[a] (fraction)		0.975
Ycum[b] (fraction)		0.976
RMSEP	% Nominal	3.6
	% m/m	0.2
R^2		0.965
Preprocessing technique		2^{nd} Derivative (11pt), SNV and OSC
Wavelength range (nm)		1150-1900

[a] Cumulative variance captured by the model for the X variables.
[b] Cumulative variance captured by the model for the Y variables.

One challenging step during multivariate calibration is the prediction of unknowns, thus a fully independent continuous blending trial was performed in order to test the prediction capability of the A1 PLS regression model. Figure 7-7 illustrates NIR predictions of the A1 levels for the

monitoring of a 25 minutes run, each point corresponds to one predicted value as well as the relative standard deviation (RSD). RSD is a mixing index widely used in industry and was calculated through the standard deviation of the predicted values presiding over a range of 10 predictions and subsequently divided by their average, the values are shifted on one unit time and the calculations are repeated, resulting in a moving RSD. RSD is an indicator of the uniformity of the blend; lower RSD values are correlated with better blend uniformity. At the beginning of the process, during the start-up stage, falling RSD values showed the steadying of the process. The RSD values as well as the in-line NIR predictions presented fluctuations during the process that could be related to inhomogeneities in the A1 level of the blend as well as artifacts in the NIR predictions. As an external evaluation, the in-line NIR predictions were compared with the measured A1 concentration obtained by the sampling of the process at different time points followed by an off-line HPLC quantification**.** The HPLC values indicated that the concentrations of A1 % varied within the 90-110% of the target value. This was in accordance with the observed behavior for the NIR predictions (Figure 7-8).

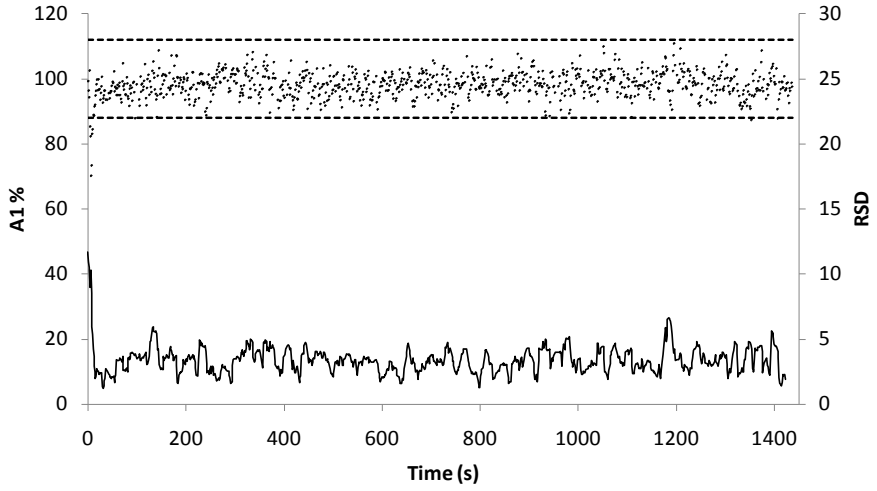

Figure 7-7 In-line NIR predicted values, the dotted line indicates ± 3SD and the continuous line refers to RSD of the predictions.

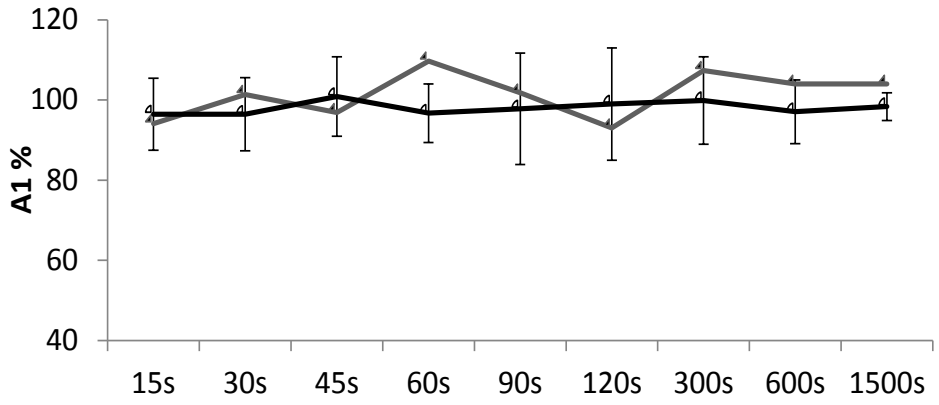

Figure 7-8 Off-line HPLC values (◆) and average of 10 NIR predictions (○), with error bar representing three standard deviations.

7.4 Conclusion

This paper described the development of an in-line PLS-model for the quantification of the API in a powder stream. The off-line calibration samples acquired in a lab-scale experimental set-up, allowed us to measure different concentrations levels of the active ingredient under dynamic conditions, on the other hand, the complexity of the powder flow at the during the filling of a container could not be fully reproduced. In order to incorporate the unaccounted variability, selected samples from the process were added to the calibration set. As the preprocessing techniques, OSC combined with second derivative and SNV, proved to focus the analysis into the chemical attribute by reducing physical and kinematic variations as well as the difference between the two NIR spectrometers. Finally the PLS model was applied to the prediction of unknown samples during the monitoring of the process under normal conditions. The NIR predictions showed good results when compared to their corresponding time-point from the off-line HPLC results. This work is a probe of concept of the feasibility of using NIR under thin flow conditions present in a process stream.

7.5 References

Ahn, H., Brennen, C.E., Sabersky, R.H., 1991. Measurements of Velocity, Velocity Fluctuation, Density, and Stresses in Chute Flows of Granular Materials. J. Applied Mech.-T. ASME. 58, 792-803.

Andersson, M., Svensson, O., Folestad, S., Josefson, M., Wahlund, K.-G., 2005. NIR spectroscopy on moving solids using a scanning grating spectrometer-impact on multivariate process analysis. Chemometr. Intell. Lab. Syst. 75, 1-11.

Barnes, R.J., Dhanoa, M.S., Lister, S.J., 1989. Standard Normal Variate Transformation and De-trending on Near-Infrared Diffuse Reflectance Spectra. Appl. Spectrosc. 43, 772-777.

Benedetti, C., Abatzoglou, N., Simard, J.-S., McDermott, L., Léonard, G., Cartilier, L., 2007. Cohesive, multicomponent, dense powder flow characterization by NIR. Int. J. Pharm. 336, 292-301.

Blanco, M., Coello, J., Montoliu, I., Romero, M.A., 2001. Orthogonal signal correction in near infrared calibration. Anal. Chim. Acta 434, 125-132.

Blanco, M., González-Bañó, R., Bertran, E., 2002. Monitoring powder blending in pharmaceutical processes by use of near infrared spectroscopy. Talanta 56, 203-212.

Cowe, I.A., McNicol, J.W., 1985. The Use of Principal Components in the Analysis of Near-Infrared Spectra. Appl. Spectrosc. 39, 257-266.

Cuesta, F., Toft, J., van der Bogaert, B., Massart, D.L., Dive, S.S., Hailey, P., 1995. Monitoring powder blending by NIR spectroscopy. Fresenius J. Anal. Chem. 325, 771-778.

Dahm, D.J., Dahm, K.D., 2007. Interpreting Diffuse Reflectance and Transmittance, IM Publications, Norfolk, UK.

Fan, L.T., Chen, S.J., Watson, C.A., 1970. Solids Mixing. Ind. Eng. Chem. 62, 53-69.

Farrell, J.A., Higgins, K., Kalivas, J.H., 2012. Updating a near-infrared multivariate calibration model formed with lab-prepared pharmaceutical tablet types to new tablet types in full production. J. Pharm. Biomed. Anal. 61, 114-121.

FDA, 2004. Guidance for Industry: PAT – A Framework for Innovative Pharmaceutical Development, Manufacturing, and Quality Assurance. http://www.fda.gov/downloads/Drugs/GuidanceComplianceRegulatoryInformation/Guidances/ucm070305.pdf, accessed June 2012.

Geladi, P., MacDougall, D., Martens, H., 1985. Linearization and Scatter-Correction for Near-Infrared Reflectance Spectra of Meat. Appl. Spectrosc. 39,491-500.

Hersey, J.A., 1970. Sampling and assessment of powder mixtures for cosmetics and pharmaceuticals. J. Soc. Cosmetic Chemists 21, 259-269.

Karande, A.D., Liew, C.V., Heng, P.W.S., 2010. Calibration sampling paradox in near infrared spectroscopy: A case study of multi-component powder blend. Int. J. Pharm. 395, 91-97.

Martens, H., Stark. E.,1991. Extended multiplicative signal correction and spectral interference subtraction—new preprocessing methods for near infrared spectroscopy. J. Pharm. Biomed. Anal. 9, 625–635.

Peinado, A., Hammond, J., Scott, A., 2011. Development, validation and transfer of a Near Infrared method to determine in-line the end point of a fluidized drying process for commercial production batches of an approved oral solid dose pharmaceutical product. J. Pharm. Biomed. Anal. 54, 13-20.

Reich, G., 2005. Near-infrared spectroscopy and imaging: Basic principles and pharmaceutical applications. Adv. Drug Deliv. Rev. 57, 1109-1143.

Roberts, A., 2003. Chute Performance and Design for Rapid Flow Conditions. Chem. Eng. Technol. 26, 163-170.

Rinnan, Å, van der Berg, F., Engelsen, S., 2009. Review of the most common pre-processing techniques for near-infrared spectra. Trends Anal. Chem. 28, 1201-1222.

Roggo, Y., Chalus, P., Maurer, L., Lema-Martínez, C., Edmond, A., Jent, N., 2007. A review of near infrared spectroscopy and chemometrics in pharmaceutical technologies. J. Pharm. Biomed. Anal. 44, 683-700.

Saeed, M., Saner, S., Oelichmann, J., Keller, H., Betz, G., 2009. Assessment of Diffuse Transmission Mode on Near-Infrared Quantification – Part I: The press effect on Low-Dose Pharmaceutical Tablets. J. Pharm. Sci. 98, 4877-4886.

Santomaso, A.C., Canu, P., 2001. Transition to movement in granular chute flows. Chem. Eng. Sci. 56, 3563-3573.

Savitzky, A., Golay, M.J.E., 1964. Smoothing and Differentiation of Data by Simplified Least Squares Procedures. Anal. Chem. 36, 1627-1639.

Sekulic, S.S., Ward II, H.W., Brannegan, D. R., Stanley, E.D., Evans, C.L., Sciavolino, S.T., Hailey, P.A., Aldridge, P.K., 1996. On-Line Monitoring of Powder Blend Homogeneity by Near-Infrared Spectroscopy. Anal. Chem. 68, 509-513.

Sjöblom, J., Svensson, O., Josefson, M., Kullberg, H., Wold, S., 1998. An evaluation of orthogonal signal correction applied to calibration transfer of near infrared spectra. Chemom. Intell. Lab. Syst. 44, 229-244.

Sulub, Y., Konigsberger, M., Cheney, J., 2011. Blend uniformity end-point determination using near-infrared spectroscopy and multivariate calibration. J. Pharm. Biomed. Anal. 55, 429-434.

Vanarase, A.U., Alcalà, M., Jerez-Rozo, J. I., Muzzio, F.J., Romañach, R.J., 2010. Real-time monitoring of drug concentration in a continuous powder mixing process using NIR spectroscopy. Chem. Eng. Sci. 65, 5728-5733.

Williams, J.C., Rahman, M.A., 1970. The continuous mixing of particulate solids. J. Soc. Cosmetic Chemists 21, 3-36.

Wold, S., Esbensen, K., Geladi, P., 1987. Principal component analysis. Chemom. Intell. Lab. Syst. 2, 37-52.

Wold, S., Antti, H., Lindgren, F., Öhman, J., 1998. Orthogonal signal correction of near-infrared spectra. Chemom. Intell, Lab. Syst. 44, 175-185.

8 Conclusions and Perspectives

This research was focused on the mixing of particulate materials. Different aspects of powder blending were studied, from particle size incompatibilities between the formulation ingredients and segregation tendencies. Pointing out the importance of a well-designed formulation and how a scientific understanding of the physicochemical properties of the formulation can deeply improve the quality of the final blend.

Near-infrared spectroscopy was the selected analytical tool for this research. NIR as a major PAT tool was a valuable technique for the blend uniformity monitoring in batch and continuous mixing. NIR offered three great advantages for blend monitoring, one was to avoid the use of thief sampling which is known to introduce bias on the measurements. The second advantage was that off-line and wet and destructive analytical methods can be eluded. The third advantage was fast data acquisition.

NIR showed great applicability for the measurement of solid samples. On the other hand careful selection, development, and application of the statistical tools is fundamental. In this research, special emphasis was given to the correct implementation of the chemometric methods in order to develop robust models for the monitoring of the quality attribute (mostly API concentration).

Continuous mixing of powders is a new technology in the pharmaceutical industry. In this study we showed the feasibility of monitoring the continuous blending of a pharmaceutical formulation. An insight into the parameters that can influence the analytical measurements was provided. Due to the novelty of NIR monitoring of a continuous blending process, there is plenty of material for future research. Some examples are: the influence of the flowing powder-layer on the quality of the spectra, the influence of high cohesion, the reliability of the system after a long process, the possibility to identify segregation issues on the flowing powder, the robustness of a the MVDA method, and validation of the final MVDA model.

Figure 8-1 illustrates the final goal of process control for a continuous blender, in which the critical variables from the continuous blender, the feeding system, and the NIR spectrometer would be all included in a general MVDA model.

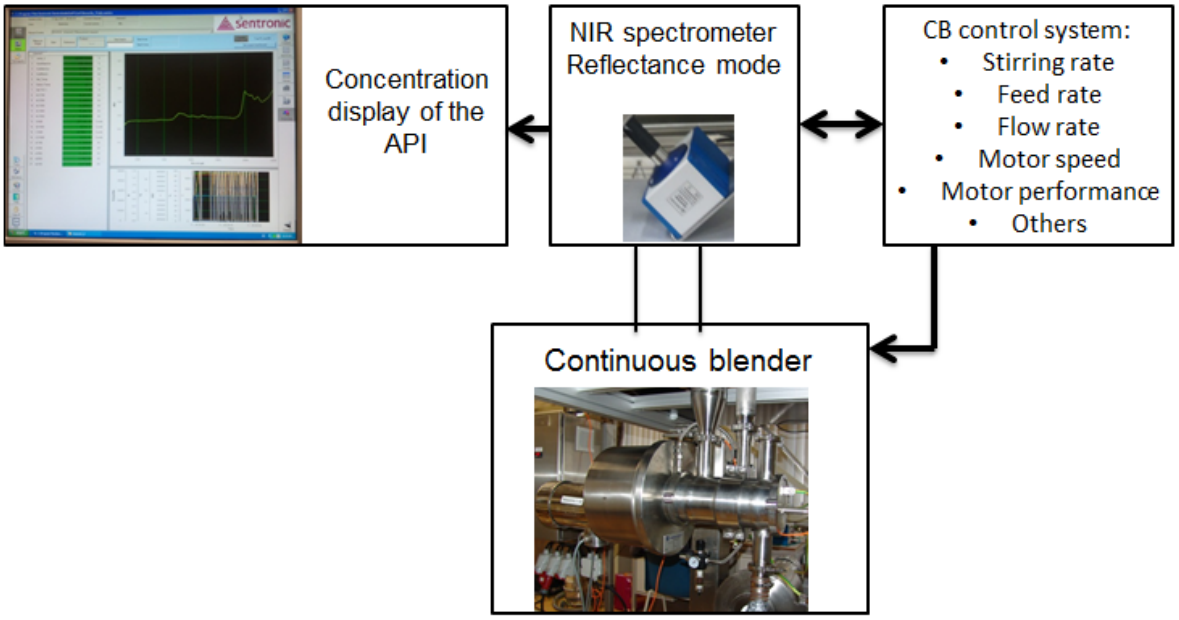

Figure 8-1 Process control for a continuous blender.

The need to produce high quality products in a short time is pushing towards continuous manufacturing. Despite the precedents of continuous manufacturing in other industries, the pharmaceutical industry is just beginning to shift to continuous production. This research is a step forward to the development of reliable systems for the control a continuous blending process in a pharmaceutical formulation. Throughout, it was observed that understanding the process, the technology, and the formulation can lead to powerful results reflected in higher efficiency and cost savings.

9 Appendix 1: Supplementary Discussion to Chapter 6

9.1 Objective

The objective of this section is to cover the parameters that may be relevant on the performance of the NIR spectrometer as well as for the continuous blending system. Among the studied parameters were the influence of high rotation rate on the mechanical stability of the granules, the selection of acquisition times and averaging of NIR spectra, and the influence of mass flow rate on the spectroscopic data.

9.2 Materials and methods

Attrition Evaluation

The morphological characterization was performed by scanning electron microscopy (SEM) (ESEM XL 30 FEG, Philips, The Netherlands) at an applied voltage of 10 kV and magnifications of 100-2000 times. The sample preparation included placing the powder on carbon adhesive, followed by gold plating.

The average particle size was measured using a laser diffraction system (Mastersizer S long bed, Malvern, Worcestershire, UK). The lens range was within the particle size range of 4.2-3500 µm. The samples were dispersed through a dry powder feeder and the measurements were carried out 5 times. Obscuration value was kept between 10-30% and residual under 1%. The analysis was set in “polydisperse” mode. The mean and median diameters and the span values were recorded.

NIR and feeding system

In order to identify the best acquisition parameters for the NIR data and also for testing the influence of different feedings rates on the quality of the spectroscopic results, a set-up including a feeding system coupled with an NIR probe was implemented. Figure 9-1 illustrates the full experimental set-up. This set-up consisted of a K-Tron T35 gravimetric

feeder, fixed with twin concave screws. The NIR equipment was a SentroPAT FO spectrometer (Sentronic GmbH, Dresden, Germany) that includes a diode array detector and acquires the data by a fiber optical connector from the diffuse reflectance probe SentroProbe DR LS (Sentronic GmbH, Dresden, Germany). The probe has tungsten halogen bulbs as the light source.

All the experiments were performed by pouring a target blend into the hopper followed by the adjustment of the feeding rate. Subsequently the hopper was emptied at different mass flow rates and the powder was continuously measured by NIR. The target blend was 4% m/m of A1, 1% m/m of the lubricant and 95 % (m/m) of granules containing a second API.

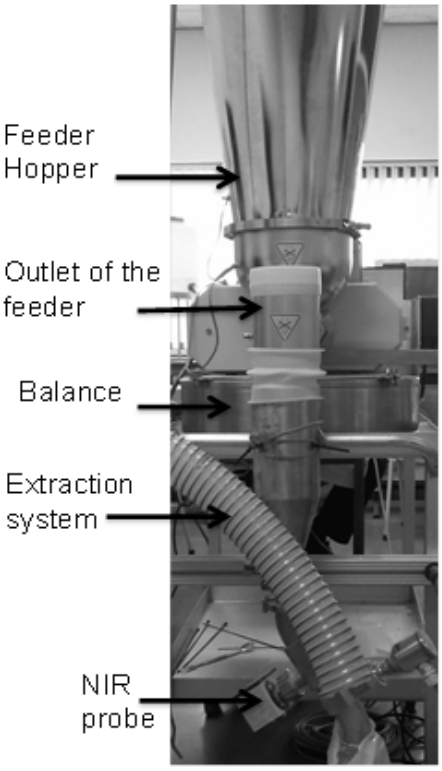

Figure 9-1 Experimental set-up consisting of a feeding system and a NIR probe.

NIR acquisition settings

This test was performed by pouring 2 kg of the target blend in the hopper. The feeding rate was kept constant at 79.2 kg/h. The material was emptied and scanned at four different acquisition parameters given in Table 9-1. These experiments were performed by triplicate.

The scan time (t) refers to the time in milliseconds in which the spectrometer measures one single spectrum, then a number n of single spectra are collected an averaged in order to get a single averaged spectrum. It is important to point out that each average spectrum required extra time in order to be stored in a file. One average spectrum was stored each 1.7 seconds for T7A60 and this time increased up to 4 seconds for T12A240.

Table 9-1 NIR acquisition settings.

Trial Code	Scan Time (t) [ms]	Total of Single averaged spectra (n)	Average spectrum NIR measurement time ($n * t$) [ms]	Total time* [s]
T7A60	7	60	420	1.7
T7A240	7	240	1680	2
T12A60	12	60	720	3
T12A240	12	240	2880	4

* Time in which an average spectrum is measured and stored into a file.

The final results were qualitatively evaluated through a PCA. Furthermore, the Mahalanobis distance by means of the Hotelling's T^2 was used for comparing the four trials. The outliers corresponding to the start-up period of the feeder were removed and only the steady-state period for each trial was used for the comparison. Hotelling's T2 values were For the PCA and the wavelength region of the combination bands was excluded; therefore the analysis was performed over the NIR frequencies of 1200 to 1900 nm.

Mass flow rate experiments

A total mass of 2 kg of the target formulation was emptied through the feeding system at different mass flow rates. Subsequently the flowing powder was scanned at two different scan times of 7 and 12 milliseconds with a total of 60 single spectra averaging. The mass flow rate ($\dot{m}$) was varied from 20 to 140 kg/h, in steps of 20 kg/hr. Table 9-2 contains the list of experiments performed.

Table 9-2 Flow rate experiments.

Trial Code	Flow rate, $\dot{m}$ [kg/h]	Single spectrum scan time [ms]
F20T7	20	7
F20T12	20	12
F40T7	40	7
F40T12	40	12
F60T7	60	7
F60T12	60	12
F80T7	80	7
F80T12	80	12
F100T7	100	7
F100T12	100	12
F120T7	120	7
F120T12	120	12
F140T7	140	7
F140T12	140	12

The resulting spectra were qualitatively analyzed through a PCA, using the wavelength range of 1200 to 1900 nm.

9.3 Results and Discussion

Attrition evaluation

Particulate materials such as the granules can suffer attrition due to mechanical stress. Attrition has different effects like changes in the internal angle of friction, particle size distribution, surface area, bulk density, fluidizing velocity, and dust release (Bemrose and Bridgwater, 1987). Changes on the particle properties can also influence the quality attributes of the final dosage form such as tensile strength, porosity, and dissolution profile. Therefore, it is preferable to avoid significant damage of the particles during the manufacture unit operations.

In this study, the particles were blended at 1000 rpm inside a continuous blender. In order to qualitatively evaluate the damage to the particles, samples from a reference blend mixed at 10 rpm were compared to the blend mixed at 1000 rpm. The micrographs of the reference blends are given in Figure 9-2 and Figure 9-3, showing different shapes and particle dimensions. The particles of interest are the granules, which correspond to 95 % m/m of the formulation. The granules are the big aggregates with amorphous shape. Visually in Figure 9-4 the granules do not show significant breakage nor apparent damage after the blending process under high shear forces.

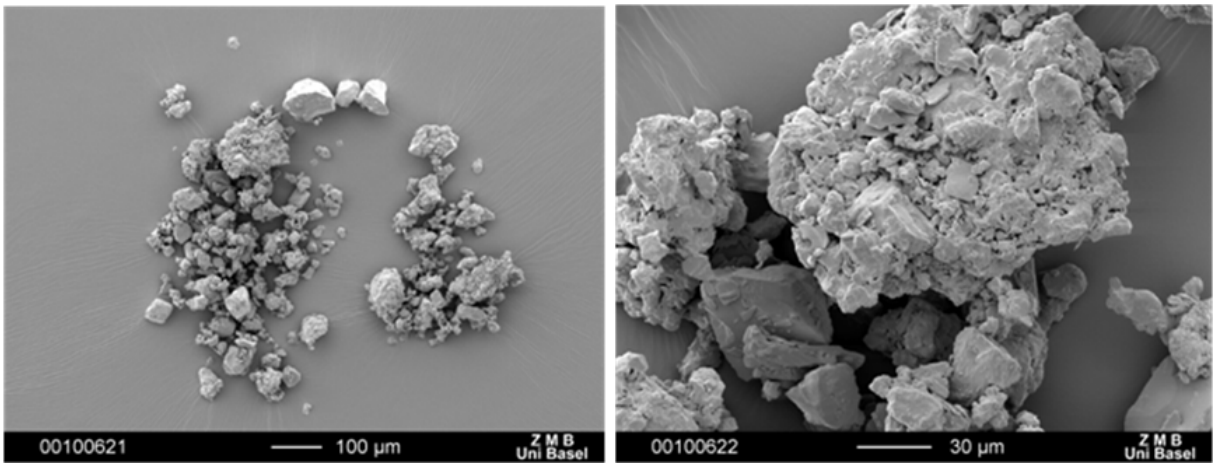

Figure 9-2 SEM micrograph for reference blend mixed at 10 rpm.

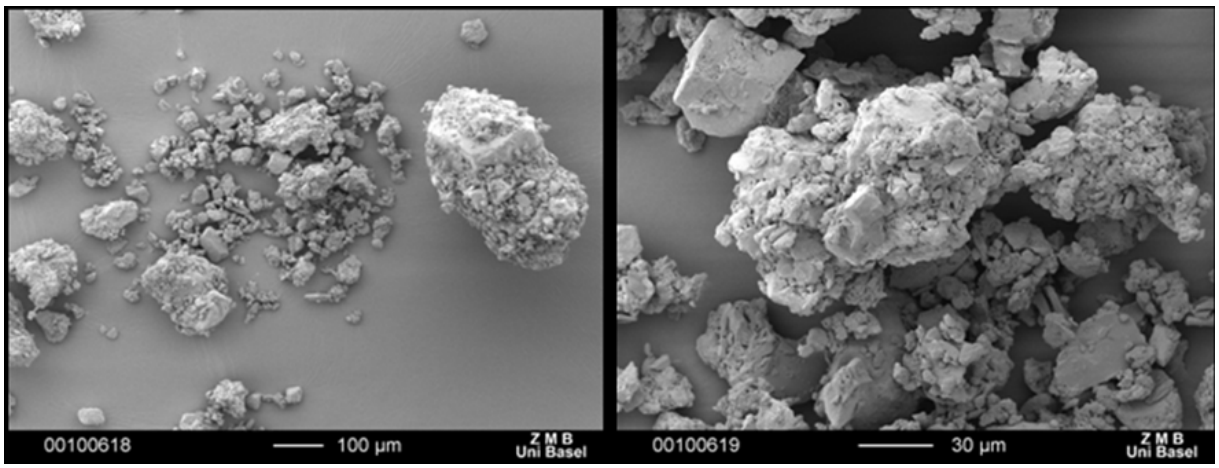

Figure 9-3 SEM micrograph for reference blend mixed at 10 rpm.

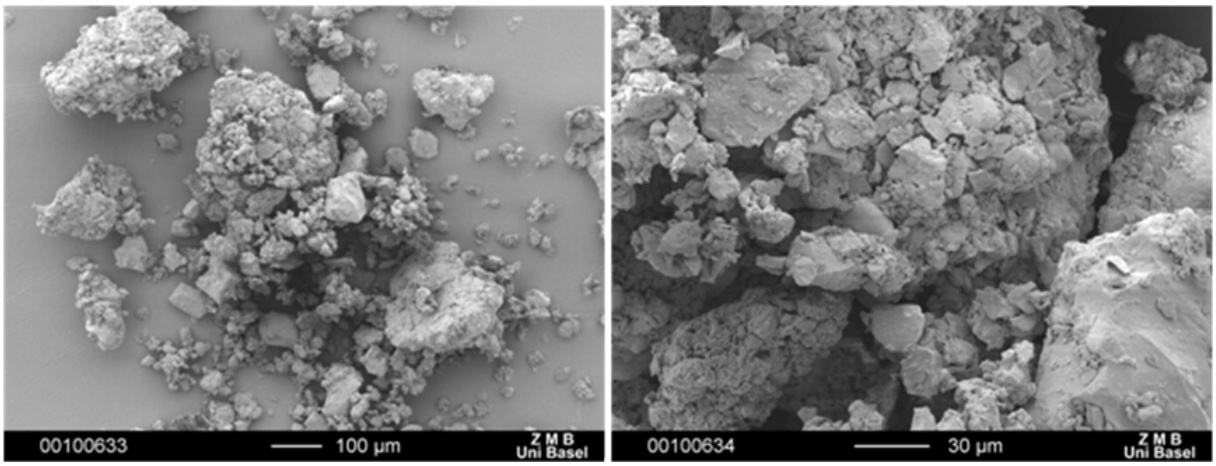

Figure 9-4 SEM micrograph for blend mixed at 1000 rpm.

The granules and the blends were measured through laser diffraction and the mean particle size was registered. The mean particle size in Figure 9-5 indicates that the blends mixed at 10 rpm had bigger particles than the particles blended at 1000 rpm. This situation may be caused by slight attrition experienced by the particles mixed at 1000 rpm which was not evident through the SEM micrographs.

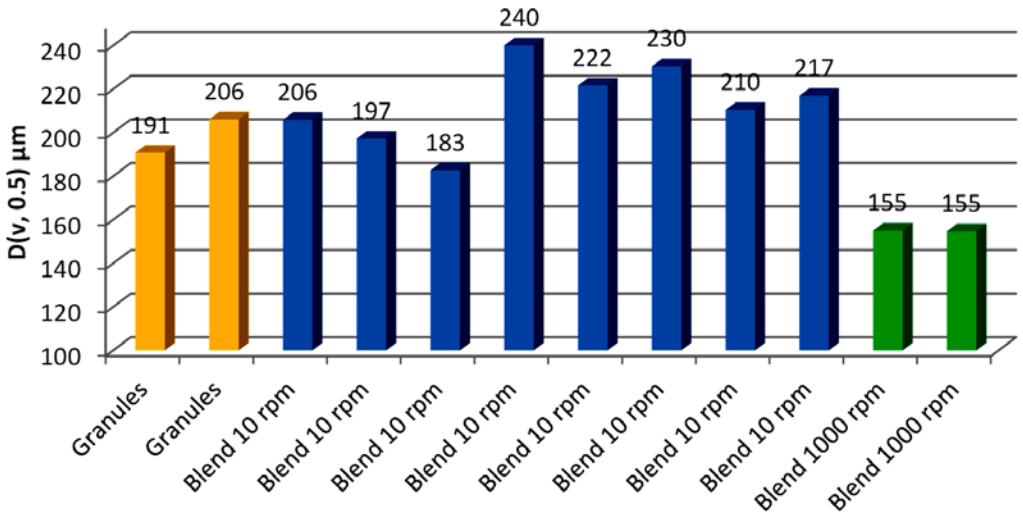

Figure 9-5 Mean particle size measured by laser diffraction.

Determination of NIR acquisition parameters

After the removal of the start-up phase for each of the trials, a PCA was performed. Figure 9-6 shows the scores plot for all the trials. There was no evidence of the formation of individual clusters, and the samples from each of the trials were distributed around the origin.

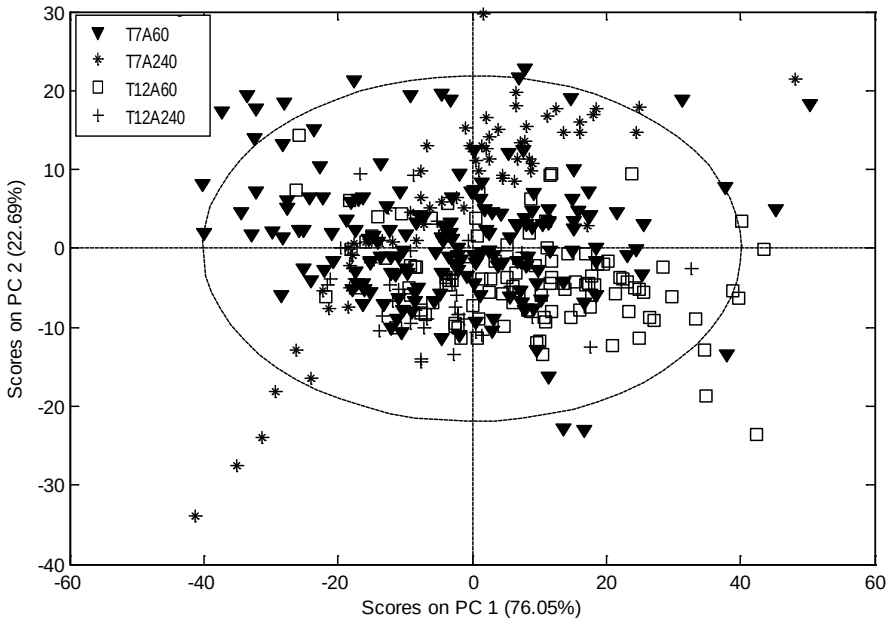

Figure 9-6 PCA for NIR spectra under different acquisition parameters.

Hotelling's T2 are associated with the distance to the center of the scored plot, thus the values are always positive. Figure 9-7 shows the Hotelling's T2 values for each of the acquisition parameters. Even though the start-up phase for each trial was previously excluded, it is possible to observe several outliers.

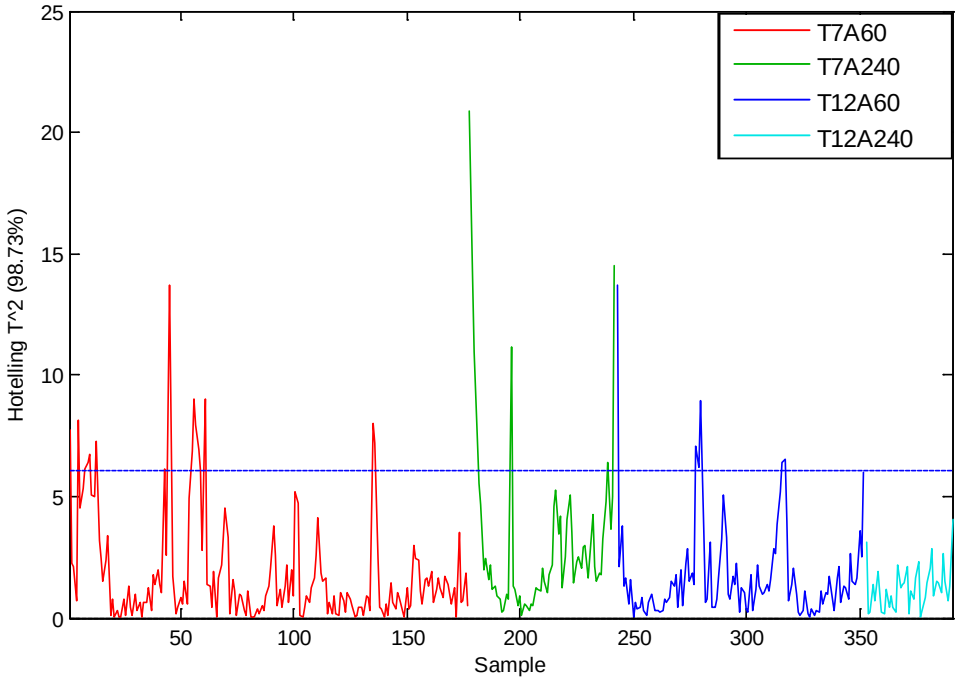

Figure 9-7 Hotelling's T^2 plot for each of the trials.

Figure 9-8 contains the Hotelling's T^2 values divided by quartiles; this plot does not assume a specific distribution of the data and it is useful for analyzing results that are not normally distributed as the Hotelling's T^2. The size of the boxes refers to the width of the distribution; therefore the values for T7A240 indicate more dispersed values which is in accordance with the interquatile range of 2.99 (Table 9-3). The * marks denote the outliers of each trial. The outliers differ from the rest of the samples and do not represent the normal conditions of the process. The higher amount of outliers was found for T7A60, which is attributed to the higher acquisition time of each single spectrum, and as a result this trial included more noise. The trial that had the lowest amount of outliers was T12A240. This trial represented the highest averaging and highest acquisition time. T12A240 had a narrow interquartile range of 1.15 and few outliers. On the other hand the number of measured spectra reduced considerably. Another disadvantage is that variation in the process or API levels could go unnoticed.

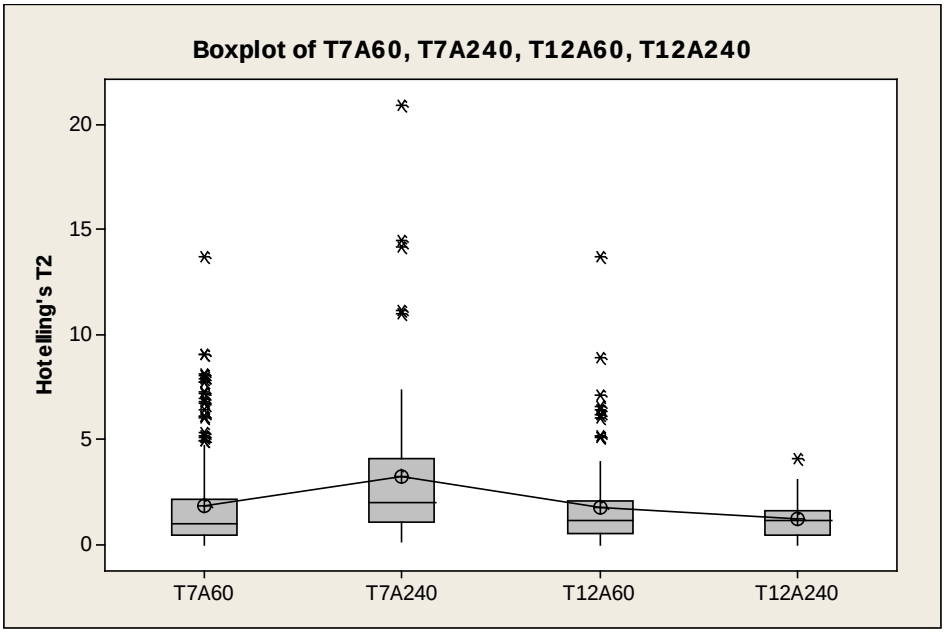

Figure 9-8 Boxplot for Hotelling's T^2 values of the different NIR acquisition parameters.

Table 9-3 gives the quartile values for each trial. Evaluation was done considering that values close to zero were closer to the center of the main cluster. Indicating less spectral variability. T7A60 has the lowest values for the first quartile and the median. T7A60 had a single spectrum acquisition time of 7 milliseconds, as a result higher amount of spectra were collected under the same conditions. These acquisition parameters would be useful when

fast spectra collection is required. In general, the averaging of 240 spectra increases the total time for each measurement. The high number of averaged spectra were correlated with a decrease of noise and in the case of T12A240 the smoothing of the signal could lead to unnoticed chemical variations.

Table 9-3 Results for the Hotelling's T2 values divided by quartiles.

Trial	Number of samples	First Quartile	Second Quartile (Median)	Third Quartile	Interquartile range
T7A60	177	0.43	1.01	1.75	1.75
T7A240	65	1.12	2.02	4.11	2.99
T12A60	110	0.55	1.13	2.08	1.52
T12A240	39	0.47	1.19	1.61	1.15

The results suggest that the best NIR conditions were achieved with a 60 single spectra averaging. In relation to the acquisition time s, 7 ms would collect higher amount of spectra faster than with 12 ms settings. Additionally 7ms had higher sensitivity to noise and to chemical and physical variations than 12 ms.

Influence of mass flow rate

Mass flow rate is a main parameter that can be easily controlled on the continuous blender and it is directly associated with the yield of the process. This section was focused on the influence that the mass flow rate exerted on the NIR spectra. From the previous section (Determination of NIR acquisition parameters), it was observed that the 60 single spectra averaging showed good performance. On the other hand, the best scan time was not fully identified. Therefore a qualitative comparison of the mass flow trials scanned at 7 and 12 ms was performed. Figure 9-9 shows the scores plots for the feeding rates ranging from 40 to 140 kg/hr. The spectra from the 20 kg/hr trials were excluded due to highly scattered data. The scores plot clearly demonstrates that the spectra from the 7 ms scan time, was more scattered than the scores for 12 ms. These results confirm that a scanning time of 7 ms was

more sensitive to noise. In contrast the scores from 12 ms scan time were clustered together, were more homogeneous, and were more robust to flow rates variations. The scan time of 12 ms may be the optimal value for the identification of the steady-state of the continuous blending process.

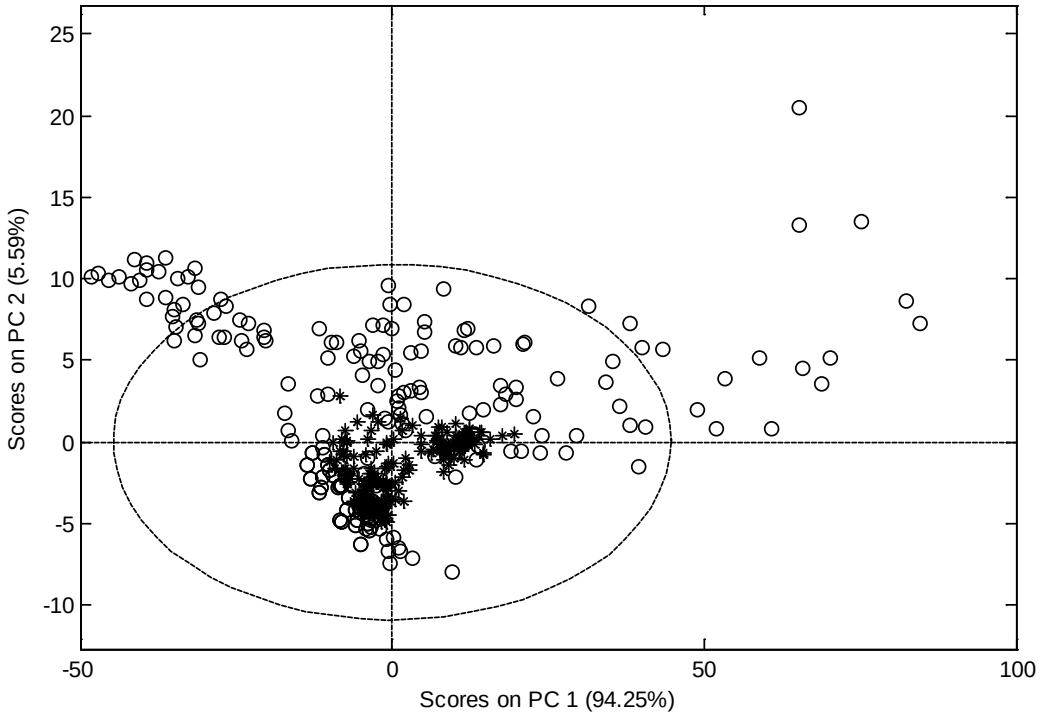

Figure 9-9 Scores plot for the flow rate trials (40 to 140 kg/h) under different scanning times (○) 7 ms and (∗) for 12 ms.

The total amount of measurements per trial is given in Table 9-4. At low feed rates, the time needed for emptying the feeder's hopper was longer, therefore greater number of spectra were collected.

Table 9-4 Number of measurements for each trial.

Trial Code	Total spectra	Trial time [s]
F20T7	176	300
F20T12	142	306
F40T7	83	142
F40T12	81	159
F60T7	56	104
F60T12	48	103
F80T7	45	78
F80T12	38	76
F100T7	33	58
F100T12	31	62
F120T7	28	49
F120T12	25	51
F140T12	22	44

The target blend was emptied through the feeder at 20 kg/h and it was measured by NIR at 7 or 12 ms of scanning time. The measured spectra of each trial were individually analyzed by PCA. Figure 9-10 shows the first PC for the trials F20T12 and F20T7., The scores of both trials showed periodic fluctuations. The trial with scan time of 7 ms (F20T7) presented fluctuations with higher frequency than the trial with 12 ms scan time. The relevance of these experiments was to identify the fluctuations due to the feeding process. The high frequency fluctuations are meant to be damped by the continuous blending process, while low frequency fluctuations can lead to inhomogeneities on the final blend. Figure 9-11 shows the scores for the first PC of the 40 kg/h trials. It was clear that the high frequency fluctuations diminished however the process did not steady.

The NIR scanning time can be adjusted in order to identify the high frequency variations. The use of NIR can lead to a better characterization of a feeding system, thus giving an insight into the performance and reliability of the equipment.

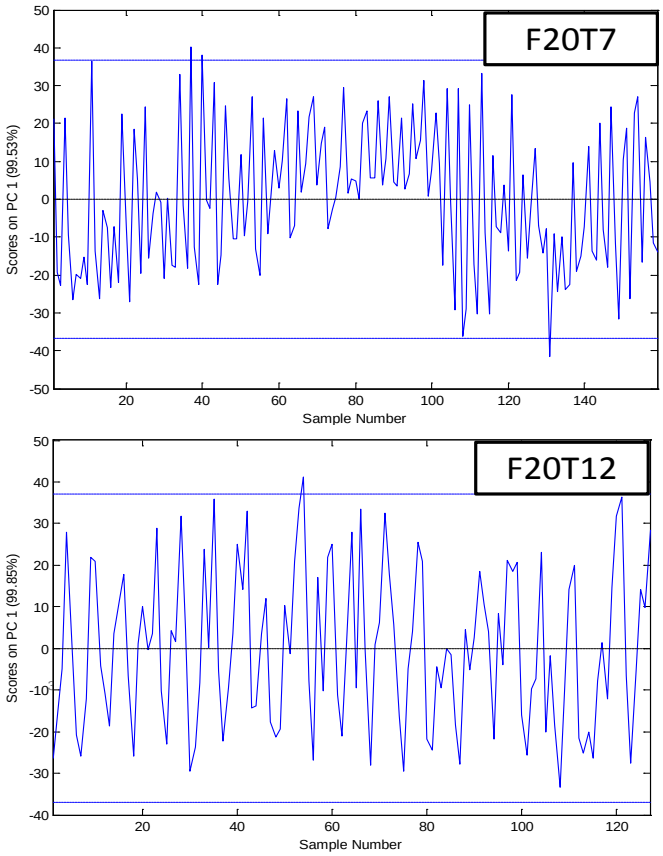

Figure 9-10 Scores for the first PC for the trials F20T7 andF20T12.

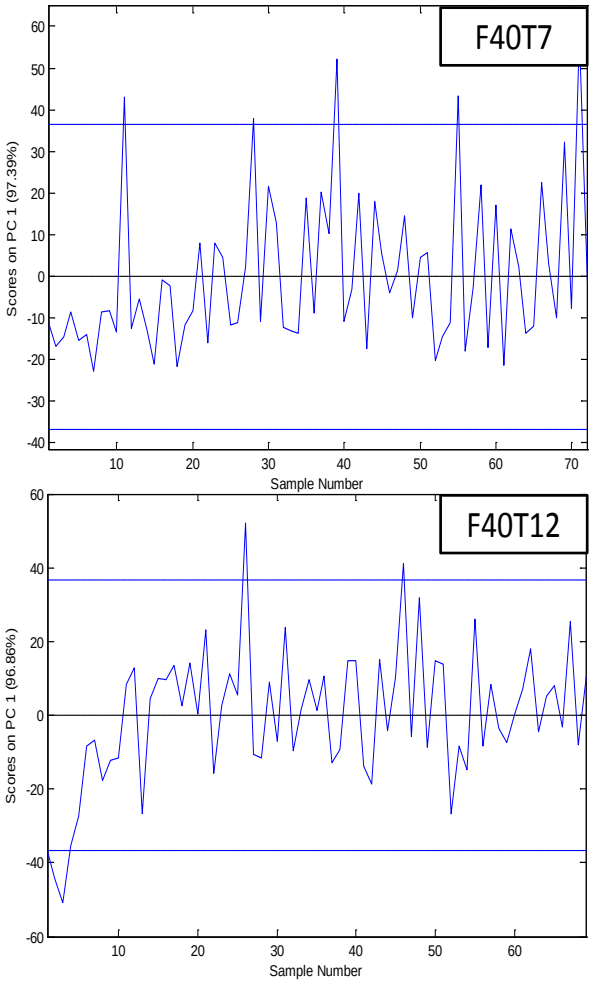

Figure 9-11 Scores for the first PC for the trials F40T7 and F40T12.

9.4 Conclusions and perspectives

Bulk solids processing is challenging as variations on the physical properties of the particles can lead to quality variations.

Part of this study consisted of assessing the impact that high rotation speed can have on the physical stability of the particles. The granules did not show significant physical damage, but slight attrition was present. In order to fully avoid the appearance of attrition, lower stirring rates may be used.

For the development of robust processes and analytical methods, it is fundamental to understand the process variables that determine the quality of the final product. These experiments showed that fluctuations in the mass flow rate could be observed on the NIR

spectral data. This study demonstrated that NIR acquisition settings could be defined according to the experimental needs. Lower scan times were more sensitive to noise, while high averaging and long scan times were less sensitive to noise and to process changes. Therefore a compromise between scan time and averaging is fundamental for the development of an NIR analytical method.

References

Bemrose, C.R., Bridgwater, J., 1987. A Review of Attrition and Attrition Test Methods. Powder Technol. 49, 97-126.

10Appendix 2. Matlab codes

10.1 Matlab code for coloring spectra

Objective: To generate a Graphical User Interface (GUI) for the visualization of NIR spectra. The spectra were color coded according to the reference values (**Y** matrix). The GUI allows the user to apply the main preprocessing techniques: original data (without preprocessing), SNV, first derivative (15 pt. smoothing), second derivative (15 pt. smoothing), autoscale and their combinations. This GUI is a useful tool for the identification of the wavelength regions associated with the reference values allowing the user to focus the analysis on the frequencies of interest. The GUI appearance together with the preprocessing techniques is shown in Figure 10-1.

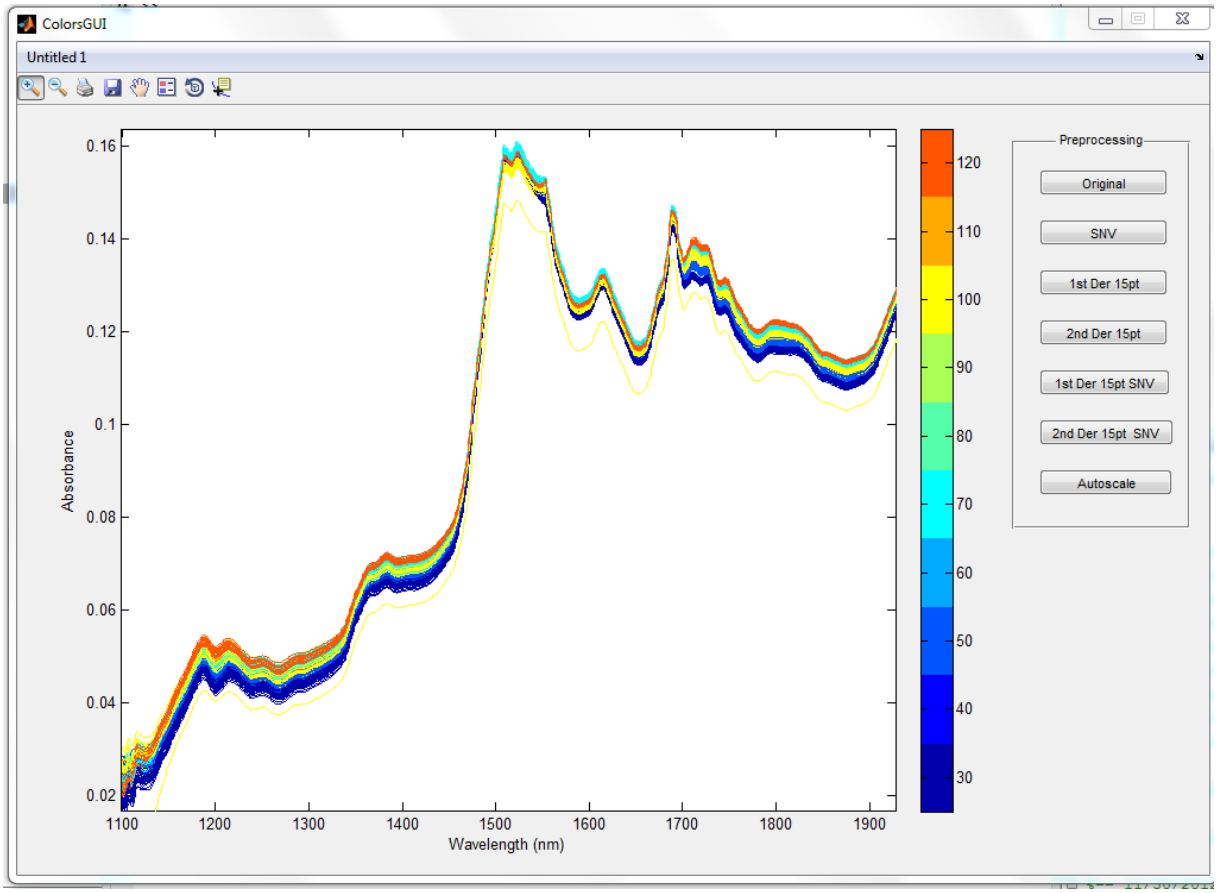

Figure 10-1 GUI for NIR spectra visualization.

GUI main code

```
function varargout = ColorsGUI(varargin)
% COLORSGUI MATLAB code for ColorsGUI.fig
%      COLORSGUI, by itself, creates a new COLORSGUI or raises the existing
%      singleton*.
%
%      H = COLORSGUI returns the handle to a new COLORSGUI or the handle to
%      the existing singleton*.
%
%      COLORSGUI('CALLBACK',hObject,eventData,handles,...) calls the local
%      function named CALLBACK in COLORSGUI.M with the given input
arguments.
%
%      COLORSGUI('Property','Value',...) creates a new COLORSGUI or raises
the
%      existing singleton*.  Starting from the left, property value pairs
are
%      applied to the GUI before ColorsGUI_OpeningFcn gets called.  An
%      unrecognized property name or invalid value makes property
application
%      stop.  All inputs are passed to ColorsGUI_OpeningFcn via varargin.
%
%      *See GUI Options on GUIDE's Tools menu.  Choose "GUI allows only one
%      instance to run (singleton)".
%
% See also: GUIDE, GUIDATA, GUIHANDLES

% Edit the above text to modify the response to help ColorsGUI

% Last Modified by GUIDE v2.5 14-Nov-2012 16:11:04

% Begin initialization code - DO NOT EDIT
gui_Singleton = 1;
gui_State = struct('gui_Name',       mfilename, ...
                   'gui_Singleton',  gui_Singleton, ...
                   'gui_OpeningFcn', @ColorsGUI_OpeningFcn, ...
                   'gui_OutputFcn',  @ColorsGUI_OutputFcn, ...
                   'gui_LayoutFcn',  [] , ...
                   'gui_Callback',   []);
if nargin && ischar(varargin{1})
    gui_State.gui_Callback = str2func(varargin{1});
end

if nargout
    [varargout{1:nargout}] = gui_mainfcn(gui_State, varargin{:});
else
    gui_mainfcn(gui_State, varargin{:});
end
% End initialization code - DO NOT EDIT


% --- Executes just before ColorsGUI is made visible.
function ColorsGUI_OpeningFcn(hObject, eventdata, handles, varargin)
% This function has no output args, see OutputFcn.
% hObject    handle to figure
% eventdata  reserved - to be defined in a future version of MATLAB
% handles    structure with handles and user data (see GUIDATA)
% varargin   command line arguments to ColorsGUI (see VARARGIN)
```

```
load x;
load y;
load NIR;
run colors
% Choose default command line output for ColorsGUI
handles.output = hObject;

% Update handles structure
guidata(hObject, handles);

% UIWAIT makes ColorsGUI wait for user response (see UIRESUME)
% uiwait(handles.figure1);


% --- Outputs from this function are returned to the command line.
function varargout = ColorsGUI_OutputFcn(hObject, eventdata, handles)
% varargout  cell array for returning output args (see VARARGOUT);
% hObject    handle to figure
% eventdata  reserved - to be defined in a future version of MATLAB
% handles    structure with handles and user data (see GUIDATA)

% Get default command line output from handles structure
varargout{1} = handles.output;


% --- Executes on button press in SNV.
function SNV_Callback(hObject, eventdata, handles)
% hObject    handle to SNV (see GCBO)
% eventdata  reserved - to be defined in a future version of MATLAB
% handles    structure with handles and user data (see GUIDATA)
load x;
load y;
load NIR;
run colorsSNV

% --- Executes on button press in MSC.
function MSC_Callback(hObject, eventdata, handles)
% hObject    handle to MSC (see GCBO)
% eventdata  reserved - to be defined in a future version of MATLAB
% handles    structure with handles and user data (see GUIDATA)


% --- Executes on button press in Der1.
function Der1_Callback(hObject, eventdata, handles)
% hObject    handle to Der1 (see GCBO)
% eventdata  reserved - to be defined in a future version of MATLAB
% handles    structure with handles and user data (see GUIDATA)
load x;
load y;
load NIR;
run colorsDer1

% --- Executes on button press in Der2.
function Der2_Callback(hObject, eventdata, handles)
% hObject    handle to Der2 (see GCBO)
% eventdata  reserved - to be defined in a future version of MATLAB
% handles    structure with handles and user data (see GUIDATA)
load x;
load y;
load NIR;
```

```
run colorsDer2

% --- Executes on button press in Der1SNV.
function Der1SNV_Callback(hObject, eventdata, handles)
% hObject    handle to Der1SNV (see GCBO)
% eventdata  reserved - to be defined in a future version of MATLAB
% handles    structure with handles and user data (see GUIDATA)
load x;
load y;
load NIR;
run colorsDer1SNV

% --- Executes on button press in Der2SNV.
function Der2SNV_Callback(hObject, eventdata, handles)
% hObject    handle to Der2SNV (see GCBO)
% eventdata  reserved - to be defined in a future version of MATLAB
% handles    structure with handles and user data (see GUIDATA)
load x;
load y;
load NIR;
run colorsDer2SNV

% --- Executes on button press in Autoscale.
function Autoscale_Callback(hObject, eventdata, handles)
% hObject    handle to Autoscale (see GCBO)
% eventdata  reserved - to be defined in a future version of MATLAB
% handles    structure with handles and user data (see GUIDATA)
load x;
load y;
load NIR;
run colorsauto

% --- Executes on button press in original.
function original_Callback(hObject, eventdata, handles)
% hObject    handle to original (see GCBO)
% eventdata  reserved - to be defined in a future version of MATLAB
% handles    structure with handles and user data (see GUIDATA)
load x;
load y;
load NIR;
run colors


% --------------------------------------------------------------------
function Untitled_1_Callback(hObject, eventdata, handles)
% hObject    handle to Untitled_1 (see GCBO)
% eventdata  reserved - to be defined in a future version of MATLAB
% handles    structure with handles and user data (see GUIDATA)
```

Scripts for the Call back functions of the GUI

SNV Callback (SNV preprocessing)

```
NIRSNV=snv(NIR);
colorsets=10; %How many color subgroups do I want to create
limits=linspace(min(y),max(y)+100*eps,colorsets+1);
[n,group]=histc(y,limits);
colours=jet(colorsets);
```

```
h=plot(x,NIRSNV); %NIR must be an array of number without axis and
description of the observations. x is the wavelength array
for i=1:length(h)% i is the wavelength accuracy, in this case 1 nm
set(h(i),'Color',colours(group(i),:))
end
colormap(colours)
caxis([min(y) max(y)])
colorbar
xlabel('Wavelength (nm)')
ylabel('Absorbance')
```

Der1 Callback (First derivative with SG 15 points smoothing)

```
NIR1st=savgol(NIR,15,2,1);
colorsets=10; %How many color subgroups do I want to create
limits=linspace(min(y),max(y)+100*eps,colorsets+1);
[n,group]=histc(y,limits);
colours=jet(colorsets);
h=plot(x,NIR1st); %NIR must be an array of number without axis and
description of the observations. x is the wavelength array
for i=1:length(h)% i is the wavelength accuracy, in this case 1 nm
set(h(i),'Color',colours(group(i),:))
end
colormap(colours)
caxis([min(y) max(y)])
colorbar
xlabel('Wavelength (nm)')
ylabel('Absorbance')
```

Der2 Callback (Second derivative with SG 15 points smoothing)

```
NIR2nd=savgol(NIR,15,2,2);
colorsets=10; %How many color subgroups do I want to create
limits=linspace(min(y),max(y)+100*eps,colorsets+1);
[n,group]=histc(y,limits);
colours=jet(colorsets);
h=plot(x,NIR2nd); %NIR must be an array of number without axis and
description of the observations. x is the wavelength array
for i=1:length(h)% i is the wavelength accuracy, in this case 1 nm
set(h(i),'Color',colours(group(i),:))
end
colormap(colours)
caxis([min(y) max(y)])
colorbar
xlabel('Wavelength (nm)')
ylabel('Absorbance')
```

Der1SNV Callback (First derivative with SG 15 points smoothing followed by SNV)

```
NIR1st=savgol(NIR,15,2,1);
NIR1stSNV=snv(NIR1st);
colorsets=10; %How many color subgroups do I want to create
limits=linspace(min(y),max(y)+100*eps,colorsets+1);
[n,group]=histc(y,limits);
colours=jet(colorsets);
h=plot(x,NIR1stSNV); %NIR must be an array of number without axis and
description of the observations. x is the wavelength array
```

```
for i=1:length(h)% i is the wavelength accuracy, in this case 1 nm
set(h(i),'Color',colours(group(i),:))
end
colormap(colours)
caxis([min(y) max(y)])
colorbar
xlabel('Wavelength (nm)')
ylabel('Absorbance')
```

Der2SNV Callback (Second derivative with SG 15 points smoothing followed by SNV)

```
NIR2nd=savgol(NIR,15,2,2);
NIR2ndSNV=snv(NIR2nd);
colorsets=10; %How many color subgroups do I want to create
limits=linspace(min(y),max(y)+100*eps,colorsets+1);
[n,group]=histc(y,limits);
colours=jet(colorsets);
h=plot(x,NIR2ndSNV); %NIR must be an array of number without axis and
description of the observations. x is the wavelength array
for i=1:length(h)% i is the wavelength accuracy, in this case 1 nm
set(h(i),'Color',colours(group(i),:))
end
colormap(colours)
caxis([min(y) max(y)])
colorbar
xlabel('Wavelength (nm)')
ylabel('Absorbance')
```

Autoscale Callback (Autoscale data)

```
NIRauto=auto(NIR);
colorsets=10; %How many color subgroups do I want to create
limits=linspace(min(y),max(y)+100*eps,colorsets+1);
[n,group]=histc(y,limits);
colours=jet(colorsets);
h=plot(x,NIRauto); %NIR must be an array of number without axis and
description of the observations. x is the wavelength array
for i=1:length(h)% i is the wavelength accuracy, in this case 1 nm
set(h(i),'Color',colours(group(i),:))
end
colormap(colours)
caxis([min(y) max(y)])
colorbar
xlabel('Wavelength (nm)')
ylabel('Absorbance')
```